INNATE IMMUNO-ONCOLOGY OF MALIGNANT PLEURAL MESOTHELIOMA (MPM)

Bioscience division, Department of Life Science, College of Health and Life Science,
Brunel University London, United Kingdom

Berkan Vural
1005863

Main supervisor: Dr Uday Kishore

Second supervisor: Dr Maria Sabrina Tosi

Research Development Advisor: Dr David Tree

Acknowledgements

I would like to thank:

My primary supervisor, Dr Kishore – for his assistance and guidance throughout my research. He has been of great help in forming collaborations with Dr Roberta Bulla, and her group, and for allowing me to travel to them and to gain skills and experience in a working clinical environment for my research, as well as arranging the necessary training to carry out my research. I would also like to thank him for being my mentor and making me strong when times were challenging, especially during frustrating times when unexpected data is present.

My second supervisor Dr Sabrina Tosi and colleague's Dr Pathan and Dr Tsolaki for their utmost encouraging support and valuable advice throughout my research, and sharing their experiences and valuable skills with me, and also allowing me to seek their assistance with open doors.

I would like to thank Dr Roberta Bulla, from Trieste University, and her group with great appreciation for accepting me in their laboratory for more than a year and giving me valuable skills to pursue my research. This was a great opportunity that I very much appreciate. I would also like to thank her for dedicating time for me, her support and feedback, and essentially giving me the skills and experience that I have gained in a working clinical and laboratory environment to enable me to succeed in my research, but also for my personal growth.

Declaration

I can confirm that this thesis presented for the degree of MPhil, has

i) been composed entirely by myself

ii) been solely the result of my own work

iii) not been submitted for any other degree or professional qualification

Any contributions from colleagues in the collaboration, such as diagrams or calibrations, are explicitly referenced in the text.

Date: 02/07/2020

Signature: *Berkan Vural*

Print Name: BERKAN VURAL

Abstract

Malignant pleural mesothelioma is a type of cancer that develops in the pleural cavity. The pleural cavity is the lining covering the outer surface of the body's most vital organs, such as the lung and heart. Asbestos is the only scientifically proven cause of the disease. My thesis involves ascertaining the role of human pulmonary surfactant protein D (SP-D) in the pathogenesis or protection against malignant pleural mesothelioma (MPM), a chronic cancer that is linked to long-term exposure to asbestos. The overall aim of my research is to determine whether our generated recombinant form of human SP-D (rfhSP-D) induces apoptosis in MPM, as it does in leukaemia, prostate and pancreatic cancers via a range of signalling pathways. An alternative hypothesis is that since SP-D can induce a potent pro-inflammatory immune response while interacting with asbestos-like particles, it creates a perfect chronic microenvironment for the development of MPM. Thus, rfhSP-D may negate the intrinsic pro-tumorigenic consequences of pulmonary SP-D-asbestos needle interaction. Our team has established apoptotic activity of rfhSP-D in pancreatic cancer, breast cancer and lung cancer. So far, I have performed immunohistochemical staining on mesothelioma biopsies sections to detect the presence of human SP-D, and I have found within these mesothelioma subtypes that human SP-D is present and saturated throughout the tissue histotypes. This raises various questions, such as what is the function of human SP-D in MPM? Is human SP-D pro- or anti-tumorigenesis, and essentially why is human SP-D being profoundly present in MPM biopsy sections received from patients? This suggest a crucial role for SP-D in mesothelioma, as its presence marks its significance in tumour growth. I have generated a recombinant fragment of human SP-D (rfhSP-D) to mimic the functional effects of human SP-D. Recombinant fragment of human SP-D (rfhSP-D) is composed of homotrimeric neck and carbohydrate recognition domain, purposely to analyse the apoptotic activity of rfhSP-D in MPM using *in vitro* assays and ultimately to provide a potential therapeutic intervention to improve upon new strategies that will potentially reduce tumour growth and in future to increase patient survival and prognosis. Firstly, the recombinant form of SP-D (rfhSP-D) is prepared using a plasmid pUK-D1 that contains collagen triple-helix consisting of cDNA sequences for repeating 8 Gly-X-Y triplets, the α-helical coiled-coil neck and CRD region of human SP-D, for which under bacteriophage T7 promoter is used to express the recombinant form of human SP-D (rfhSP-D) (177 residues: Gly179 to Phe355) that is transformed into *Escherichia coli* BL21 (λDE3) pLysS. Once rfhSP-D is produced an purified in large batches, it then undergoes endotoxin removal, as toxins produced from *E. coli* is potent to all cells and creates an inflammatory

response that will overpower rfhSP-D when carrying out *in vitro* assays, potentially causing false positive results. Here, I have provided data and an insight into a new area of research, that was not carried out before. This includes the ability of rfhSP-D to bind to malignant pleural mesothelioma (MPM) cell line (MSTO) in a calcium dependent manner on its carbohydrate moiety structure, and rfhSP-D induces apoptosis in MPM cell lines (MSTO and Met-5a), which are confirmed using a number of valid *in vitro* experimental techniques.

Table of Contents

List of Abbreviations

ABPA	Allergic bronchopulmonary aspergillosis
AM	Alveolar macrophages
CT	Computerised tomography
CRD	Carbohydrate recognition domain
DPT	Diffuse pleural thickening
DVL	Dishevelled
EGFR	Epidermal growth factor receptor
EGF	Epidermal growth factor
EPP	Extra-pleural pneumonectomy
H & E stain	Haematoxylin and eosin
HA	Hyaluronic acid
IgM	Immunoglobulin M
IgG	Immunoglobulin G
IHC	Immunohistochemistry
IPTG	Isopropyl β-D-1-thiogalactopyranoside
IL	Interleukin
IMRT	Intensity-modulated radiotherapy technique
IPA	Invasive pulmonary aspergillosis
LPS	Lipopolysaccharide
MBL	Mannan binding Lectin
MPM	Malignant plural Mesothelioma
NK cells	Natural killer Cells
PET	Positron emission tomography
PBMCs	Peripheral blood mononuclear cell
rfhSP-D	Recombinant fragment of human surfactant protein D
RICTOR	Rapamycin-insensitive companion of mammalian target of rapamycin
RPTOR	Regulatory-associated protein of mTOR
SMRP	Soluble mesothelin-related peptides
SP-D	Surfactant protein D
TNF-α	Tumour necrosis factor - Alpha
VATS	Video-assisted thoracoscopic surgery
VEGF	Vascular endothelial growth factors

1. General introduction

1.1 ***An overview of malignant pleural mesothelioma***

Pleural mesothelioma is a type of cancer that develops in the pleura, which is known to be the protective layer that lines one of the most vital organs, the lungs, and the chest cavity. Malignant pleural mesothelioma is the most common type of mesothelioma, and it is commonly caused by the exposure of asbestos (Cugell and Kamp, 2004). Mesothelioma remains critically under-researched, despite its potentially deadly effects world-wide. The cause of its deadly nature stems from its poor prognosis and lack of effective treatment or cure. The median survival after treatment ranges from 9-18 months. The lack of effective treatment has led to high mortality rates across the globe, with 2,180 estimated new cases diagnosed in the United States in 2013 alone, and 2,697 new cases of MPM in the UK in 2015 (MesotheliomaHelp.org, 2017). The main contribution to its high mortality rate is because MPM is almost always diagnosed at a stage where it is too late to cure, due to its latency period of 20 to 40 years, whereby current forms of treatment can only be effective in reducing symptoms and pain, as symptoms usually get noticed when patients reach their senior years of around 50 - 60 years of age. The epidemic severity of mesothelioma has been underestimated for many years. It is essential to widen our knowledge as well as awareness of mesothelioma, particularly malignant plural mesothelioma (MPM), critically to reduce the rising number of deaths each year (Pass *et al*., 2005). According to various sources, asbestos exposure is the primary cause of mesothelioma. However, the vast majority of sources still pertain to the common misconception that asbestos has now been eradicated for many years, which is the most common misconception in society in relation to mesothelioma. Malignant mesotheliomas are primarily developed from the surface serosa cells of the pleural, peritoneal and pericardial cavities, as well as the tunica vaginalis (Sluis-Cremer., 1991; Pass *et al*., 2005; and Cugell, 2004)

MPM is known to be the most common among the mesothelioma types, accounting for approximately 90% of the disease, which may be due to the major risk factor of occupational exposure to asbestos. Most mesotheliomas occur in the pleura. Development of the disease is between 20 and 60 years after from first contact (O'Brien *et al*., 2006). Three main histologic subtypes of mesothelioma are epithelioid (Figure 1A), sarcomatoid (Figure 1B) and biphasic (Figure 1C). Epithelioid tumours are known to be the most common and have a better prognosis than sarcomatoid and biphasic tumours. My study is focused on MPM which is the most aggressive and common form of mesothelioma. MPM, amongst other forms of mesothelioma,

is most challenging to treat because of its aggressive nature and the median overall survival varies between 9 and 18 months.

MPM is confined to the pleural cavity, which is a protective layer formed over the lungs and beneath the chest wall, called the pleura. The pleura is a serous membrane, lining the thoracic cavity and covering the lung. In healthy pleurae, the parietal and visceral pleura are both in contact (Figure 2). Both left and right pleural cavities each constitutes a closed unit not connected to the other. The surface of the pleural cavity composed of a sheet of flat cells, known as the mesothelium, covers an underlying layer of loose elastic tissue. In normal pleura, it is known to exude fluid to maintain its moist and lubricated environment. A list of major disorders arising from the pleura include 1) pleurisy; the occurrence of inflammation in the pleura 2) plural effusion; the build-up of excess fluid between the two pleurae 3) empyema occurs when build-up of pus occurs in the pleural space, and 4) mesothelioma is when tumour develops in the pleura (Cugell and Kamp, 2004).

Three subtypes of Mesothelioma

A)

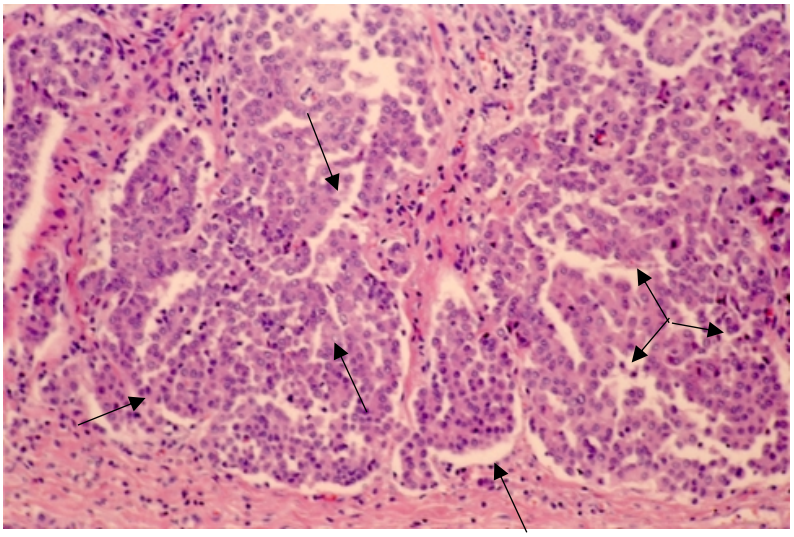

B)

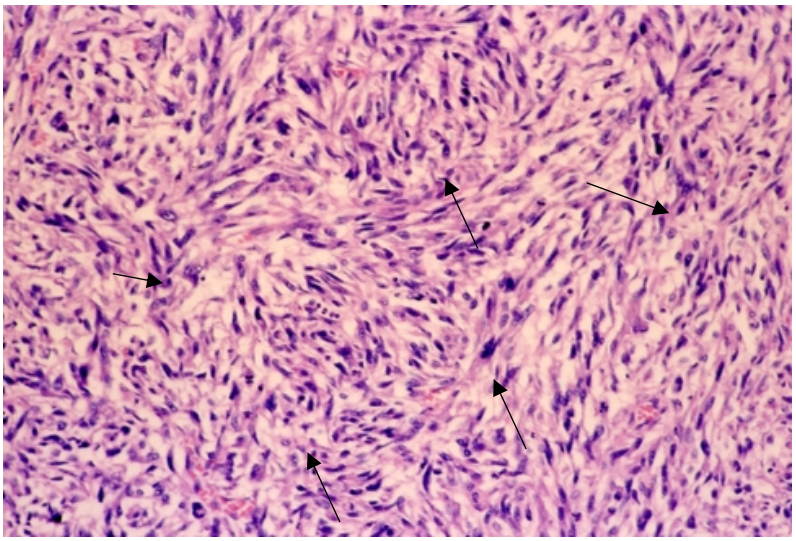

C)

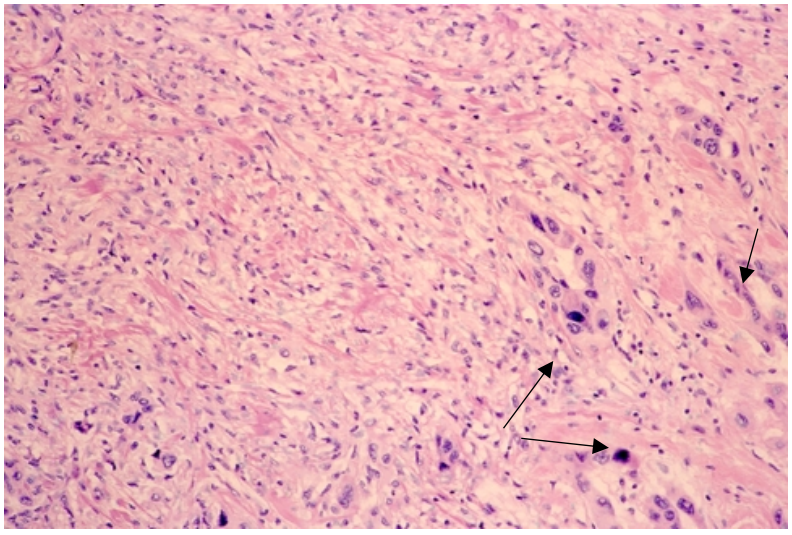

Figure 1. Immunohistochemical classification at x100 magnification showing mesothelioma. A) Epithelioid mesothelioma (H&E stain), shows prominent and distinctive papillo-tubular structure (indicated by black arrows). B) Sarcomatoid Mesothelioma (H&E stain), as clear display of proliferation specifically of spindle cells, which is a distinctive marker for sarcoma (indicated by black arrows). C) Biphasic mesothelioma (H&E stain), this subtype shows both features of epithelioid mesothelioma and that of sarcomatoid mesothelioma within one tumour (indicated by black arrows) (Adapted from Kouki, 2008).

Based on the haematoxylin and eosin (H&E) staining on Figure 1, eosin stained cytoplasm and extracellular matrix pink, and haematoxylin stains the nucleus light blue. This ultimately turns red in presence of acid, as differentiation is achieved by treating the tissue with acid solution. The bluing step converts the initial soluble red colour within the nucleus to an insoluble blue colour. The counterstaining is achieved by using eosin which imparts pink colour to the cytoplasm (Cugell and Kamp, 2004).

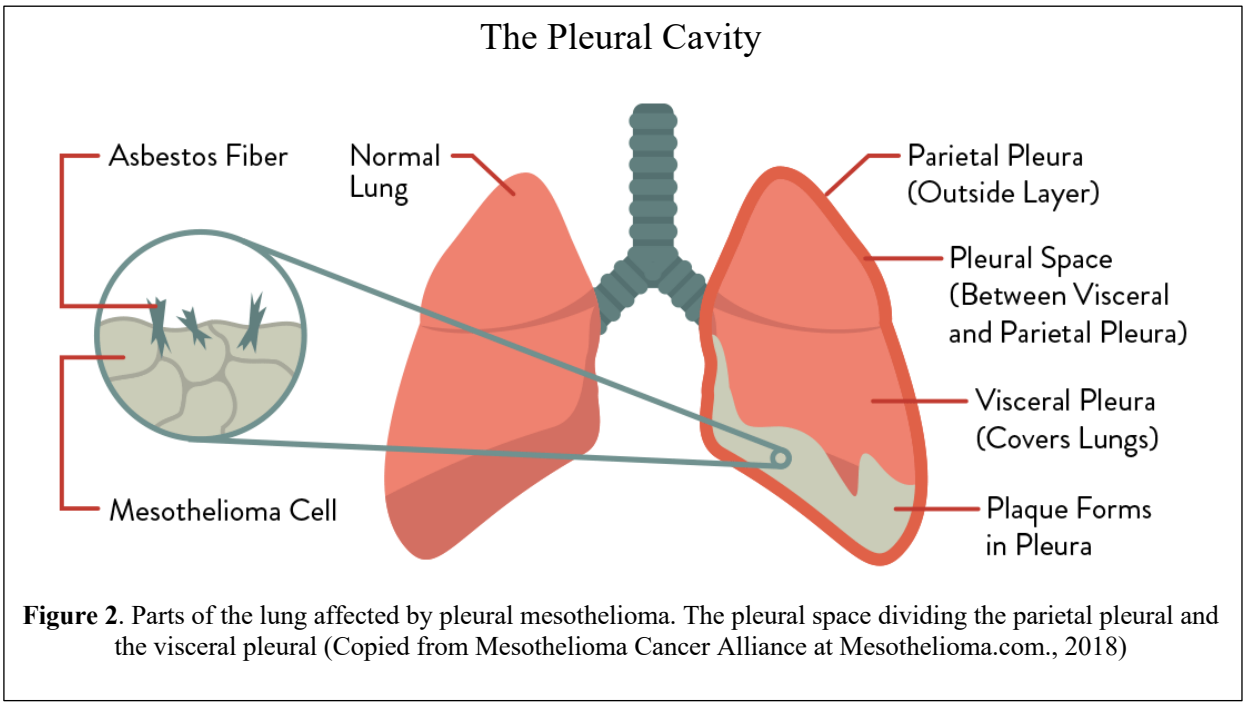

Figure 2. Parts of the lung affected by pleural mesothelioma. The pleural space dividing the parietal pleural and the visceral pleural (Copied from Mesothelioma Cancer Alliance at Mesothelioma.com., 2018)

Since the primary and most common cause of mesothelioma is the exposure to asbestos, the extremities of mesothelioma began to appear at the start of the industrial revolution in the 1800's, where mining for asbestos were common and widely sought-after. Asbestos was used on an industrial scale despite the subsequent discovery of its harmful effects. According to Cancer Research UK, there are around 2,700 new mesothelioma cases in the UK every year, equating to more than seven every day (2013-2015) (Cancer Research UK., Feb 2018). Furthermore, since the early 1990's, mesothelioma incidence rates have increased by around two thirds (67%) in the UK. According to mesotheliomahelp.org (Joseph., 2018) mesothelioma occurs four times more often in men than in women, this may be due to occupational exposure. In the UK, mortality rates have significantly increased by 887% since the early 1970's, which is an alarming rate (Cancer Research UK., Feb 2018).

Asbestos was used industrially because of its valuable physical properties which allow it to be resistant to chemicals, heat, water and electricity; it turned out to be the most suitable insulator for turbines, steam engines, ovens and electrical generators (Carbone *et al*., 2012). Asbestos became the backbone of the industrial revolution. Going back in history, during the late 1800's the mining and manufacturing of asbestos was revolutionized and become a booming industry. However, as a sheer consequence of the lack of understanding the effects of asbestos, serious health effects were evident in individuals who were involved in mining and refining the mineral, as well as people who became directly exposed to it (Mauney, 2018). The development of malignant mesothelioma was first associated with the widespread use on an industrial scale of asbestos in the early and mid 20th century (Carbone *et al*., 2012). Pleural mesothelioma has been the most common type of mesothelioma in Europe in the 1990's. Currently, Scotland and England are estimated to have the highest European incidence rates at ages 40-74. While the increase in incidence slowed down or remained static in most European countries between the late 1980's and mid-1990's, the rates continued to increase significantly in England and France.

During the early 19th century, crocidolite (blue asbestos fibres) was found in Free State, Africa. In 1876 chrysotile, known as white asbestos, was first discovered in the Thetford Township, in south-eastern Quebec. Canada established the world's first commercial asbestos mines and joined Russia in excavating the mineral, which is found in more than 95 percent of all asbestos products (Mauney, 2018). The serpentine form of asbestos, known as chrysotile, as well as the amphibole forms of asbestos, are common and well known to be the main concern for those who had been exposed within their working environment. However, evidence collected from the deceased suggests resultant user exposure may involve both forms, chrysotile and amphibole. Amphibole and crocidolite are far more potent carcinogens in comparison to serpentine asbestos, such as chrysotile in the causation of malignant mesothelioma (Sluis-Cremer, 1991; Sluis-Cremer *et al*., 1992; Boutin *et al*., 1996; Boffetta, 2007). However, chrysotile can cause lung cancer, and is a known carcinogen that accounts for 95% of asbestos related deaths worldwide; therefore, chrysotile evidently is the foremost cause of malignant mesothelioma (Carbone *et al*., 2012).

Eventually, in 2002, the last U.S asbestos mine closed, bringing to an end more than a century of asbestos production in the country. There are several bills in Congress and around the world seeking to establish the first national mesothelioma registry as well as renewed interest in abolishing asbestos use and exposure. Although we are heading in the right direction in eliminating the use of asbestos, we may face tremendous challenges if we are to eliminate

all the asbestos created during the industrial revolution, when this fine mineral was assumed to be harmless (Mauney, 2018). As evident from the media across the world, especially in the UK, we are still discovering sites where asbestos was used. Around the world there are an estimated 14,200 new cases of mesothelioma diagnosed each year, with incidence rates varying across the continents (Cancer Research UK, 2018).

Pathological manifestations of asbestos exposure in affected individuals, include pleural plaques, chunky substances that form on the lungs because of calcification and diffuse pleural thickening (DPT), fibrous tissue that fills the pleural space (Figure 3). MPM and DPT are likely to become common in the future because of the growing trend of new cases. Clearly, the overall prevalence of DPT and pleural disease are rising. The Worker's Compensation Dust Diseases Board of New South Wales have shown a rise in DPT cases from 65 in 2002 to 133 cases in 2006 (Miles, 2008).

Asbestos-related diffuse pleural thickening

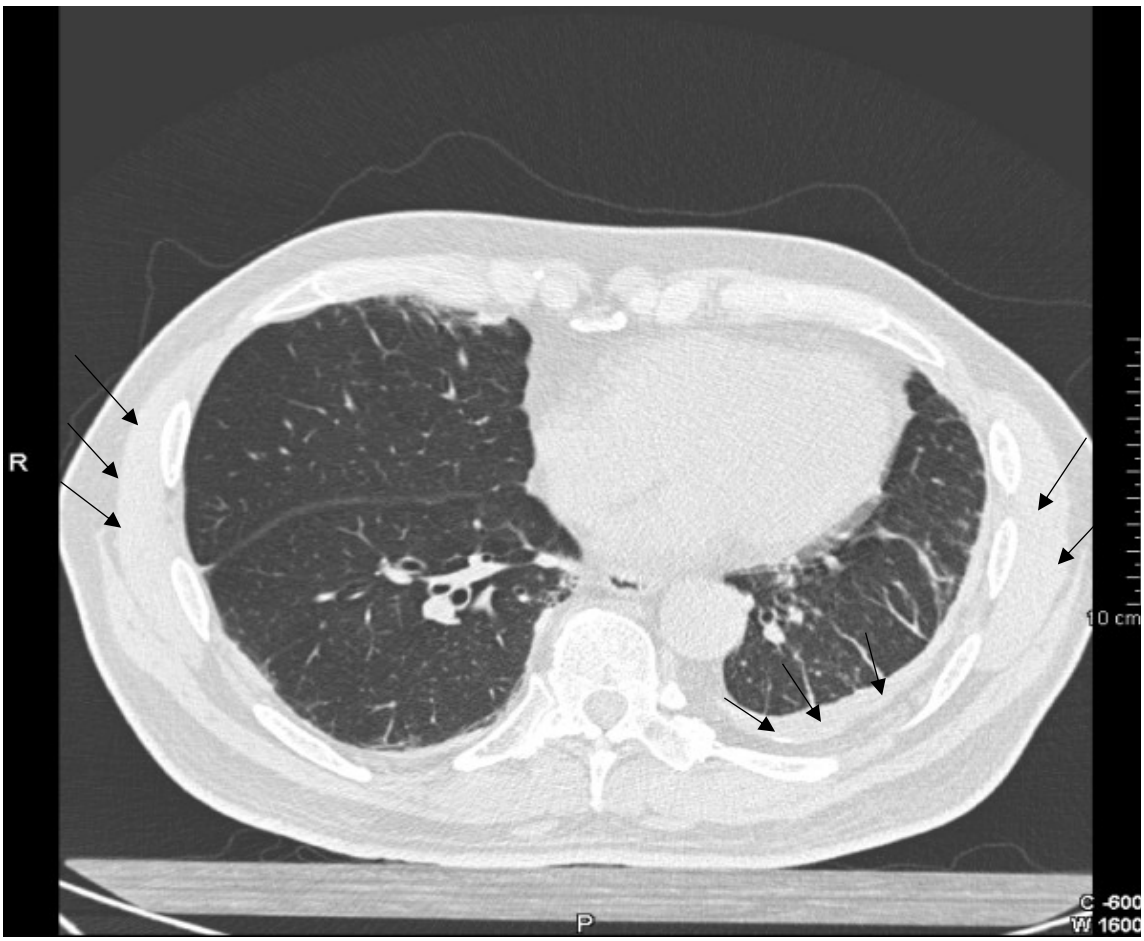

Figure 3. Computed tomography (CT) scan of the thorax demonstrating asbestos-related diffuse pleural thickening. The diagram clearly shows "crow's feet" or better known as parenchymal bands that are shown on the left, and an overall reduction in the lung volume. Black arrows, see diagram, showing the abnormal growth of the MPM (Adapted from Miles, 2008).

According to Cancer Research UK, Feb 2018, the incidence and rates for males and females both combined has shown a dramatic increase in new cases by 67% in the UK between 1993-1995 and 2013-2015. The increase was larger in males than in females, is mainly due to the occupational exposure to asbestos fibres. Over the last decade in the UK (between 2003-2005 and 2013-2015), the number of new cases of MPM has increased by 7% (Figure 7).

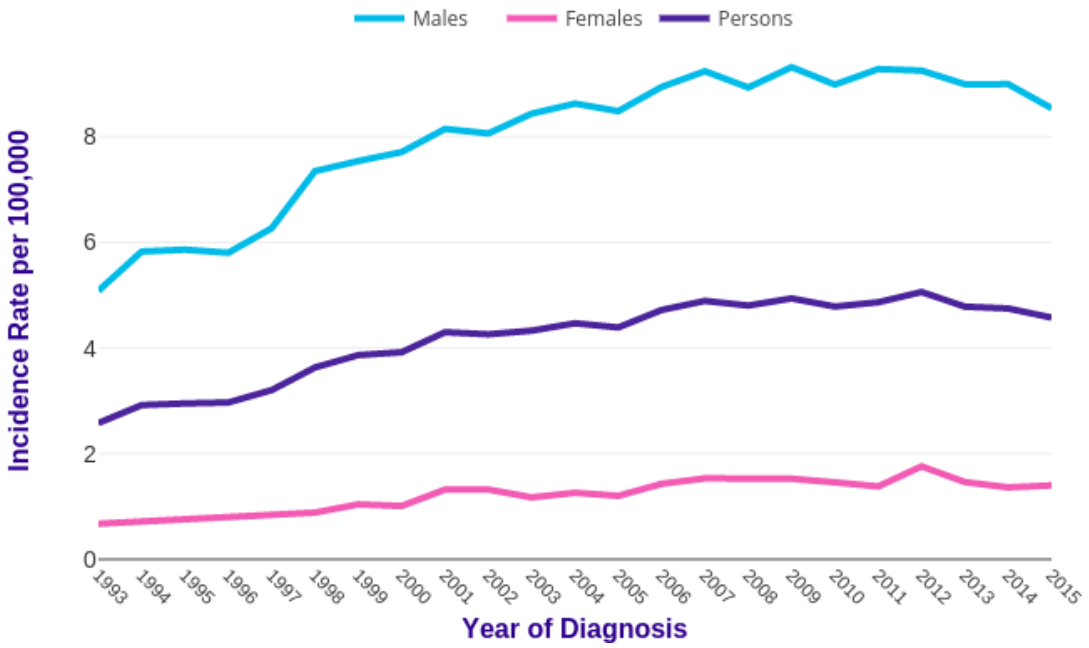

Figure 4. Mesothelioma incidence trends from 1993 to 2015. For males, mesothelioma age-standardised (AS) incidence rates in the UK increased by 58% between 1993-1995 and 2013-2015. For females, mesothelioma AS incidence rates in the UK increased by 96% between 1993-1995 and 2013-2015 (Copied from Cancer Research UK. Feb 2018).

The majority of cases of mesothelioma from asbestos can be preventable by using personal protective equipment, including facial masks and air filters, and carry out cooperate risk assessments will allow for more effective monitoring of employees. Many corporations and businesses that manufactured or mined asbestos and have profited from it, were justifiably aware of the hazards and risks of this deadly mineral to the workers and to civilians. However, those who profited from asbestos did not warn of the risks or protect workers, because of its value and capitalizing potential, which has led to a greater number of people suffering. There are a growing number of lawsuits against companies who were involved in mining asbestos. Essentially, it is the duty and obligation of these businesses to fully understand their products

and the risks involved in mining these minerals, and they should issue warnings about the dangers involved and to be fully aware, which may have prevented deaths. There are suspusion that many corporations withheld information regarding risk assessments and health consequences to protect themselves from liability. As a result, workers have unnecessarily developed life-threatening complications that resulted in eventual death. According to the World Health Organization, it is estimated that asbestos causes half of all deaths from occupational cancer, and 125 million people have been exposed to asbestos in the workplace (MesotheliomaHelp.org., Jan 2017). Despite these statistics from around the world, the long latency period of MPM and the continuous consumption and distribution of asbestos products that is currently available to the public, will only cause new cases and mortality rate to continue to rise around the world.

1.2 Immune-oncology and pathogenesis of MPM

The mechanism underlying development of the predisposition to MPM from the exposure of asbestos remains widely unknown and critically under-researched. The mechanism through which mesothelial cells undergo neoplastic transformation is not known. Recent evidence has unveiled a multistep process involving both the activation of oncogenes as well as the inactivation of tumour suppressor genes. Critically, what is also unknown is whether asbestos fibres, which are the main causing factor of MPM, act directly on mesothelial cells, or indirectly through the formation of reactive oxygen species and growth factors (Robinson, 2005).

The most common hypothesis is that MPM exists as a multifactorial carcinogenesis mechanism, which is prone to stimulation by asbestos fibres when inhaled which then migrates to the pleura where it is trapped and initiates a cascade of inflammatory responses. Asbestos fibres enter the pleural space where repeated cycles of tissue damage are established through inflammation, as the foreign object (fibres) stimulates an immune response. As asbestos fibres are phagocytosed by macrophages, this triggers the release of oxygen free radicals, which causes intra-cellular DNA damage and abnormal repair. Fibres that are phagocytosed also initiate an oncogenic cascade of events, this includes activation of c-Myc and c-Jun oncogenes, binding with epidermal growth factor receptors (EGFRs), and promotion of anti-apoptotic genes including Bcl-xl (Robinson, 2005). However, it is argued that certain types of asbestos fibres cannot be phagocytosed by pulmonary macrophages because of their larger diameter in size, such as the family of amphibole fibres (Cugell and Kamp, 2004). The amphibole fibres are most carcinogenic, and it is known to be bio-persistent and contain high iron content that

catalyses the production of reactive oxygen radicals. When inhaling amphibole fibres, it cannot be phagocytised by the body's natural immune response to foreign agents, this is because of its size in nature, instead these fibres get deposited and burrowed over the years in the serosal surfaces of the pleural, specifically the pericardium and peritoneum. This increases the chances of developing a variety of other life-threatening complications, such as plural plaques, diffuse pleural thickening and benign pleuritis with effusion, also high risk of developing asbestosis which is a chronic lung disease caused by inhaling asbestos fibres (Cugell and Kamp, 2004).

Asbestos fibres penetrating mesothelial cells and interfering with mitosis, generate mutations within the DNA and also modify chromosome structure (Sekido, 2013). As a result of asbestos-exposed mesothelial cells, inflammatory cytokines are released into the extracellular matrix, as well as tumour growth factor-β, platelet-derived growth factor and vascular endothelial growth factors (VEGF). The release of these humoral factors into the extracellular matrix creates a favourable microenvironment for tumour development and growth. The local microenvironment has been examined in MPM. It is known to encourage growth, survival, and invasion of cancer cells, and plays a critical role in the development of cancer. The extracellular matrix (ECM) is a crucial constituent of the microenvironment. Hyaluronic acid (HA) is a member of the glycosaminoglycan family and an abundant and ubiquitous component of the ECM. HA is a negatively charged high-molecular-weight (HMW) polysaccharide (4.0 – 800 kDa) and it is made up of the repeating disaccharide, specifically glucuronic acid and *N*-acetylglucosamine. In the tumour microenvironment of MPM, HA forms a molecular 3D-scaffold structure for cells *via* the assembly of ECM, for which it modulates stromal as well as tumour cells. HA has multiple functions that are dictated by its molecular size and tissue concentration, and it relies on balanced biosynthetic and degradation processes. Increased HA synthesis has been examined and known to be associated with cancer progression and metastasis, supporting the hallmarks of cancer. Patients diagnosed with MPM have been found to have large quantities of HA in their tumour tissue, although both malignant and benign mesothelial cells have been found positive for intracytoplasmic HA (Lorusso and Ruegg, 2008).

1.3 Immune aspects of MPM and its links to the innate immune system

The local microenvironment of MPM is composed of many different important constituents, HA is one of the main constituent that make up the local environment for tumour growth. The complement system is also a constituent of the local environment for cancer.

Understanding the tumour microenvironment and its constituents, including the complement system and HA, will allow for a more effective immunotherapy modality to treat MPM. The complement system acts as an immune surveillance against malignant cells for its advantageous ability to promote inflammation and cause direct cell killing (Rickin *et al*., 2010). C1q is an important factor in the functionality of the complement system. This is mainly because the forming C1 complex triggers and activates the complement system. C1q is a subcomponent protein that binds to C1r and C1s to form the C1 complex. C1q is primarily synthesised by hepatocytes, macrophages and epithelial cells, and is a member of the collectin family. C1q (460 kDa) is made up of 18 different polypeptide chains, composing of 6A (223 residues), 6B (226 residues) and 6C (217 residues) chains, each have a short N-terminal region linked to a collagen sequence and a C-terminal globular region (Sellar *et al*., 1991). Three genes within the chromosomes 1 (long arm) is responsible for encoding C1qA, C1qB and C1qC homologous proteins. One of each of the three C1q polypeptides are able to combine to form the C1q subunit, and six subunits are able to combine to form the C1q protein. The C1q protein is able to bind to CH3 domain of the IgM and the CH2 domain of the IgG. C1q is also able to bind to a number of cellular receptors saturated on fibroblast, lymphocytes, as well as amongst cell surfaces and intercellular membranes, including mitochondrial membranes.

The binding activity of these cell receptors to C1q may induce a number of physiological responses, which includes chemotaxis, phagocytosis and pro-coagulant activity (Rickin *et al*., 2010). The C1q complex has important functions in the protection of the host and also contributes to supporting the immune system. Important functions of C1q also includes clearance of apoptotic bodies, recognising immune complexes and initiating the classical complement pathway. The activation of the classical pathway through C1q is achieved by the engagement of C1q subunits structures with two additional subunits of C1s and C1r, which are held by ionic bonds in the presence of calcium. Upon activation, these two subunits are known to achieve enzymatic activity. C1s activates two essential complement proteins, complement component 4 (C4) and complement component 2 (C2). C1q has a number of different roles mediated through its direct interaction with other C1q receptors. These roles include recognising apoptotic cells and removing them, regulate T cell activation through specific receptors (T cell – C1q receptors), and C1q is able to activate polymorphonuclear leukocytes through neutrophil C1q receptors. C1q has the ability to effect cell differentiation and proliferation and dendritic cell maturation. Therefore, its presence in normal healthy host provides a crucial support for the development of the immune system (Sellar *et al*., 1991).

Sellar *et al.* (1991) has shown the importance of C1q by carrying out a study to understand C1q deficiencies. C1q deficiencies are presented in two different forms, an absent C1q protein or an abnormal C1q protein. A number of cases of C1q deficiencies have shown infections, including otitis media, urinary tract infections, oral infections and meningitis, as well as skin lesions and glomerulonephritis. An estimated 93% of cases are linked to systemic lupus erythematosus, which is triggered by mutations within the C1qA, C1qB or C1qC genes, and known to be inherited in an autosomal recessive pattern.

C1q is also found in placenta during pregnancy to modulate the endovascular and interstitial invasion of trophoblast cells (Bulla *et al*., 2008). C1q is saturated in several solid human tumour tissues and is profoundly involved in the progression of tumour (Agostinis et al., 2010). In MPM, C1q have been shown to bind to HA. More specifically, globular head of the C1q A chain (ghA) has a greater binding affinity to HA, compared to ghB and ghC. This interaction suggests a differential categoric nature between C1q domain and HA. In MPM tumour, the interaction between HA and C1q mediates pro-tumorigenic properties, that supports cellular adhesion, proliferation and migration of human mesothelioma cells. A research group performed immunohistochemistry on MPM biopsies, and unravelled C1q present in all variant types of mesothelioma tissues examined, including epithelioid, sarcomatioid and biphasic type. Interestingly, monocytoid cells are primarily associated with C1q, which indicates that these cells are the main source of C1q locally. C1q is also highly radiant in small vessels, which raise the possibility of exhibiting pro-angiogenic activity (Bulla *et al*., 2008), which is also found in wound healing (Agostinis *et al*., 2010). HA is found to be highly saturated in MPM tissues mainly because it is responsible for lubricating pleural membranes, allowing the membranes to slide without greater friction, and are also secreted in mesothelial cells. In tumour, the function of C1q seems to be highly dependent on the microenvironment. It is clear from previous studies, that C1q is locally produced by cells of non-tumour form and is able to bind differentially to various components present in the extracellular matrix of the tumour microenvironment. The composition of the mesothelioma tumour microenvironment contains a heterogenous mixture of immune cells, including natural killer cells and T cells, epithelial and stromal cells, which differs upon administration of therapies and also between individuals, as no one individual is the same or react in a similar manor (Marcq *et al*., 2017).

Immune cells that are present in the tumour microenvironment is a crucial aspect in therapeutic therapies, as it paves the way of potentially controlling tumour growth. This is because immune filtration occurring in tumours includes dendritic cells (DCs), neutrophils,

mast cells, macrophages, myeloid-derived suppressor cells (MDSCs), natural killer (NK) cells, B and T lymphocytes, which some are known to have anti-tumorigenic properties. While, MDSCs, type 2 macrophages and regulatory T cells, known as Tregs, are known to supress immune response and support the hallmarks of cancer. In MPM, the tumour microenvironment is stimulated through the exposure of mesothelial cells to asbestos fibres and leads to a highly immunosuppressive state caused by an infiltration of immunosuppressive cells, including type 2 tumour associated macrophages. Various histologic types of mesothelioma show different tumour microenvironments. Specifically, for MPM, macrophages are abundantly present in all histological types, and the stroma of MPM tissue is known to be infiltrated by MDSCs (Yamada *et al*., 2010).

The immune expression profile in MPM reveals leukocyte infiltration in all variant types of mesothelioma, with higher levels in non-epithelioid mesothelioma (Mudhar and Wallace, 2002). Furthermore, NK cells, T helper cells and cytotoxic T cells were all shown abundantly present in MPM (Marcq *et al*., 2017). T cell subsets revealed heterogeneity as well as high coefficient variations in various studies (Yamada *et al*., 2010). B cells and Tregs were also revealed to be present in MPM biopsies and pleural fluid of mesothelioma. The microenvironment surrounding MPM is also known to have tumour growth promoting cancer-associated fibroblasts, as well as programme death ligand 1 (PD-L1), with high concentrations seen in non-epithelioid histologic types. In addition, it is found that in MPM there is an infiltration of immune effector cells and immune suppressive cells, including Tregs and M2 (repair) macrophages, as well as expression of PD-L1 (Anraku *et al*., 2008).

It is common for tumours to exploit ways of bypassing the immune system in order to capitalise on a network of natural resources to assist in growth and development, ultimately achieving all the hall marks of cancer. However, the ability to map the composition of the tumour microenvironment will prove to be advantageous in target therapy in mesothelioma, in order to reduce or lesson the effects of pro-tumorigenic activity. More specifically, tumours containing high levels of T effector cells and Tregs could be treated using combination therapy targeting cells of interest, as this will help control their functions and improve upon the efficacy of immunotherapy, for example patients with tumours that are shown to have an infiltration of MDSCs will most likely benefit when using celecoxib, which have shown in a study to have reduced its suppressive function (Mudhar and Wallace, 2002). The microenvironment of MPM with expression of cytotoxic T cells and PD-L1, using PD-L1 inhibitors as a form of treatment has shown most effective. Furthermore, other forms of treatment include emactuzumab or nintedanib, which used for treating tumour microenvironment infiltrated by M2 macrophages,

as it is effective in converting M2 macrophages into M1 subtype, altering its function and purpose. Further to this point, stimulating OX40 as it is known to regulate cytokine production and stimulates cytotoxic T cell, can be used as part of therapeutic immunisation strategy for treating MPM and other forms of cancer (Marcq *et al*., 2017). Essentially this provides a new approach for treating cancer, especially MPM, and the opportunity to develop a tailored form of treatment using immunotherapy. However, there are possibilities in which the tumour will overcome cytotoxic killing elicited by the response of the immune system, therefore, effective treatment is likely to be found in heterogeneity of tumours and the tumour microenvironment.

1.4 Signalling pathways and MPM

A study conducted by Robinson., (2005) have shown asbestos fibres to stimulate phosphorylation of various kinases, including mitogen-activated protein and extracellular signal-regulated 1 and 2, which stimulate an increase in the expression of proto-oncogenes and induction of cellular proliferation. Genetic profiling of MPM tumours have shown common mutations, which include a significant reduction in the expression of key molecules in the p53 tumour-supressing gene pathway, such as p14, p16 and NF2-MERLIN (Robinson, 2005). Loss mutations and deletions of other genes, including BRCA-associated protein 1 (BAP1) and set domain bifurcated 1 (SETDB1) amongst others have also been demonstrated in MPM (Illei, 2003). MPM have shown to have a low frequency of protein-altering mutations (~25 mutations per tumour), which consequently limits the potential for molecular targeted therapy, as oncogene-addiction is less likely to occur in MPM. The term oncogene addiction is best described in cancer cells, which contain multiple genetic and epigenetic abnormalities. Despite this complexity, the growth and survival of the cancer cells can often be impaired by the inactivation of a single oncogene. This phenomenon, known as “oncogene addiction,” provides a rationale for molecular targeted therapy (Bibby *et al*., 2016).

Wnt pathway activation is unique to mesothelioma, as it is not known to be activated in this condition but is typically active in normal cells during development. β-catenin accumulation has been demonstrated as well as transcriptional activation of specific target genes, such as the TCF target gene and overexpression of c-myc, during development (Uematsu *et al*., Aug 2003). E3 ubiquitin-protein ligase (Siah-1) links the p53 pathway to β-catenin and promotes its degradation. Nearly 80% of MPM have wild-type p53, but they do have homozygous deletion of p14, which results in the inactivation of the p53 pathway (Matsuzawa and Reed, 2001 and Liu *et al*., 2001). As a result of p53 inactivation, the

production of β-catenin is excessively stimulated. Primary β-catenin mutation results in the dysregulation of β-catenin signaling, which is a vital event in the genesis of several human malignancies, however it is not found in MPM. In MPM, Wnt signalling pathway is activated through Dishevelled-1 overexpression and downstream signalling through β-catenin (Uematsu *et al*., 2003). MPM tumours appear to be relatively stimulated by the over-expression of transcriptional regulation of translocated β-catenin. This suggest that MPM cells may require Dvl-β-catenin pathway as an essential source for tumour formation. As evident from the data, overexpression of Dvl causes cytoplasmic accumulation of β-catenin, transcriptional activity, and tumour growth. Furthermore, it is demonstrated that activation of the dishevelled (Dvl-β-catenin) signalling pathway contributes to tumorigenesis and that targeted inhibition of dishevelled (Dvl) inhibits tumour growth (Uematsu *et al*., 2003).

1.5 Clinical presentation

The majority of MPM patients show progressive dyspnea and steady chest wall pain. Dyspnea occurs as a result of large pleural effusion, and non-pleuritic chest pain is commonly elicited by significant chest wall invasion. Patients diagnosed with MPM also experience non-specific symptoms which are common, such as dry cough, sudden weight loss, night sweats and fever, which are all insidious symptoms which add to the complexity to diagnose MPM. The latency period can be of around 20-50-years, following asbestos exposure and development of malignancy (Ismail *et al*., 2006).

1.6. Diagnosis

1.6.1 Clinical perspective

Effective diagnostic approaches include computerised tomography (CT), which can reveal pleural effusion, the size of the lymph nodes in the mediastinum and hilum, as well as the presence of pleural masses, and trans-diaphragmatic spread, as the tumour tends to form a coat of tissue that encases the lung and extending to the fissures and along the mediastinal pleural and diaphragm (Scherpereel *et al*., 2010). Although preliminary signs of MPM tumour is visible using a CT scan, it is not used as a sole diagnosis tool for MPM. Magnetic resonance imaging (MRI) of the chest can be a useful tool, but not a stand-alone diagnostic tool, to diagnose MPM. MRI of the chest is more sensitive and advanced in extracting images of coronal and sagittal views from patients with MPM, and fundamental when considering curative surgery for the patient (Ismail *et al*., 2006). However, MRI is not relevant for the

diagnosis of mesothelioma (grade 1B). Positron emission tomography (PET) is a favourable tool amongst other diagnostic tools for staging MPM, as it reliably detects contralateral chest involvement and extra-thoracic metastasis, such as supraclavicular nodal disease (Scherpereel *et al*., 2010).

1.6.2 Pathological perspective

Histopathological examination of MPM is a far more accurate tool to use as a diagnostic method for patients. However, diagnosis can be challenging as mesothelioma is essentially a heterogenous cancer, therefore, it creates various misleading histopathological pitfalls. The pleura is also known to be a common ground for metastatic disease (Scherpereel *et al*., 2010).

Essentially, diagnosis must involve a broad and wide range of methods and tools to detect and investigate any suspicion of MPM, which require the need for sampling of pleural fluid for biochemical and cytological examination. As pleural effusion is a common clinical sign, cytology is usually the first diagnostic examination to be performed. In MPM, usual observation amongst patients using CT scan show pleural thickening at the parietal pleura and a small amount of pleural effusion, homogeneous mass with inhomogeneous contrast enhancement, deviation of the mediastinum toward the side of the lesion because of the contraction of the hemithorax caused by tumour, and invasion of nearby structures with rib destruction or below the diaphragm into the retroperitoneum (Scherpereel *et al*., 2010). However, this carries a high risk of diagnostic error. Further investigation is essential for diagnosing mesothelioma, as low clinical suspicion can result in misdiagnosing or discharging patients. Confirmation of diagnosis therefore requires sampling of pleural fluid for biochemical and cytological examination. However, cytological yield is low in MPM, and therefore biopsies are used to confirm the diagnosis and identify histological subtype. It is necessary to obtain adequate tumour tissue to allow for definite diagnosis and essential to determine which of the histological subtypes is present. Epithelial mesothelioma is most common, as it is found in 50% of cases and elicits best prognosis (Scherpereel *et al*., 2010).

By using radiological guidance or under direct vision at thoracoscopy, biopsies can be successfully obtained percutaneously, either with local anaesthetic procedure or surgical intervention, such as video-assisted thoracoscopic surgery (VATS), which have shown to reach 95% sensitivity. Electron microscopy is used only in equivocal cases, as it is significantly advanced, compared to other tools, in distinguishing between the neoplasms, although costs are far greater (Bibby *et al*., 2016).

Immuno-histochemical stains of biopsy tissue are necessary for definite diagnosis of MPM, as there are histomorphology similarities to adenocarcinoma. Characterizing mesothelioma is achieved through staining for calretinin in 88% and vimentin in 50% of patients. Adenocarcinomas have shown to lack these markers, therefore stains positive for carcinoembryonic antigen (84%), CD15 (77%) and Ber-EP-4 (82%) (Scherpereel *et al*., 2010). In order to receive a reliable diagnosis, a wide range of immunostaining must be used.

It is vital, as with all malignancies and diseases, to attain a reliable diagnostic biomarker. A biomarker that offer high diagnostic sensitivity and specificity is vitally important and would be a pioneering step forward for MPM. Despite current research carried out into biomarkers, there are currently no such biomarkers available for MPM.

However, mesothelin has exhibited diagnostic value in MPM. Mesothelin is a cell-adhesion glycoprotein (Hollevoet *et al*., 2012). Serum mesothelin, or serum mesothelin-related proteins, is detected at a significantly higher level in patients with MPM, as compared to asbestos-exposed controls. Mesothelin is an excellent biomarker for the advance stage epithelioid tumours. Sarcomatoid subtypes, however, rarely express mesothelin. This study has revealed meta-analysis of data from 4,491 individuals, of whom 1,026 had MPM, revealing specificity of 95% and sensitivity of 32% for serum mesothelin. Although specificity is high, sensitivity is insufficient for diagnostic purposes (Figure 5 and Table 1).

Mesothelin as an effective biomarker for Epithelioid MPM

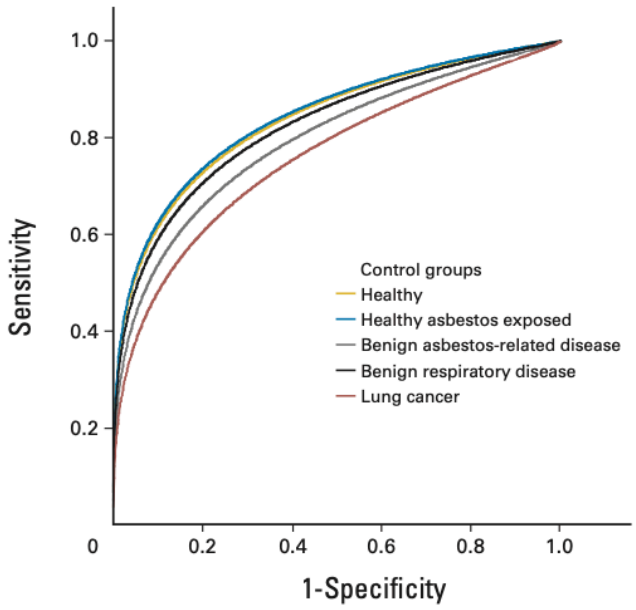

Figure 5

Control groups	AUC (95% CI)	AUC compared with healthy
Healthy	0.84 (0.81 to 0.87)	—
Healthy asbestos exposed	0.84 (0.81 to 0.87)	$P = .91$
Benign asbestos-related disease	0.80 (0.77 to 0.82)	$P < .05$
Benign respiratory disease	0.82 (0.79 to 0.86)	$P = .53$
Lung cancer	0.76 (0.73 to 0.79)	$P < .01$

Table 1

Histologic Subtype and Tumor Stage	AUC	95% CI
Epithelioid		
I-II	0.79	0.77 to 0.81
III-IV	0.84*	0.82 to 0.86
Sarcomatoid		
I-II	0.56†	0.51 to 0.60
III-IV	0.64*†	0.60 to 0.68
Biphasic		
I-II	0.70‡	0.66 to 0.75
III-IV	0.77*‡	0.73 to 0.80

Table 1 Statistics showing effectiveness of mesothelin as a biomarker for diagnosing three different subtypes of malignant pleural mesothelioma. Mesothelin is highest in epithelioid type mesothelioma compared to sarcomatoid, as can be deduced from the statistics using the key below (Copied from Hollevoet *et al*., 2012).

Key

*$P < .001$ when comparing stage III and IV patients from stage I and II patients in each histologic subtype
†$P < .001$ when comparing patients from the epithelioid subtype in the associated tumour stage
‡$P < .001$ when comparing patients from the sarcomatoid subtype in the associated tumour stage

Pleural fluid mesothelin levels also revealed similar diagnostic performance to serum, with meta-analysis of 11 studies showed sensitivity of <60% and specifically of 90%. Based on these findings, high serum or pleural fluid mesothelin require further investigations for malignancy (Cui *et al*., 2014).

Soluble mesothelin-related protein (SMRP) is present in 84% of patients suffering from MPM (Robinson, 2003). SMRP is easily detected with a simple blood test, which may not only provide an essential diagnostic test for MPM but may also show the need to monitor treatment responses. SMRP is a useful biomarker for screening at-risk individuals, as SMRP is elevated in only 2% of patients suffering from other pleural diseases. Thus, a commercial SMRP tumour marker assay kit is available now. In addition to SMRP, high levels of serum osteopontin in MPM patients have also been reported compared to those who have been exposed to asbestos or with fibrosis alone. In immunohistochemical analysis, osteopontin stains positive in 36 out of 38 samples of pleural mesothelioma (Pass *et al*., 2005). This indicates that there are useful novel markers available that will facilitate early diagnosis.

1.6.3 Staging of MPM

Based on the most widely accepted and comprehensive classification staging system by TNM-type system of the International Mesothelioma Interest Group (IMIG), there are four crucial stages of MPM tumour development. Stages one and two patients have a potentially resectable tumour. *Stage I* involves minimal tumour growth, confined to the parietal pleura, with lymph node negative patients (stage Ia), or insignificant visceral pleural involvement (stage Ib). *Stage II* also involves lymph node negative patients, but with confluent superficial tumour on the entire pleural surface, or the involvement of the lung parenchyma or diaphragmatic muscle. *Stage III* is known to be the most common stage of tumour development, which includes metastasis to hilar (N1) or ipsilateral mediastinal (N2) lymph nodes. Tumour extends into the soft tissues of the chest wall, mediastinal fat, the endothoracic fascia or the pericardium (T3 tumour). *Stage IV* is the final stage which includes patients with locally advanced tumour invading the ribs or spine, the chest wall extensively, trans-diaphragmatic spread or contralateral plural spread. This may also include contralateral, supraclavicular lymph node involvement (N3), or distant metastasis (Ismail *et al*., 2006).

1.7 Treatment

Unfortunately, there is currently no curative form of treatment for patients suffering with MPM. However, there are systemic treatment options currently available. These include

surgery radiotherapy and chemotherapy, and targeted therapy that are delivered either as part of multimodality treatment or separately (Bibby *et al*., 2016). Surgery is limited to patients with good functional status (normal functioning organs) and early stage disease and tends to be of controversial practice. It is of high importance in patients suffering from MPM to receive palliative care and symptom management, despite having no curative treatment available. It is an essential factor to control pleural effusions to reduce distressing chest pain and allow patients to breathe normally (Ismail, *et al*., 2006). There are currently a number of novel therapeutic agents under investigation, which may provide an optimistic decrease in mortality rates of this malignancy and further treatment options in the future (Rimner, *et al*. 2016).

1.7.1 Surgery

There are currently two approaches to surgery in MPM, one of which is the radical removal of all visible disease or a more conservative 'debulking procedure', involving tissue-sparing. The radical and more aggressive option is extra-pleural pneumonectomy (EPP), aiming to eradicate all macroscopic tumour, which involves en bloc resection of the parietal and visceral pleura with the involvement lung, diaphragm, mediastinal lymph nodes and pericardium (Bibby *et al*., 2016). The procedure involves reconstruction of the diaphragm and pericardium with Gortex or Marlex mesh. These surgical approaches may be used with MPM for palliation and treatment, depending on the patient circumstances and the extent of the tumour development. This includes video-assisted thoracoscopic surgery (VATS) talc pleurodesis, EPP and pleurectomy/decortication. However, there are no randomized studies comparing these surgical techniques, and results are generally in retrospective series that uses different staging systems, and other confounding comparisons (Bibby *et al*., 2016).

More specifically, VATS is useful for collecting diagnostic tissue by permitting directed biopsies. During this procedure, effusion is drained, loculations are lysed, and pleurodesis is achieved with aerosolized talc. Open thoracotomy or closed VATS can be performed for debulking pleurectomy/decortication, which is defined as a significant but incomplete macroscopic clearance of plural tumour. The objective of this operation is intentionally to relieve an entrapped lung by extracting the visceral tumour cortex. However, pleurectomy/decortication is not proposed in a curative intent, but considered as valuable in symptom control, especially symptomatic patients suffering from entrapped lung syndrome who cannot benefit from chemical pleurodesis. VATS pleurodesis does not prolong survival, but it is preferred in patients with comorbidities or advance stage disease, who then will undergo systemic chemotherapy (Ismail, *et al*., 2006). Unfortunately, there is currently limited

evidence to support debulking surgery, as there is an absence of randomized trials. However, there is an ongoing national study in the UK, supported by the National Cancer Research Institute, comparing VATS debulking with chemical pleurodesis. Despite the morbidity of thoracotomy that may diminish the benefits, emerging evidence based on VATS shows good symptom control and a beneficial effect on survival (Ismail, *et al*., 2006).

1.7.2 Radiotherapy

There are two main settings for using radiotherapy in patients suffering from MPM. This includes using radiation as a palliative measure to treat symptoms, or an adjuvant to surgery and chemotherapy as part of tri-modality treatment. However, tri-modality treatment is not considered as standard care for MPM and tends to be a highly controversial issue, because of unreliable studies that have been carried out in highly selected patients.

Radiation in MPM consists of a highly precise intensity-modulated radiotherapy technique (IMRT). However, the alternative, high-dose external- beam hemi-thoracic radiotherapy is considered highly toxic in patients. According to a study, intensity-modulated radiotherapy technique is not without risk of toxicity, as 8 out of 27 patients experienced radiation pneumonitis. Despite this risk, this technique can treat unresected tumour and allows accurate three-dimensional mapping of the tumour and will deliver a homogeneous dose to the tumour with significantly reduced radiation injury to surrounding organs (Rimner, *et al*. 2016).

Radiotherapy is used effectively to treat localised chest wall recurrences in MPM patients. Hemithoracic adjuvant radiotherapy can be employed, after EPP, for treating resected hemithorax. It can also be used to treat known residual localised unresected tumour. It is a common practice to use adjuvant radiotherapy, along with chemotherapy, after radical EPP, but there are no known studies to support any added value to adjuvant chemotherapy alone in the setting of a fully resected tumour. In terms of palliative treatment, radiotherapy can be used to reduce the bulk of a tumour and relieve symptoms, particularly in the case of chest wall invasion, nerve root involvement or painful cutaneous metastasis. A recent prospective phase II SYSTEMS trial revealed that a dose of 20 gray, delivered at five consecutive fractions, reduced patient-reported pain scores in 14 out of 40 participants. Further ongoing trials are evaluating the optimum radiotherapy dose and choice of regimen. Radiotherapy fractions is implicated when the full dose of radiation is divided into a number of smaller doses called fractions. This allows healthy cells to recover between treatments (Rimner *et al*., 2016).

1.7.3 Chemotherapy

Combination chemotherapy, with pemetrexed and cisplatin, is currently considered as the first-line systemic therapy in patients but limited to those with good performance status and unresectable MPM. Alimta ® also known as its generic name pemetrexed (manufactured and marketed by Eli Lilly and Company), is a cytotoxic multi-targeted antifolate compound that effectively blocks the activity of several enzymes in the folate metabolism pathway involved in producing nucleotides, the genetic materials of cells, preventing cells from dividing and proliferating (Ismail *et al*., 2006). Pemetrexed, activated more readily in cancer cells than in normal cells, which leads to a higher level of active form and longer duration in cancer cells, limiting its effects in normal cells. The active form of pemetrexed acts as potent inhibitor of thymidylate synthase (TS), the rate-limiting enzyme in the production of thymidylate, a necessity for DNA synthesis (Haas and Stermen, 2013). The reported phase III trial involving cisplatin and pemetrexed has demonstrated a significant survival advantage of 12.1 months for the combination, and 9.3 months in the case of cisplatin. Significant improvements in objective response rate (ORR) (percentage of patients whose cancer shrinks or disappears after treatment) also reported in addition to improve lung function, dyspnea and pain (Ismail *et al*., 2006).

Alternatively, the combination of gemcitabine and carboplatin has shown good response rate, acceptable toxicity profile and palliative effects, and is currently used as treatment in patients with pleural mesothelioma and considered as a first-line option for MPM. A single-arm trial phase II study of gemcitabine and carboplatin in patients suffering from MPM have reported a 26% partial response rate, significant palliative benefits and a median response duration of 55 weeks (Lee *et al*., 2009; Ceresoli *et al*., 2006; Favaretto *et al*., 2003). The median survival for patients in this study was 66 weeks. However, in phase three of clinical trial involving randomised studies have shown no benefits with the addition of bevacizumab to this regimen (Lee *et al*., 2009).

Unfortunately, there is no second-line chemotherapy in mesothelioma, following treatment with cisplatin and pemetrexed. Gemcitine or other drugs with single-agent activity, such as vinorelbine, are commonly used as a second-line regimen. There is no sufficient evidence in randomised or single-arm studies to recommend second-line chemotherapy as a standard treatment. However, MPM patients, with adequate performance status, should be enrolled into clinical trials of second-line treatment (Haas, 2013). Performance status is essential to quantify MPM patients' general well-being and activities of daily life. This is used to determine whether MPM patients can receive chemotherapy, whether dose adjustment is necessary, and

as a measure for the required intensity of palliative care. A large double-blinded randomised clinical trial of the histone deacetylase inhibitor, known as vorinistat used in second-line therapy for MPM, revealed no survival benefits (Ceresoli *et al*., 2011).

Although, all patients suffering from MPM will eventually experience a recurrence after first-line chemotherapy, the standard of care (platinum- pemetrexed therapy) shows a response rate at around 45%, a median progression-free survival (PFS) of up to 7.3 months and an overall survival (OS) up to 16 months (Zalcman *et al*., 2016). This provides a need of creating an effective immunotherapy agent, potentially from understanding and using SP-D which shows promising results amongst other cancer cell lines, which may be used to target MPM and reduce mortality rate and increase OS. Furthermore, it is essential to establish a suitable biomarker to select the optimal candidate for immunotherapy among patients clinically diagnosed of MPM in terms of efficacy and tolerance, and to avoid substantial costs and unnecessary complications.

1.8 Surfactant Protein D

1.8.1 The correlation between HA and C1q, and the association of SP-D

As HA is a major constituent of the local microenvironment, the complement system also constitutes the local environment for cancer as an immune surveillance against malignant cells. This is due to its ability to promote inflammation and direct cell killing. Studies have focused their investigation on C1q, which is known to be the first recognition subcomponent of the complement classical pathway (Eggleton *et al*., 1998; Duncan and Winter, 1988). C1q is an interesting protein as it elicits a strong link between the innate and adaptive immune system. This is due to its ability to bind immunoglobulinG (IgG)- and IgM-containing immune complexes. In addition of C1q being involved in the clearance of apoptotic cells, and thus maintenance of immune tolerance, C1q has shown to have the ability to directly affect cell differentiation and proliferation, dendritic cell maturation, and synaptic pruning, which are functions that are not dependent on complement activation by C1q (Duncan and Winter, 1988). It has also been shown some involvement of C1q in pregnancy via its ability to modulate the endovascular and interstitial invasion of trophoblast cells in placenta. Further to this point, C1q is involved in tumour progression and present in a variety of solid human tumour tissues, including MPM (Bulla *et al*., 2008). A Study based in Trieste, Italy, have been focusing on the involvement of C1q in the proliferation and invasiveness of MPM, which has found that C1q bind to HA and elicit pro-tumorigenic properties, leading to heightened adhesion, proliferation

and migration of human mesothelioma cells (MES) (Bulla *et al*., 2016). A similar innate immune molecule is SP-D, belonging to the collectin family.

C1q is similar to some extent to SP-D for the reason that they contribute to the innate immune system and the overall immunity of the human body. C1q also possess a region of galactose–glucose disaccharides that is attached to the collagenous regions of each protein, which suggest that carbohydrate regions on pathogens as well as apoptotic cells provide targets by which C1q can bind, eliciting a crucial function of removal of self-waste. C1q and SP-D both possess lectin-like activities, which shows the extent in which C1q and SP-D are similar (Eggleton *et al*., 1998; Païdassi *et al*., 2008).

1.8.2 Structure of Human Surfactant Protein D

The most common areas in the human body in which SP-D is secreted includes the trachea, brain, testis, salivary gland, heart, prostate, kidneys, small intestine, pancreas, and placenta. SP-D is also secreted in the serous glands of proximal human trachea, intestinal epithelia, in the endocytic compartment of macrophages, and in human and mesentery as well as the human inner ear (Madsen *et al*., 2000; Herías *et al*., 2007). Its presence in saliva and tear as well as in the epithelial lining strongly suggests that SP-D is a general scavenging defence molecule within the human body with a likely role in the modulation of mucosal immunity. Mucosal immunity is an area of limited research, it is essentially the involvement of the immune system in mucosal membranes of the intestine, respiratory system and the urogenital tract (Madsen *et al*., 2003; Hartshorn *et al*., 2003).

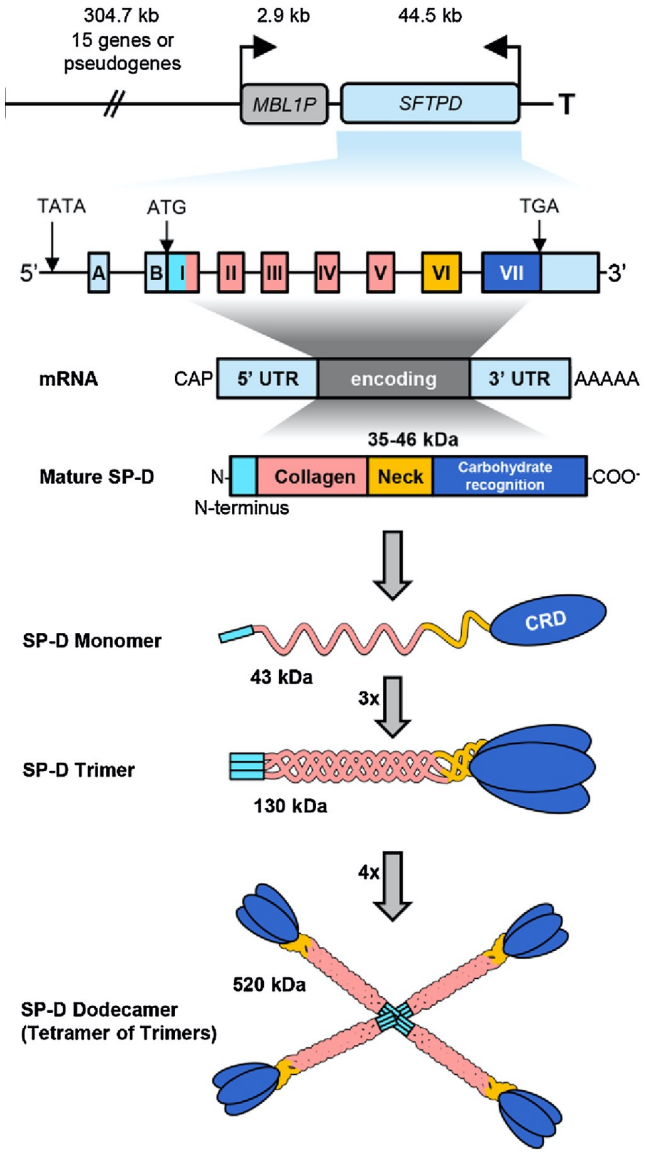

Figure 6 - The diagram illustrates the molecules of (B) SP-D, whereby a clear comparison of the different functional regions of the molecules is identified. The CRD region of the SP-D protein structure is known to mediate calcium dependent ligand-binding to molecules, such as carbohydrate, pathogens and phospholipids. The molecules are first shown as monomers and trimers. They are divided into four sub-units, the N-terminal non-collagenous domain linked to a collagenous region followed by alpha-helical coiled coil neck and the C-terminal carbohydrate recognition domain. Each sub-unit has different ligand binding affinities. SP-D assembles into a cruciform dodecamer as can be seen on the diagram below the SP-D trimer (130 kDa) (Copied from Vieira *et al*., 2017).

SP-D belongs to a group of collagen-containing mammalian lectins, called collectins, and encoded by the SFTPD gene. SP-D is a complex structure and it is shown on Figure 6. The primary structure of SP-D is organised into four distinct regions: firstly, a cysteine-containing N-terminal triple-helical collagen section, required for disulphide-dependent oligomerisation,

which is linked to triple-helical collagen that is composed of 8 repeating amino acid sequence Gly(glycine)-X-Y triplets, known to maintain the molecule shape, stability, dimension and oligomerisation. This is followed by an alpha-helical coiled neck region, by which its main function is forming a trimerization link between three monomer SP-D proteins. The alpha-helical coiled neck is connected to a globular structure at the C-terminus composing of a C-type lectin (homotrimeric ligand recognition domain), which is known as the carbohydrate recognition domain (CRD), known to mediate calcium dependent ligand-binding (Kishore *et al*., 2006). As can be seen on Figure 6, the structure of SP-D and illustrates the distinct functional regions. The diagram illustrates the molecule of SP-D as monomers and trimmers, whereby they are clearly divided into four distinct sub-units (Nayak *et al*., 2012).

SP-D is known as large oligomeric structures, in which each is assembled from multiple copies of either a single or two polypeptide chain. SP-D is composed of oligomers of a 130-kilo Dalton (kDa) sub-unit and contains three identical polypeptide chains of 43 kDa. Human SP-D is assembled into a 520 kDa tetrameric structure containing four of the homotrimeric sub-units connected through their N-terminal regions, but also possible with multimers, trimmers, monomers and dimers structures, as can be seen on Figure 6 (Vieira *et al*., 2017).

1.8.3 Endogenous role of Human SP-D

SP-D is well known to bind various self and non-self ligands through CRDs on the target surface in a carbohydrate- and calcium-dependent manner (Madsen *et al*., 2000). The collagen region stimulates the recruitment and activation of the immune cells for the purpose of removing pathogens and apoptotic cells as well as necrotic cells (Madsen *et al*., 2003). SP-D is known to play a vital role in the process of controlling inflammation initiated by self, non-self and altered-self cells and molecules. Further to its functions, SP-D plays a critical role and a significant contribution in reducing allergic reactions (Madan *et al*., 2001), inhibition of microbial growth (Wert *et al*., 2000), activation of phagocytosis and maintenance of pregnancy (Madsen *et al*., 2000) as SP-D is significantly found in amniotic fluid, as demonstrated on Figure 7 (Nayak *et al*., 2012).

More specifically, cells undergoing apoptosis (programmed cell death) and necrotic cells are removed by supporting biological mechanism. This is an essential process and vital for sustaining a balance in normal health, and this supports the resolution of inflammation. This is achieved by clearing a range of inflammatory cells that has been recruited as a consequence of inflammation, which includes plasma cells, lymphocytes, neutrophils and eosinophils from the site of injury. Removing necrotic cells and cells undergoing apoptosis is vital, as it

essentially prevents the activation of neutrophil microbial defence mechanisms and its activation. This mechanism also supports normal embryonic development and maintains tissue homeostasis (Wyllie *et al*., 1980; Haslett *et al*., 1994). Without this mechanism or ineffective clearing of cells that are undergoing necrosis and apoptosis, will lead to an abnormal accumulation of secondary necrotic cells and late apoptotic cells in the lungs (Bianchi *et al*., 2008). As a result of this accumulation, this will initiate the inflammatory immune response in order to reduce this accumulation of unwanted dying cells. However, without eliminating apoptotic cells will lead to a variety of health complications, including cancer and the development of tumours (Janssen *et al*., 2008).

In a study using murine models, apoptotic cell removal was assessed to determine the contribution of SP-D, as well as C1q, in the naïve lung. The experiments conducted includes apoptotic polymorphonuclears leukocytes (PMNs) being installed into mice intratracheally. After 30 minutes, the lungs were washed (lavage colleted) and the assessing of the clearance of apoptosis began by measuring the alveolar macrophages ingestion of the apoptosis cells and quantifying recovered apoptotic PMNs. In this study, data have strongly suggested that the clearance of exogenous apoptotic PMNs, from naïve mouse lung, had specifically been affected by SP-D itself. Therefore, SP-D was shown to contribute in enhancing clearance of apoptotic cells in resident murine and human alveolar macrophages *in vitro,* also suggesting that SP-D is a potent modulator in the clearance of apoptotic cells in naïve lungs (Vandivier *et al*., 2002). SP-D has the ability to interact with apoptotic cells by binding through its CRD region, enhancing apoptotic cell uptake by phagocytes. This mechanism is dependent on CD91, a receptor found in plasma membrane involved in receptor mediated endocytosis, and calreticulin, located on the endoplasmic reticulum and first identified as a calcium binding protein and involved in phagocytic activity. The entire collectin family, including SP-D, MBL and SP-A, functions using a common receptor complex that boosts removal of apoptotic cells (Vandivier *et al*., 2002).

Human surfactant protein D (SP-D) is a member of the soluble C-type lectin family and plays a fundamental role in linking the innate and adaptive immunity to protect against infection, allergy and inflammation (Stahlman *et al*., 2002). More importantly, this innate immune molecule (SP-D) forms a part of the host defence against respiratory pathogens and allergens, and is considered to serve a number of immunological functions, including microbial growth inhibition, recognition and clearance of necrotic and apoptotic cells, recognition and agglutination as well as phagocytosis of viral, bacterial and fungal pathogens (Wright and Dobbs, 1991). Furthermore, SP-D has been shown to exert anti-proliferative effects on B and

T lymphocytes as well as involving pattern recognition of non-self glycoproteins (Madsen *et al*., 2000; Kishore *et al* 2006). The primary site of SP-D production is within the lungs, where alveolar type II cells, as well as non-ciliated bronchial epithelial cells (also known as Clara cells) have been shown to synthesize significant amounts of these proteins (Stahlman *et al*., 2002; Madsen *et al*., 2000). The formation process of SP-D involves it being packaged into intracellular organelles, known as lamellar bodies and tubular myelin, which are then secreted into the alveolar lining layer. Studies have also provided evidence of an extra pulmonary existence of SP-D (Haagsman and van Golde, 1991; Wright and Dobbs, 1991).

SP-D contributes to the normal functioning of the innate immune system by means of binding tightly to arrays of carbohydrate structures on the surface of pathogens, allowing opsonisation which is crucial for the uptake by phagocytes, as can be seen on Figure 7 (Nayak *et al*., 2012; Mahani *et al*., 2008). SP-D bind mannose and glucose residues, which are part of most microbial ligands, more avidly than galactose, fructose and sialic acid, which are common components of glycoproteins of higher eukaryotes (Kishore and Reid, 2001; Holmskov *et al*., 2003). It is also known to regulate inflammatory responses by interacting with immune cells, such as helper T-cells and cytokines, and modulate their functions (Herías *et al*., 2007). SP-D is known to have a major role in the adaptive immune response too, as it has been shown to be an important host defence component against respiratory pathogens and allergens. Therefore, it is likely that SP-D inactivation, under physiological conditions with multiple sites of cleavage or degradation results in reduced capacity to bind to pathogens or engage in agglutination with bacteria, which will ultimately lead to susceptibility to lung inflammation and infection due to the invasion of pathogens and lack of immune response elicited by SP-D (Kishore *et al*., 2002).

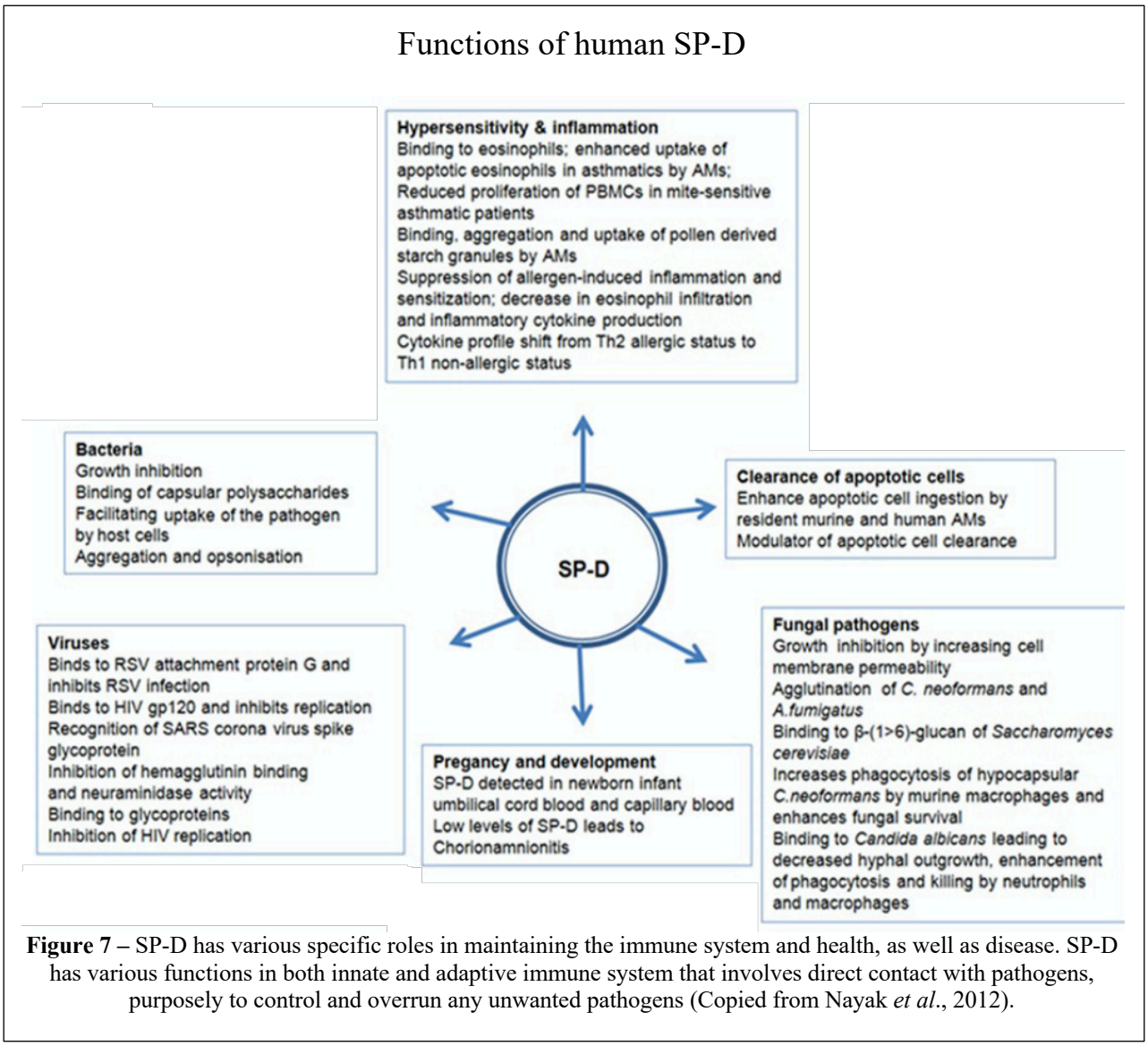

Figure 7 – SP-D has various specific roles in maintaining the immune system and health, as well as disease. SP-D has various functions in both innate and adaptive immune system that involves direct contact with pathogens, purposely to control and overrun any unwanted pathogens (Copied from Nayak *et al*., 2012).

There are various extrapulmonary tissues where its role is poorly understood such as kidney, human trachea, brain, testis, prostate and pancreas. It has been shown that SP-D deficiency in animal models are associated with significant clinical outcome in a number of infections. SP-D gene knockout mice showed fibrosis and chronic inflammation caused from the accumulation of surfactant phospholipids in the lungs, monocytes infiltration and activation of pro-inflammatory alveolar macrophages (Ikegami *et al*., 2005 and Wert *et al*., 2000).

In addition, the absence of SP-D in children increases their risk of frequent pneumonia, as compared to SP-D sufficient children (Griese *et al*., 2008). It has been shown from various studies that SP-D coding gene (SFTPD) polymorphisms leads to greater susceptibility to chronic and infectious lung disease, emphysema, tuberculosis, Crohn's disease and ulcerative colitis (Ishii *et al.*, 2012, Silveyra, 2012 and Tanaka *et al*., 2009). This represent the extent in

which SP-D contributes to the immune system and its contribution in preventing the development of diseases.

1.8.4 Endogenous role of human SP-D in allergy

Based on a study conducted by Tanaka (2009) used murine models possessed with allergic bronchopulmonary aspergillosis (ABPA) that had been induced by *Aspergillus fumigatus* (three-week culture filtrate antigens; 3-wcf) using the BALB/c (Bagg Albino, inbred research mouse strain) strain of mice shows fascinating data in relation to how SP-D can control and maintain allergic response. ABPA, known as allergic bronchopulmonary aspergillosis, is clinically characterized by episodic bronchial obstruction, positive immediate skin reactivity, elevated *A. fumigatus* specific IgG and IgE antibodies in serum, peripheral and pulmonary eosinophilia, expectoration of brown plugs or flecks and central bronchiectasis. Intranasal administration of rfhSP-D, three doses on consecutive days, revealed significant reduction in eosinophilia and specific antibody levels, as well as specific IgE levels and Th2 cytokines in the spleen. Lung sections dissected from allergic bronchopulmonary aspergillosis mice revealed extensive infiltration of lymphocytes and eosinophils that were significantly reduced following treatment. The levels of IL-2, IL-4 and IL-5 were also shown to have reduced significantly, while that of IFN-γ was raised in supernatants of the cultured spleen cells, indicating a marked Th2 to Th1 polarization of helper T-cell (Th) immune response (Mahajan *et al*., 2008). Further to this, similar protective effects of rfhSP-D have been observed in a murine model of lung allergy induced by Derp (Derp mice) as evident from significant decrease in Derp-specific IgE levels, blood eosinophilia and pulmonary cellular infiltration following therapy (Tanaka *et al*., 2009 and Madan *et al*., 2001).

Another study which associates the use of SP-D in allergy, involves intranasal administration of SP-D and rfhSP-D in a murine model of invasive pulmonary aspergillosis (IPA), immunosuppressed with hydrocortisone and challenged intranasally with *A. fumigatus* spores, has been shown to have protective effect. However, untreated IPA mice showed 100% mortality at 7 days. As a result of this study, the data shows that with treatment of rfhSP-D, it has managed to rescue ~80% of the mice (Madan *et al*., 2001). In accordance with this, a group of researchers build upon this idea and started to investigate the therapeutic effects of exogenous rfhSP-D (composed of eight GLy-X-Y collagen repeat sequences, homotrimeric neck and lectin domains) in murine models of lung allergy and eosinophilia SP-D gene-deficit mice (Mahajan *et al*., 2008). In this study, data strongly suggests that treatment with rfhSP-D down-regulates pulmonary and peripheral eosinophilia with murine models of allergy,

potentially rescuing hyper-eosinophilia in SP-D gene-deficient mice. Data from this study had also shown that the CRD region, located on SP-D, to be vital for its protective effects in ovalbumin-induced model of eosinophilic pulmonary inflammation, however in comparison to a mutant form of SP-D (altered CRD domain of SP-D) and SP-D knockout mice, had shown no effect, therefore this suggests strongly that the CRD is fundamental in this research using murine models (Mahajan *et al*., 2008). This study also assessed the possibility of a direct interaction with rfhSP-D and human eosinophils derived from allergic patients (symptomatic allergic asthma; termed as allergic patients) and healthy donors (Mahajan *et al*., 2008). In this study conducted by Mahajan (2008), rfhSP-D showed a sugar- and calcium-dependent binding to human eosinophils, which shows significant involvement of its carbohydrate recognition domain. Furthermore, rfhSP-D mediated an increase of apoptosis of primed (sensitised) eosinophils, while not affecting normal eosinophils and had increased phagocytosis of apoptotic eosinophils. The data from this study may be of significant importance depicting the significance of the mechanisms performed by rfhSP-D, and plausibly SP-D-mediated resolution of allergic eosinophilic inflammation in vivo (Mahajan *et al*., 2008).

1.8.5 Endogenous role of human SP-D in cancer

Human SP-D has shown to have a role in a variety of cancers, including leukaemia. An interesting study had used proteomics analysis on eosinophilic leukaemia cell line AML14.3D10 (model cell line for leukaemia) to detect protein expression patterns and functional protein networks to determine the underlying protein interaction with leukaemia. AML14.3D10 cell line was used mainly because it exhibits advanced eosinophilic differentiation and is the result of autocrine activation, particularly of intracellular cytokine, such as interleukin 3 and 5, signalling pathways by production of the endogenous granulocyte-macrophages colony-stimulating factor (GM-CSF), which is also known to be responsible for stimulating the cell line proliferation. The purpose of these two particular studies was to dissect the molecular mechanisms involving apoptosis induction by rfhSP-D. More specifically, understanding the immunomodulatory properties of SP-D, and how it can selectively induce apoptosis using primed eosinophils. Data from this study revealed various interesting points highlighting the role of SP-D in eosinophilic leukaemia cell line, one of which is an up-regulation of the p53 pathway (Mahajan *et al.*, 2013). Furthermore, as a result of this study, SP-D and rfhSP-D has both shown to induce G2/M phase of the cell cycle arrest, and time and dose-dependent apoptosis in AML13.3D10 eosinophilic leukaemia cell line. In addition, levels of a variety of apoptotic markers, including activated p53, cleaved caspase-9 and poly (ADP-

ribose) polymerase (PARP), as well as G2/M checkpoints including p21 and Tyr15 phosphorylation of cdc2, all showed an increase in levels in these cells. This indicate apoptotic activity and a tumour suppressive reaction. Mahajan *et al.*, (2013) had used proteomic analysis to explain the underlying mechanisms of rfhSP-D induced apoptosis. For the first time, this analysis revealed changes initiated by SP-D in a human cell. These changes include a decreased in survival related proteins, such as high mobility group box 1 (HMGA1) protein, also reported was an increase in proteins involved in protecting the cell from oxidative burst, and a decrease in proteins involved in mitochondrial antioxidant defence system. Furthermore, rfhSP-D mediated enhanced oxidative burst in the cell line, AML14.3D10, while interestingly antioxidant, N-acetyl-L-cysteine, had shown to abrogate rfhSP-D induced apoptosis (Mahajan *et al.*, 2013). However, the results from this study suggests that rfhSP-D mediated reduced viability was only specific to the cell line used, and viability of human PBMCs from healthy controls was shown to be not affected. In this study, SP-D acts as an inducer of apoptosis in eosinophilic and other cancer cells and shown to enhance the apoptotic cell up-take by macrophages (Pandit *et al*., 2014). Furthermore, this study supports other related studies in the conclusion that SP-D is an integral component of human innate immune immunosurveillance against cancer cells. Therapeutic potential of rfhSP-D in eosinophilic leukaemia as well as other cancers is a growing interest and a potential novel approach strategy.

Complimenting this investigation, another study conducted by Kumai *et al*., (2019), have shown interesting results in ovarian cancer in relation to rfhSP-D treatment. In this study, they have demonstrated the treatment of rfhSP-D in ovarian cancer using cell line SK-OV-3. This cell line is extracted from the ascites of a Caucasian female diagnosed with ovarian cancer, with an ovarian serous cystadenocarcinoma. This cell line was used because SK-OV-3 are positive for many of the antigens used to identify cancers of epithelial origin. This includes vimentin (VIM), in which acts a positive control in some experiments and epithelial membrane antigen (EMA) and leucocyte common antigen (LCA). The study conducted by Kumai *et al*., (2019), just recently published data revealing interesting effects when treating ovarian cancer with rfhSP-D. rfhSP-D treated in SKOV3 cells, revealed a decrease in proliferation of tumorigenic cells, which compliments the anti-proliferative effects of rfhSP-D in cancer cells. In addition, decrease in velocity, distance and displacement was recorded when treating rfhSP-D in SKOV3 cells, this was compared to untreated cells. Findings from this study indicate that rfhSP-D elicits cytotoxic or cytostatic properties, as this is evident from inducing caspase 3 cleavage *in vitro*. These findings also compliment a study conducted by Mahajan *et al.*, (2013), in the proposition that rfhSP-D acts an anti-tumorigenic agent. The study conducted by Kumai

et al., (2019) also reveal that human SP-D is express in clear cell adenocarcinomas, serous adenocarcinoma, mucinous adenocarcinomas and endometrioid adenocarcinomas. This was validated by immunohistochemistry using tissue microarrays, whereby the expression of SP-D was unchanged in type or grade, but only an increase of expression was recorded from stage I to stage II. Further to this study, rfhSP-D treated SKOV3 cells shown to down regulate rapamycin-insensitive companion of mammalian target of rapamycin (RICTOR) and regulatory-associated protein of mTOR (RPTOR). RICTOR is a protein which is encoded by the human RICTOR gene and form an essential component with mTOR forming a complex which integrates nutrient and growth factor derived signals, which in turn regulates cell growth (Zhang et al., (2010). RICTOR and RPTOR form essential components of the signalling pathway that regulates cell growth, as well as a positive role in maintaining cell size and mTOR protein expression (Zhang et al., (2010). In turn, rfhSP-D downregulates RICTOR and RPTOR, up-regulates pro-apoptotic factors, such as Fas and tumour necrosis factor alpha (TNF- α) and activates caspase-3-cascade to induce apoptosis *in vitro*. This together leads to a decrease in cell motility and cellular proliferation. However, based on immunohistochemistry and quantitative real time polymerase chain reaction (qPCR) analysis, natural levels of human SP-D are shown to be overly expressed in ovarian cancer patients, serous cystadenocarcinoma, compared to healthy controls. Low human SP-D mRNA expression reported an improvement in overall survival and progression free survival compared to high SP-D mRNA expression. This was also reported in another study on non-small cell lung cancers (NSCLC), whereby an increase in SP-D mRNA expression in the lungs of NSCLC patients revealed poor outcome and correlated with metastasis (Chong *et al*., 2006). The data from these studies reveal a higher order of complexity in the function and regulation of human SP-D in cancer. In contrast, a study involving gastric, lung and breast cancers have reported lower expression of SP-D mRNA compared to a healthy control group. This study reported that in lung cancer, the presence of SP-D is associated with favourable prognosis. In contrast, in relation to breast and ovarian cancer, it is reported that the presence of SP-D is correlated to an unfavourable prognosis (Mangogna *et al*., 2018). The studies carried out in relation to cancer, suggest that SP-D acts in a cell and tissue specific manner, and it is dependent on the composition of the tumour microenvironment. Based on these observations, it is a necessity to provide a wider repertoire of clinical sample and cell lines, however, it is seen from these studies that SP-D has emerged to become a potential biomarker for ovarian cancer. More importantly, high levels SP-D in ovarian cancer associated with poor survival, along with *in vitro* effects of rfhSP-D is a fascinating discovery. A reason for this outcome is that SP-D in ovarian cancer tissues is non-

functional, as this is also observed with a recent study conducted by Murugaiah *et al*., (unpublished data) using breast cancer, whereby triple-positive breast cancer cell line secreted the non-functional form of SP-D, although the cell line still remain susceptible in undergoing apoptosis with the treatment of rfhSP-D. Based on the ovarian cancer study, another theory is that human SP-D that is seen to be overly expressed may be functionally active, however SP-D can bind to the components of the tumour microenvironment, this includes hyaluronic acid (HA). In relation to *in vitro* studies, it is shown that when SP-D interacts with HA, the protective effects of SP-D is shown to be negated.

Collectively, these previous studies have shown a similar conclusion on the influence of rfhSP-D in the control of pancreatic cancer, which has recently been examined by Kaur *et al.,* (2018). This study has reported the ability of rfhSP-D to stimulate apoptosis via TNF-α/Fas-mediated apoptosis pathway independent of the p53 status in human pancreatic adenocarcinoma. This study has used various types of pancreatic cell lines to record its findings, including using Panc-1 (p53; mutant), MiaPaCa-2 (p53; mutant), and Capan-2 (p53; wildtype) cell lines. Treatment of these cell lines with rfhSP-D for 24 h showed growth arrest in G1 cell cycle phase and triggered transcriptional upregulation of pro-apoptotic factors such as NF-κB and TNF-α. rfhSP-D treatment also upregulated pro-apoptotic marker Fas, which then activated caspase cascade, as evident from cleavage of caspase 8 and 3 at 48 h, followed by apoptosis of the cells. Based on these findings, rfhSP-D can be used to therapeutically target pancreatic cancer cells irrespective of their p53 phenotype (Kaur *et al*., 2018). In a more recent study, rfhSP-D have shown to supress epithelial-to-mesenchymal transition (EMT) in pancreatic cancer cell lines through inhibiting transforming growth factor beta (TGF-β) expression, leading to the reduction in invasive potential. Pancreatic cell lines that was used in this study includes, Panc-1 (pancreas-duct; epithelioid carcinoma), Capan-2 (pancreatic tissue; adenocarcinoma) and MiaPaCa-2 (epithelial cells from carcinoma). In addition to this finding, an interrupted signal transduction lead to a negative impact on the transcription of key mesenchymal genes, this was evident from a decrease in expression of Smad2/3 (signal transducers for receptors of TGF-β) in the cytoplasm in cells only treated with rfhSP-D, as opposed to untreated cells. This led to a downregulation, when treated with rfhSP-D, on the expression of Snail (promotes repression of adhesion molecules), Vimentin (cell adhesion molecule) and Zeb1 (inducer of EMT) (Kaur *et al*., 2018). This recent study collectively supplements similar findings with rfhSP-D in other studies relating to cancers in the light of repressing tumour growth, in this case through interrupting EMT. This study also forms a parallel conclusion and contributes with other relating studies in highlighting the role of SP-D

as a novel innate immune surveillance, where it supresses EMT by reducing TGF- β pathway in pancreatic cancer cells. Further to this point, a study used human lung adenocarcinoma cells (A549 cell line) were exogenously treated with rfhSP-D supresses epidermal growth factor (EGF) and effects the EGF signalling pathway by reducing EGF binding to its receptor, EGFR. The subsequent reaction induces reduction in cell proliferation, invasion and migration of the cancer cells, ultimately showing signs of anti-tumorigenic activity by repressing tumour growth and acting as a novel innate immune surveillance (Hasegawa *et al*., 2015).

In addition to previous studies, SP-D have shown to be expressed in prostate cancer tissues with higher tumour volume and Gleason score. A study conducted by Thakur *et al*., (2017), elicited the role of rfhSP-D in prostate cancer by using a range of various cell lines, including primary prostate cancer cells, including LNCaP (androgen-sensitive human prostate adenocarcinoma cells) and PC3 cell lines which do not express androgen receptor (AR) and prostate specific antigen (PSA) and their proliferation is independent of androgen. rfhSP-D was found to induce apoptosis both in PC3 and LNCaP cell lines in a dose and time dependent manner. Based on this study, it was shown that anti-prostate tumour effects using rfhSP-D, as a form of treatment, was recognised in isolated primary epithelial cells from prostate cancer patients. Interestingly, on normal prostate epithelial cells, using the similar concentrations of rfhSP-D, no adverse effects on viability were recorded. However, in LNCaP cells, rfhSP-D treatment up-regulated phospho p53 and transcripts of Bax and also reduced Bcl2 transcripts, therefore shown to cause p53 mediated apoptosis in this cell line. In PC3 cells, rfhSP-D induced apoptosis through reducing phosphor ERK1/2 levels and caused an increase bcl-2 associated agonist of cell death (BAD) transcript. BAD is a pro-apoptotic protein that orchestrates programme cell death. Further to this study, in both cell types, an increase in cytochrome C release was recorded upon treatment with rfhSP-D establishing the activation of intrinsic apoptotic (mitochondrial mediated) pathway. In addition, rfhSP-D induces a downregulation of Bcl-2, while upregulating p53 up-regulated modulator of apoptosis (PUMA) transcripts. A study has established that PUMA plays a vital role in inducing apoptosis initiated by the binding of nuclear p53 to specific sites on the PUMA promotor, a necessity for its tumour suppressive ability (Hasegawa *et al*., 2015). rfhSP-D induces apoptosis in prostate cancer tissues biopsies, confirmed after using terminal deoxynucleotidyl transferase-mediated dUTP nick-end labelling (TUNEL) apoptotic assay. Collectively, this study carried out on prostate cancer and using rfhSP-D as a form of treatment to the cells, has concluded similar findings from different cancers using rfhSP-D, which is that rfhSP-D has an integral role in immune

surveillance against prostate cancer, which has shown to be mediated by distinct mitochondrial apoptotic mechanisms (Thakur et al., 2017).

2. Research purpose

There is a growing body of evidence linking the impact of rfhSP-D as an therapeutic immunotherapy agent by inducing apoptosis in various malignancies, such as human lung epithelial cancer, leukaemia, prostate and pancreatic cancer. Due to the limitation of the current therapeutic intervention in MPM management, there is currently a need for an effective new form of treatment to reduce or prevent reoccurrences and reduce mortality rate. Current methods of treatment for MPM are not effective in eliminating this disease and reoccurrence rates are a huge factor. Currently, there is no cure nor there is a clear-cut form of treatment that will eradicate MPM despite the severity of this disease and the growing numbers of cases year-by-year. Therefore, a new form of treatment modality needs to be exploited in order to effectively overcome the growing cases of patients suffering from MPM, and most importantly prevent reoccurrences which is the main problem for patients. Studies have shown how SP-D can reduce cell proliferation, migration and invasion in cancer using *in vitro* studies. This has been shown in human lung adenocarcinoma and other forms of cancer, and SP-D may also have the same effect in MPM, based on current research on rfhSP-D. MPM is of sarcomatoid and epithelial origin, rfhSP-D has been shown to induce apoptosis and reduce tumorigenesis in epithelial tissue from ovarian, lung and pancreas with *in vitro* studies, and may have the same suppressive effects in the tumour.

2.1 Hypothesis

Given the growing evidence of the pro-apoptotic effects of rfhSP-D in lung adenocarcinoma, ovarian, leukaemia, prostate and pancreatic cancer, as well as breast cancer (unpublished data), the hypothesis of this study is that rfhSP-D has pro-apoptotic effects on MPM cell lines. Provided that MPM is closely associated with the lungs, and rfhSP-D has binding ability to MPM cells, this provides an interesting area of research to test the hypothesis. In order to test the hypothesis, the overall aim was to:

2.2 Overall Aim

In this area of research I propose to understand the effects of rfhSP-D in MPM cell lines. In order to achieve this and my hypothesis, my overall aim is to investigate if rfhSP-D has anti- or pro-apoptotic effects on MPM cell lines.

2.3 Specific Objectives

The first objective of my project is to examine if human SP-D is present in a range of MPM tissue and cells. This will involve examining human MPM biopsies surgically extracted directly from patients and carrying out immunohistochemistry to establish the presence of human SP-D. Secondly, I intend to express and purify a recombinant form of human SP-D, also known as rfhSP-D. Thirdly, i intend to use a repertoire of laboratory techniques to establish the anti- or pro-apoptotic effects of this rfhSP-D on MPM cell lines.

3. Methods and Materials

3.1 Cell Culture and Treatments

This stage was carried out by myself at the University of Trieste, Italy for which I had close supervision from Dr Roberta Bulla. Mesothelioma cells were isolated from pleural biopsy specimens at the University Hospital of Trieste, Italy. This was carried out in accordance with the recommendations of governmental guidelines and approved by the CEUR (Comitato Etico Unico Regionale, FVG, Italy; number 34/2016), with written informed consent from human subjects, and all subjects gave written informed consent in accordance with the Declaration of Helsinki. Prior to isolating cells, the tissue was finely sliced into smaller sections and shredded using a sterilized scalpel, and incubated with digestion solution containing only 0.5% trypsin (sigma-Aldrich, Milan, Italy) and 50 μg/ml DNase I (Roche, Milan, Italy) in Hanks Balanced Salt solution with Ca^{2+} Mg^{2+} (0.5 mM) (Sigma-Aldrich) overnight at 4 °C. This was followed by replacing the enzymatic solution with collagenase type 1 (3 mg/ml) (Worthington Biochemical Corporation, DBA) diluted in Medium 199 with Hank's salts (Euroclone Spa, Milan, Italy) for 30 min at 37°C in 5% v/v CO_2. 10% fetal bovine serum (FBS, Gibco, Life Technology) was used to block further digestion, and cell suspension was filtered through a 100 μm pore filter (BD Bioscience, Italy). The cells were cultured using 45% Roswell Park Memorial Institute (RPMI) medium 1640 with GlutaMAX (Life Technologies, Milan, Italy), 45% human endothelial cells serum-free medium (HESF, Life Technologies), 10% FBS (heat-

inactivated) heated to 56°C for 30 min to inactivate complement (reduce unwanted influence) and supplemented with epidermal growth factor (EGF) (5 ng/ml), basic fibroblast growth factor (FGF) (10 ng/ml), and 5% penicillin-streptomycin (Sigma-Aldrich). MES 6, 8 2, and 16 (Primary tumour MPM cell lines, isolated from MPM biopsies) cells were used at their five to eight passages for all *in vitro* experiments.

A human lung biphasic (sarcomatoid and epithelioid phenotype) mesothelioma cell line, MSTO (ATCC, Rockville, MD, USA) (mesothelioma tumour cell line), derived from metastatic site of pleural effusion, was used as an *in vitro* model for fibroblast MPM. Cells were cultured in RPMI-1640 media containing 10% v/v FBS, 2 mM L-glutamine, and penicillin (100 U/ml) / streptomycin (100 μg/ml) (ThermoFisher). Cells were incubated at 37°C with 5% v/v CO_2 until cells reach 80-90% confluency (normally within 48 hours).

Human pleural fluids obtained from normal non-cancerous individual cell line, MeT-5A (ATCC, Rockville, MD, USA) (normal mesothelial) derived from mesothelium, and was used *in vitro* model for epithelial malignant pleural mesothelium. Cells were cultured in human endothelial serum free medium containing 10% v/v fetal bovine serum (FBS), 2 mM L-glutamine, and penicillin (100 U/ml)/ streptomycin (100 μg/ml) (ThermoFisher), and 20 ng/mL of fibroblast growth factor (FGF), and 10 ng/mL of human epidermal growth factor (EGF). Cells were incubated at 37°C with 5% v/v CO_2 until cells reach 80-90% confluency (normally within 48 hours).

3.2 Immunohistochemical analysis using in human MPM

This stage was carried out at the University of Trieste, Italy with the supervision of Dr Roberta Bulla. The tissue samples collected from patients suffering from MPM and who have been exposed to asbestos, include malignant pleural mesothelioma biphasic (Mes2), epithelioid (Mes6) and sarcomatoid (Mes8), attained from pleural effusions and biopsies. The samples of different MPM histotypes were fixed in 10% buffered formalin and paraffine embedded. The sections were initially fixed with xylene, subsequently with 100% ethanol (EtOH) and 95% EtOH. The sections were then dipped into a coplin-staining jar containing Tris (pH 9) buffer and ethylenediaminetetraacetic acid (EDTA) (1X pH 9), which were then dipped into a slide hybridization system chamber (HyChrome Euro lane) for 10 minutes at 90℃. The sections were then kept at room temperature to cool for 30 minutes. The sections were transferred into a jar containing distilled H_2O for 3 minutes, and into 1X tris-buffered saline (TBS) (dH_2O and 20% of 5X TBS pH 7.6) two times, each for 5 min. The slides were then transferred into 3%

H_2O_2 (hydrogen peroxide) for 5 min, and finally, washed with 1X TBS twice each for 5 min. The sections were then incubated with phosphate-buffered saline (PBS) + 2% w/v BSA + 4% w/v casein for 20 min, in order to block non-specific sites, and then probed with primary rabbit anti-human SP-D polyclonal antibodies (MRC Immunochemistry Unit, Oxford) (polyclonal) (1:300) overnight at 4 ℃. The bound antibodies were visualised using the Vectastain Elite ABC® (Vector Laboratories®, DBA, Italy). Secondary antibodies (Biotinylated secondary antibody solution; VECTASTAIN® Elite ABC kit) were added and incubated for 30 min, this was detected by DAB (3, 3 -diaminobenzidine) HRP substrate. Before adding DAB, the slides were washed with 1X TBS, twice each for 5 min and briefly air dried and ABC Reagent (VECTASTAIN®) was applied onto each section at room temperature for 30 min. The sections were then washed with 1XTBS, twice each for 5 min. After washing the sections were incubated with 3,3'-Diaminobenzidine (DAB). The sections were subsequently counterstained with haematoxylin (Dako®). Slides were examined using a Leica® DM 3000 optical microscope and images were extracted using a Leica® DF320 digital camera (Leica Microsystems®, Wetzlar, Germany).

3.3 Fluorescence Microscopy

This stage was carried out at Brunel University London with the supervision of Dr Uday Kishore. MSTO cells (0.5 x 105) were grown on coverslips, in a 12-well plate, overnight for 24 hours (37°C with 5% v/v CO_2) and incubated with recombinant rfhSP-D (10 µg/ml) in serum-free Roswell Park Memorial Institute (RPMI) media 1640 (without FBS) each well containing the coverslips for 1 hour at 4°C. This is to analyse cell binding of rfhSP-D to the cell line. The coverslips were washed three times with PBS and then incubated for 1 hour with primary rabbit anti- human SP-D polyclonal antibody (MRC Immunochemistry Unit, Oxford) (1:2000 dilution) at 4°C. Coverslips were washed three times with PBS, and then incubated for 1 hour with secondary antibodies (Alexa Flour® 488; 1:200, Thermo Fisher) and Hoechst (1:1000, Thermo Fisher) for immunofluorescence analysis at 4°C. Coverslips were washed three time with PBS, and then fixed using 2% paraformaldehyde (PFA) for 1 minute, followed by washing with PBS three times; images were extracted using a fluorescence light microscope (Leica®, DM4000 microscope).

3.4 Determine the presence of human SP-D from the supernatant of MSTO cell line

This stage was carried out at Brunel University London with the supervision of Dr Uday Kishore. Supernatant from MSTO cell line (50 ml) was collected after 24 hours of culturing and stored at -20°C. 50 ml of supernatant was dialysed against one litre of calcium/affinity buffer (50 mM Tris-HCL pH 7.5, 100 mM NaCl and 5 mM $CaCl_2$) overnight at 4°C. The dialysate was passed through a maltose-agarose column (5 ml) (Sigma-Aldrich) (equilibration in affinity buffer), before being wash once with 1 M Salt buffer (50 mM Tris-HCL pH 7.5, 100 mM NaCl and 10 mM $CaCl_2$) and calcium/affinity buffer. After passing the supernatant through the column, the column was then washed once again with 1 M Salt buffer and calcium/affinity buffer. 50 ml of Elution buffer (10 mM EDTA, 100 mM NaCl and 50 mM Tris-HCL) was then passed through the column and collected using Eppendorf tubes (Thermo Fisher). The optical density (OD) was taken (240 nm) for each Eppendorf tube, containing the eluted fractions. To confirm the presence of human SP-D a western blot was performed using the method described earlier.

3.5 Transformation of E. coli cells

This stage and the following subsequent stages in this methods and material sections was carried out at Brunel University London with the supervision of Dr Uday Kishore. Firstly, competent cells needs to be achieved to incorporate the plasmid followed by transformation, this is done by using plasmid pUK-D1, containing cDNA sequences for eight Glycine-X-Y amino acid triplets, the α-helical coiled-coil neck and CRD region of human SP-D, under bacteriophage T7 promoter to express the recombinant form of human SP-D (rfhSP-D) (Dodagatta-Marri *et al*., 2014; Singh *et al*., 2003) (177 residues: Gly179 to Phe355) transformed into *Escherichia coli* BL21 (λDE3) pLysS (Invitrogen™). The expression cassette included eight N-terminal Gly-X-Y triplets with substitution of S for P in position 2, residue 180, followed by the alpha-helical coiled-coil neck region (protein structure; amino acid residue from 203-235) and the globular CRD region (protein structure; amino acid residue from residue 236-355).

Initially, a single colony of grown BL21 (λDE3) pLysS (Invitrogen™) in a petri-dish (agar plate), the day before, was inoculated into a new petri-dish containing 10 ml Luria broth (LB) (Invitrogen™ miller's LB broth base; tryptone, yeast extract and sodium chloride) supplemented with chloramphenicol (50 μg/ml) (Gibco®, MA, USA) and ampicillin (50 μg/ml) (Gibco®, MA, USA) and incubated overnight in a 37°C shaker at 2000 rpm. The

following day, 500 µl of primary inoculum was transferred into 25 ml LB medium (Invitrogen™) containing 100 µg/ml of chloramphenicol and ampicillin (50 µg/ml) (Gibco®, MA, USA). This was incubated for 3 hours at 37°C incubator, constant shaking at 200 rpm, for cells to grow to log phase indicated by 0.3 - 0.4 optical density (OD) against plain LB medium at 600 nm. After reaching 0.3 – 0.4 optical density (OD), the sample was centrifuged (3000 rpm for 10mins) to collect BL21 (λDE3) pLysS cells to pellet. The supernatant was discarded the pellet was resuspended in 12.5 ml of 0.1 M $CaCl_2$. The resuspended pellet was incubated on ice for 1 hour. After incubating on ice, the cells were then centrifuged at low speed centrifugation (2000 rpm) for 5 mins to form a pellet. After centrifugation, the supernatant was discarded and the pellet containing cells was resuspended in 2 ml of 0.1 M $CaCl_2$. Competent cells are achieved through this process.

After achieving competent cells, 200 µl of competent cells was transferred into a sterile 2 ml Eppendorf tube and 100 ng of specific plasmid (pUK-D1 containing cDNA sequences for 8 Gly-X-Y triplets, the α-helical coiled-coil neck and CRD region of human SP-D) was added, before mixing thoroughly. This was mixed again by flicking the tube to allow DNA to enter the competent cells followed by incubation on ice for 1 hour before applying heat shock at 42°C for 2 minutes to allow transfer of DNA material. The nuclear pore was closed by transferring the tube to ice for 5 minutes. Followed by adding 800 µl of LB medium to the cells and placed in an incubator at 37°C for 45 mins, to allow 1 complete cell cycle replication to take place. 100 µl of competent cells was spread on a LB agar plate (containing ampicillin; 50 µg/ml, and chloramphenicol 50 µg/ml) (Gibco®, MA, USA).

Note: After transformation, cells were streaked onto agar containing ampicillin plates and chloramphenicol and allowed to grow overnight in an incubator (37°C). The next day the culture were inoculated and colonies taken and placed in LB media (containing ampicillin; 50 µg/ml, and chloramphenicol 50 µg/ml) (Gibco®, MA, USA).

3.6 Pilot Scale

The expression cassette included a short stretch of triple collagen helix of eight repetitious amino acid sequence Glycine-X-Y repeat (where X and Y are frequent proline and hydroxyproline) followed by the α-helical coiled-coil neck region (residues 203–235) and the globular CRD region (residues 236–355). A primary inoculum of 30 ml bacterial culture, grown in LB (50 µg/ml ampicillin, 50 µg/ml chloramphenicol) overnight in a shaking culture at 37°C, was then inoculated into 500 ml LB (50 µg/ml of ampicillin and 50 µg/ml

of chloramphenicol) and grown to A_{600} of 0.6–0.8 (OD). Cells were induced with 0.5 M isoproyl-β-thiogalactoside (IPTG) (Sigma-Aldrich, UK) for 3h at incubator (37°C), followed by centrifugation at 4°C (5000 rpm) for 10 minutes. After centrifugation, the supernatant was discarded, and the formed pellet was kept and analysed on a sodium dodecyl sulphate-polyacrylamide gel electrophoresis (SDS-PAGE) gel; this is a quality control check to determine whether rfhSP-D was formed, also used to establish whether the transformation process was successful by observing bands at 20 kDa (representing rfhSP-D) on the SDS-PAGE gel.

3.7 Large-scale expression and purification of rfhSP-D

After determining whether the transformation process was successful using SDS-PAGE, the remaining pellet undergone lysis and sonication of the insoluble proteins in inclusion bodies; the cell pellet was re-suspended in the lysis buffer (50 mM Tris–HCl pH 7.5, 200 mM NaCl, 5 mM EDTA, 0.1% v/v Triton X-100, 0.1 mM phenylmethylsulfonylfluoride (PMSF) (Sigma-Aldrich, UK), pH 7.5, and 50 μg/ml lysozyme (Sigma-Aldrich, UK) and sonicated 15 cycles at 40 kHz for 30 seconds with 2-minute intervals. All stages of sonication were carried out on ice to prevent proteins denaturing. The sonicated sample underwent centrifugation using a high-speed centrifuge at 13,000 rpm for 10 min to collect protein rich pellet.

After centrifugation, the recovered pellet was solubilized in 50 ml buffer I (50 mM Tris–HCl, pH 7.5, 100 mM NaCl, 10 mM β-merceptoethanol, and 8 M urea) (Sigma-Aldrich®, UK) for 1 hour at 4°C (add magnetic stirrer to maintain constant movement). After solubilising, this was then poured into a dialysis bag and dialysed (Biodesign™ cellulose dialysis tubing roll) stepwise against buffer 1 containing 4 M urea for 2 hours, then with buffer 1 containing 2 M urea for 2 hours, and then with buffer 1 containing 1 M urea for 2 hours, and finally with buffer 1 without urea overnight at 4°C. Each step contains buffer 1 with varying urea concentrations and incubated for 2 hours each, constantly stirring using a magnetic stirrer. Finally, after overnight incubation with buffer 1 without urea, dialysis with affinity buffer (50 mM Tris-HCL pH 7.5, 10 mM NaCl and 5 mM $CaCl_2$) for 48 hours stirring at 4°C. The dialysate was then centrifuged using a high-speed centrifuge (12,000 rpm for 15 minutes). The following day, the proteins were purified by affinity chromatography on a maltose-agarose column.

The rfhSP-D created was then loaded onto a maltose-agarose column (Pierce™, Thermo Fisher), before being washed extensively with 20 ml of 1 M salt buffer (50 mM Tris-

HCL pH 7.5, 1000 mM NaCl and 10 mM $CaCl_2$, pH 7.5) followed by 20 ml of affinity buffer (50 mM Tris-HCL pH 7.5, 10 mM NaCl and 5 mM $CaCl_2$). The maltose–agarose column (Pierce™, Thermo Fisher), was washed extensively again with 20 ml of 1 M salt buffer (50 mM Tris-HCL pH 7.5, 100 mM NaCl and 10 mM $CaCl_2$, pH 7.5) followed by 20 ml of affinity buffer (50 mM Tris-HCL pH 7.5, 10 mM NaCl and 5 mM $CaCl_2$) and the bound rfhSP-D was eluted with elution buffer (50 mM Tris-HCL pH 7.5, 100 mM NaCl and 10 mM EDTA, pH 8). As rfhSP-D binds to the maltose–agarose column (Pierce™, Thermo Fisher) and then eluted with 10 mM EDTA (pH 8) confirms that rfhSP-D binds maltose in a calcium-dependent manner, and was used as a quality control measure prior to its use in the experiments to confirm that it is biologically active and able to bind via its CRD structure. Any unbound rfhSP-D will flow through and discarded as it is either biologically inactive or has not folded correctly, as it was unable to bind to the maltose agarose column. The rfhSP-D bound to maltose–agarose column was eluted using EDTA (pH 8). The OD_{280} was checked to obtain protein yield. After elution, 6 different batches of purified rfhSP-D were collected. A good batch of rfhSP-D will have an OD (A_{280}) reading of between 0.6 – 0.8. This was measured using a spectrophotometer at 280 nm. The concentration of rfhSP-D protein was accurately measured using the bicinchoninic (BCA) colorimetric assay (Pierce™ BCA Protein Assay Kit; Fisher scientific®, UK), in which a standard curve is created based on a range of known BCA and bovine serum albumin (BSA) protein concentrations as a standard. The OD taken from samples containing rfhSP-D is read against the standard curve and the concentration is determined.

3.8 Endotoxin removal from rfhSP-D

The levels of endotoxin present in rfhSP-D sample preparation was further minimized by passing each sample through a spinning column containing endotoxin removal resin (Pierce™ high capacity endotoxin removal spin columns, Thermo Fisher™). The resin (Thermo Fisher™ Pierce™ High Capacity Endotoxin Removal Resin) contains porous cellulose beads modified to possess covalently attached ε-poly-L-lysine (polylysine). This modified attached polylysine possess a high affinity for endotoxins present in the rfhSP-D samples, which enables it to easily bind. The binding capacity of this resin is two million endotoxin units (EU) per ml, reducing endotoxin levels typically by 99%, below 5 EU/ml, which is of acceptable range. The resin and columns provided in the kit were followed as instructed based on the manufacturer's specification. Initially, the column containing the resin was regenerated by incubating it with five-resin-bed volumes (5ml) of 0.2N NaOH in 95% ethanol for 2 hours, at room temperature (22°C). After regenerating, the column was washed with five-resin-bed volumes (5ml) of 2M

NaCl, and then washed with 5ml of endotoxin-free ultrapure-water. After washing, the column was equilibrated by passing through 5ml of endotoxin-free buffer (0.2M NaCl containing Tris-HCl, pH 7.5). After equilibration, the samples were added into the column and tightly sealed and placed on a shaker at 5°C overnight. The next day, the flow-through was collected and proteins eluted from the column by adding two-resin-bed of endotoxin-free buffer (0.2M NaCl containing Tris-HCl, pH 7.5) at a flow rate of 10-15 ml/h, and collected into endotoxin-free tubes and stored at 5°C. The flow-through and the fractions of purified protein was run on 12% SDS-PAGE gel, to determine the presence of rfhSP-D and absence of endotoxins or background interferences. Endotoxins levels was then measured in each fraction collected using Limulus Amebocyte Lysate (LAL) assay (Thermo Fisher, Pierce™). After the endotoxin column was used, it was cleaned by 5ml of 0.2N NaOH in 95% ethanol for 2 hours at room temperature (22°C). Five-resin-bed volumes of 2M NaCl followed by 5-resin-bed volumes of endotoxin-free ultrapure water was then passed through the column containing the resin, and stored in 20% ethanol at 5°C.

3.9 Limulus Amebocyte Lysate (LAL) assay to detect LPS in samples

An endotoxin chromogenic LAL assay kit (ToxinSensor™ Chromogenic Endotoxin Assay Kit) was used to quantify endotoxins levels present in various fractions collected during large scale purification of rfhSP-D. It is used as a quantitative *in-vitro* test for gram-negative bacterial endotoxin. LAL reagent is used as it causes the protein sample to change colour to yellow, as it reacts with the liposaccharide (LPS) present, and the optical density is measured using a spectrophotometer at 545 nm. Once LAL is bound to endotoxins, the concentration is then measured by attaining the OD_{545} for each sample, because the absorbance readings is in direct proportion to the endotoxin levels present, therefore the concentration can be deduced from a standard curve. The LAL is essential as it contains lyophilised lysate from Limulus Polyphemus, extracted from blood cells from horseshoe crab, has a fundamental property of being exquisitely sensitive to bacterial toxins and LPS. More specifically, LPS present in the fractions of purified rfhSP-D catalyses a pro-enzyme in LAL to an active enzyme. Once activated enzymes catalysis further reaction to split peptide nucleic acid (pNA). The release of this colour producing substrate from this reaction is detected and measured spectrophotometrically against a linear gradient, created using a range of known endotoxins standards (Maloney *et al*., 2018).

LAL reagent was prepared by reconstituting the lyophilised lysate present in the LAL reagent by adding 1.7 ml of LAL reagent water provided, and gently mixed for 30 seconds to

avoid foaming. This reconstituted lysate is stable when stored at -20°C for a maximum of one week.

Chromogenic substrate reconstituted by adding 1.7 ml of LAL reagent water to yield a concentration of ~2 mM and can be stored in dark for up to one month at 5°C to maintain its stability.

Stop solution was prepared by adding 10 ml of buffer S (follow manufactures specification; ToxinSensor™ Chromogenic Endotoxin Assay Kit) to Colour-stabiliser #1. It is stored at 5°C to maintain its stability for up to one week.

Colour stabiliser #1 and #2 was reconstituted by adding 10 ml of LAL reagent water to each and can be kept in 5°C for up to one week.

The endotoxin standard stock solution was prepared by adding 2 ml of LAL reagent water and mixed thoroughly for 15 min using a vortex. The stock is stable for up to one week when stored at 5°C. After preparing 1 EU/ml endotoxin solution from the stock solution, four endotoxin standard solution was made from the 1 EU/ml endotoxin solution, ranging from 0.1 – 0.01 EU/ml, by serial dilution using LAL reagent water, this was then used to generate the standard curve by obtaining the OD_{545}. A blank was used only containing LAL water reagent, to determine false positive results and to detect any background interferences.

After preparing all reagents, 100 µl of samples was added to individual endotoxin-free vials (ToxinSensor™) and mixed thoroughly using a vortex to prevent any foam forming. This included a blank, only containing LAL reagent water instead of the test sample. After mixing, 100 µl of reconstituted LAL, prepared earlier, was added to each vial containing the test samples, a mixed thoroughly. The vials were then incubated at 37°C for T1 using a water bath. After incubation, 100 µl of reconstituted chromogenic substrate solution was added to each individual vial and swirled gently, not mixed or shaken, followed by incubation at 37°C for 6 minutes. After incubating with chromogenic substrate solution, 500 µl of reconstituted colour-stabiliser #1 to each vial and swirled gently, and then 500 µl of reconstituted colour-stabiliser #2 was added to each vial and swirled gently. And finally, 500 µl of reconstituted colour-stabiliser #3 was added to each vial and gently swirled. The absorbance of each vial was read using a spectrophotometer at OD_{545}, after standardising the reader using a blank (distilled water) to zero absorbance.

The endotoxin levels of each vial containing rfhSP-D was found to be insignificant (~ 4 pg/µg). The assay carried out was linear over a range of 0.01 – 0.1 EU/ml (10 EU = 1 ng of endotoxin) as determined by limulus amebocyte lysate (LAL) test. The amount of endotoxin

present in all rfhSP-D batches made throughout this study was found to be ~ 4 pg/µg of rfhSP-D.

3.10 SDS-PAGE

A 15% v/v Sodium dodecyl sulfate-polyacrylamide gel electrophoresis (SDS-PAGE) was prepared, as a quality control stage, to observe the correct bands representing rfhSP-D (20 kDa) samples. Briefly, 20 µL of one batch containing purified rfhSP-D (~600 µg/ml protein) was mixed with 2X treatment buffer (50 mM Tris pH 6.8, 2% β-merceptoethanol, 2% SDS, 0.1% bromophenol blue, and 10% glycerol) (Invitrogen®) and denatured by heating at 100°C for 10 min, using a standard heating block. Samples were then loaded onto the gel, cast as per measurement detailed in Table 1 and Table 2. Only 5 µl of unstained protein molecular weight protein marker (Thermo Fisher™ Pierce™) were loaded in the first lane (ladder) and 10 µl of each of the rfhSP-D samples were loaded in each well. Electrophoresis was performed at room temperature (22°C) for approximately 90 min using a constant voltage (120V) in solution of 1X running buffer (10% 10X running buffer, 10% SDS and distilled H_2O) (Invitrogen®) until the dye front reached the end of the 60 mm gel. The gel was then stained with staining solution (50% Methanol, 40% acetic acid with 0.1% Coomassie blue) (Thermo Fisher®) for 1 hour on a shaker, followed by de-staining (50% Methanol, 10% acetic acid and 40% distilled H_2O), overnight.

A 15% SDS-PAGE was prepared by making a 15% resolving gel followed by a stacking gel. The resolving gel is composed on various solutions as outlined on Table 1:

Table 1 – The exact recipe for preparing 15% resolving SDS- PAGE gel

Component (15% Resolving Gel)	Volume (µl)
De-ionised Water	1100
30% Acrylamide Mix	2500
1.5M Tris-HCL, pH 8.8	1300
10% sodium dodecyl sulfate (SDS)	50
10% Ammonium persulfate (APS)	50
Tetramethyl ethylenediamine (TEMED)	15

The resolving gel was left to polymerise at room temperature (22°C) for 10 minutes. Followed by making the stacking gel and loaded on top with a separating comb fixed in place. The stacking gel for all SDS-PAGE is various solutions outline on Table 2:

Table 2 – The exact recipe for preparing 15% resolving SDS-PAGE gel

Component (Stacking Gel)	Volume (µl)
De-ionised Water	2100
30% Acrylamide Mix	500
1M Tris-HCL, pH 6.8	380
10% sodium dodecyl sulfate (SDS)	30
10% Ammonium persulfate (APS)	30
Tetramethyl ethylenediamine (TEMED)	15

3.11 Western Blot

After making the SDS-PAGE (12% w/v), the separated proteins were then electrophorectically transferred onto a nitrocellulose membrane (Sigma®) using transfer buffer (25 mM Tris, 190 mM glycine, and 20% methanol, pH 7.5) for 3 hours at 320 mA. This is followed by blocking with 5 % w/v dried milk powder (Sigma®) in 100 ml PBS in room temperature (22°C) for 2 hours on a rotary shaker (200 rpm). The nitrocellulose membrane (Sigma®) was then washed with PBST (phosphate-buffered saline (PBS) + 0.05% Tween 20) three times (10 minutes each) and incubated with primary rabbit anti-human SP-D polyclonal antibody (1:1000 dilution) at room temperature (22°C) for 1 hour. The nitrocellulose membrane (Sigma®) was washed with PBST (three times, 10 minutes each) before being incubated with secondary antibody goat anti-rabbit IgG horseradish peroxide (HRP-conjugate) (1:1000 dilution; Thermo Fisher®) for 1 hour at room temperature. The bands were visualised using 3,3-diaminobenzidine (DAB) substrate (Sigma-Aldrich).

3.12 MTT Assay

MTT (3-(4,5-Dimethylthiazol-2-yl)-2,5-Diphenyltetrazolium Bromide) (ThermoFisher ® Invitrogen™) assay was carried out by incubating MSTO cells (0.5×10^5) in a 96-well microtiter plate, each well containing different concentrations of rfhSP-D (5 µg/ml, 10 µg/ml and 20 µg/ml) and a well containing untreated control in serum-free RPMI (without FBS)

medium for 24 hours and another plate for 46 hours of incubation (37°C and 5% v/v CO_2). After the incubation periods, 12 mM MTT (5 mg/ml stock) was added to per well and incubated for 4 hours at 37°C and 5% v/v CO_2. The plate was then gently tipped over a paper towel to remove most of the content of each well, and a total volume of 50 µl of dimethyl sulfoxide (DMSO) was added to each well and incubated for another 10 minutes at 37°C and 5% v/v CO_2. Avoid direct light exposure at all times. The final stage is to measure the optical density (OD) of each well at 540 nm using a multi-well spectrophotometer.

3.13 Flow cytometry

Cell lines were plated in three separate 6-well plates ($0.1x10^7$) and incubated with rfhSP-D (10, 20 and 40 µg/ml) and an untreated negative control (without rfhSP-D). One plate was incubated for 24 h, the second plate was incubated for 48 h and the third plate was incubated for 72 h (37°C with 5% v/v CO_2). After the incubation periods, cells was detached by using 5 mM EDTA, pH 8, and centrifuged (1200 x g for 5 min). Apoptotic analysis was carried out using flow cytometry, and fluorescein isothiocyanate (FITC) conjugated annexin V apoptosis detection kit with PI (BioLegend™) was used, as per manufacturer's instructions. After culturing MSTO cells and detaching using EDTA, cells was washed twice with cell staining buffer (BioLegend™) and resuspended in annexin V binding buffer at a concentration of 0.25-1.0 x 10 cells/ml. 100 µl of cell suspension was then transferred in each individual test tube (5 ml capacity test tube). 5 µl of FITC conjugated annexin V and 10 µl of propidium iodide (PI) solution was added to each of the test tube containing cells, followed by gently vertexing and incubation for 15 minutes at room temperature (22°C) in the dark. After incubation, 400 µl of annexin V binding buffer (BioLegend™) was added to each labelled tube. The samples in each labelled tube was then inserted into the flow cytometer (NovoCyte™; ACEA Biosciences Inc) and analysed using appropriate software (NovoExpress®). Compensation parameters were acquired using unstained, untreated FITC stained, and untreated PI stained cells was used to standardised data.

3.14 Statistical Analysis

GraphPad Prism (software V 7.04) was used to construct the graphs, and the statistical analysis was carried out using unpaired one-way ANOVA test and Tukey's range test (a multiple comparison analytical test) on data presented on Figure 20. Significance values were considered based on *$P < 0.0024$ (UT vs 5 µg/ml) and **$P < 0.0416$ (UT vs 20 µg/ml) between

the treated and untreated control conditions. **P < 0.0416 (UT vs 20 μg/ml) is considered as significant. A value of p < 0.05 was considered statistically significant. Error bars show the SD, as indicated on Figure 20.

4. Results

4.1 Human SP-D is present in panel of invasive Malignant Pleural Mesothelioma Specimens

The presence of human SP-D is clearly identified in all of the panel of invasive MPM specimens. This includes specimens of epithelioid (MES 6; Figure 9A, B, and C), biphasic (MES 2; Figure 8A, B and C) and sarcomatoid (MES 8; Figure 10A, B and C) histotypes. As shown on figure 8, 9 and 10, a strong detection of human SP-D is identified in all invasive tumour specimens examined, particularly in biphasic histotype (Figure 8), where SP-D shown to be more prominent. This is compared with the negative control (Figure 11). This is to ensure non-specific staining or background interferences was present and validates the images received from staining SP-D (Figure 8, 9, and 10).

MES 2 – MPM Biphasic

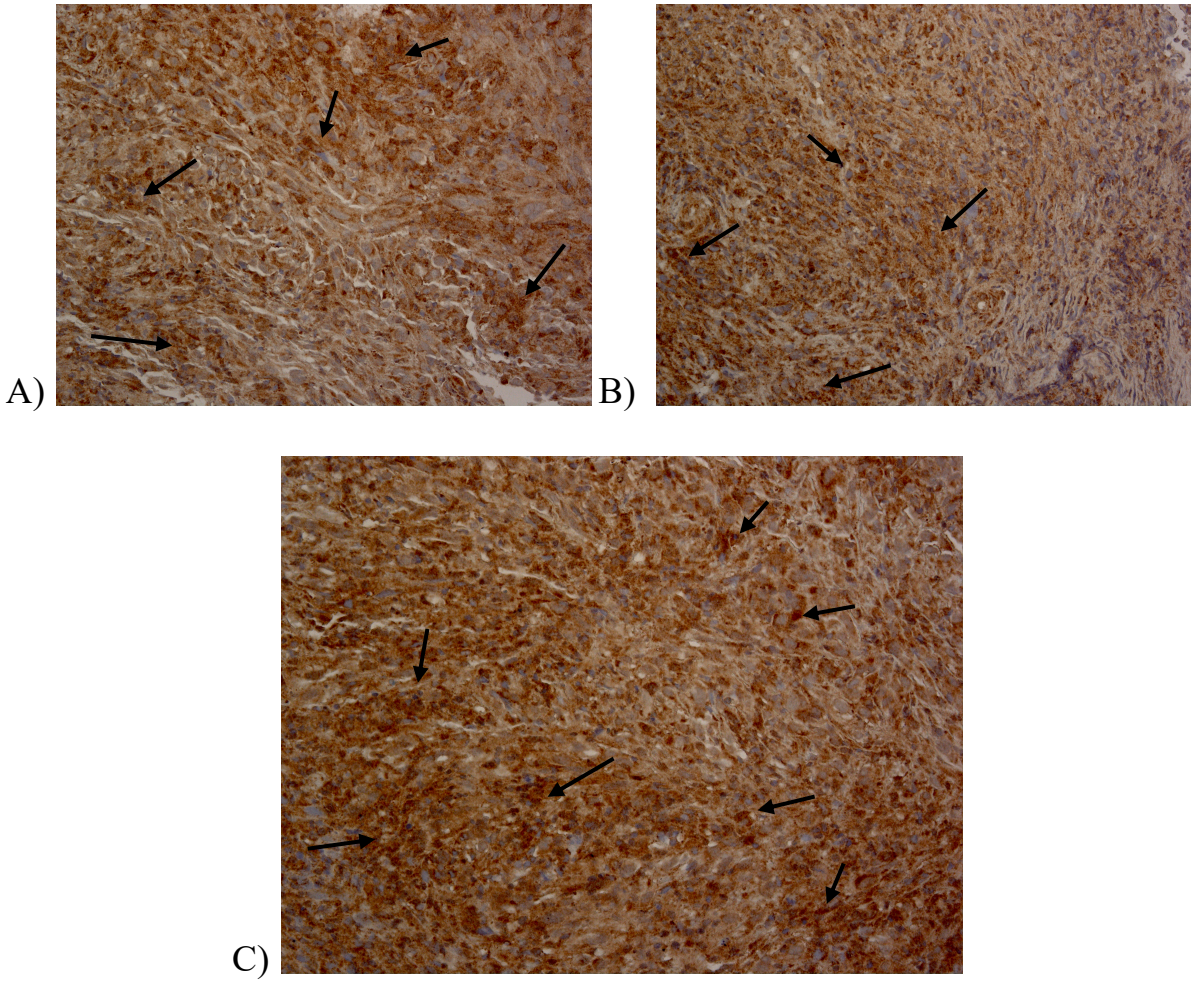

Figure 8: Immunohistochemical analysis at 100x (A) (B) and 200x (C) magnification showing SP-D (brown) in human mesothelioma (MPM) biphasic. A, B and C are biphasic type MPM, shown in different sections of the same tissue. SP-D shown as brown, see black arrows for guidance. Hematoxylin (deep blue/purple) stains the nucleus. Primary antibody - Anti-SP-D (1:300) polyclonal rabbit anti-human (MRC Immunochemistry Unit, Oxford). Secondary antibody - Biotinylated secondary antibody solution (Vectastein Elite ABC® kit (Vector Laboratories®, DBA, Italy). SP-D stained with DAB (3-3'-Diaminobenzidine) (brown).

MES 6 – MPM Epithelioid

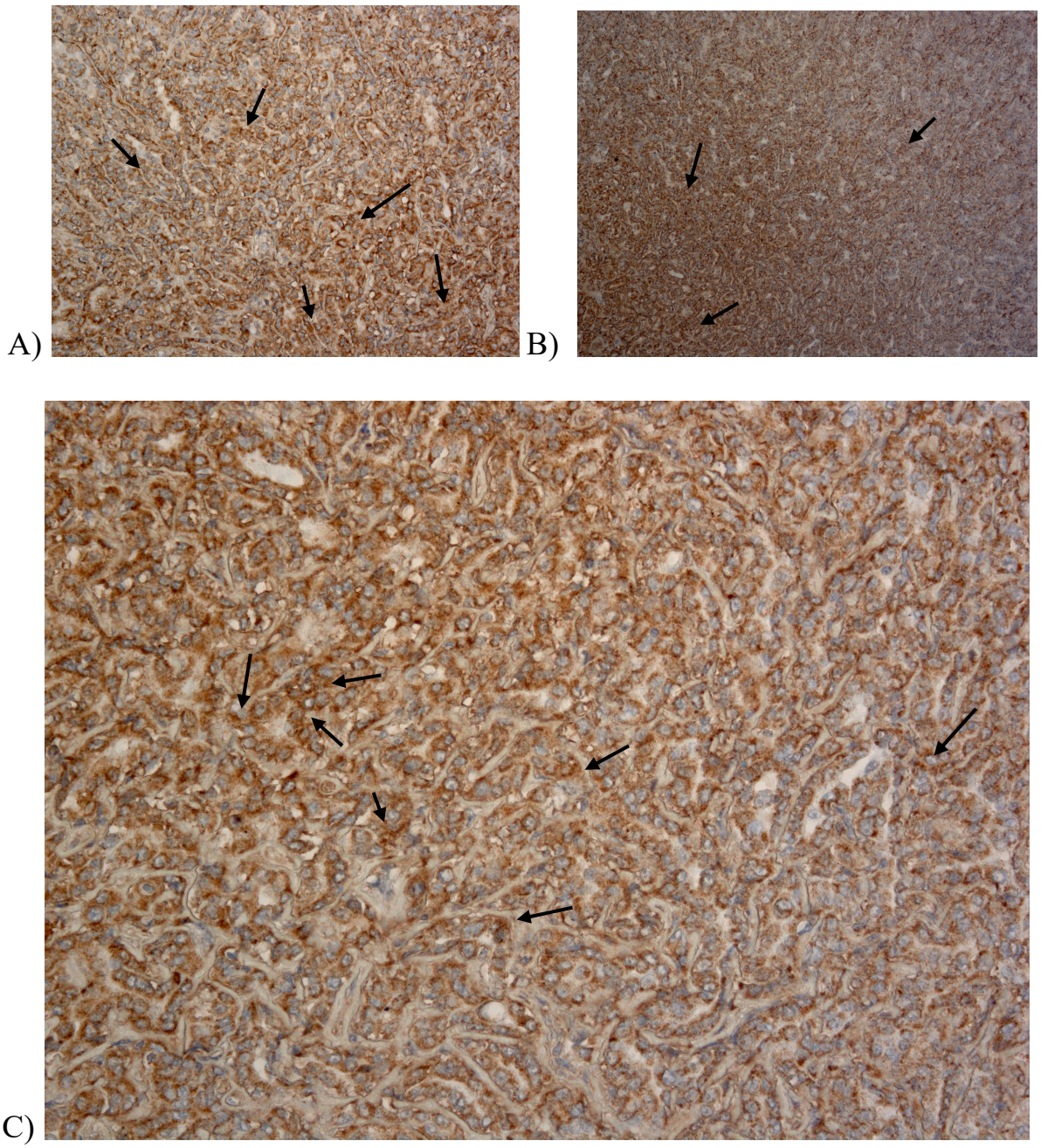

Figure 9: Immunohistochemical analysis at 100x (A), 40x (B) and 200x (C) magnification showing SP-D (brown) in human mesothelioma (MPM) epithelioid. A, B and C are epithelioid MPM, shown in different sections of the same tissue. SP-D shown as brown, see black arrows for guidance. Hematoxylin (deep blue/purple) stains the nucleus. Primary antibody - Anti-SP-D (1:300) polyclonal rabbit anti-human (MRC Immunochemistry Unit, Oxford). Secondary antibody - Biotinylated secondary antibody solution (Vectastein Elite ABC® kit (Vector Laboratories® DBA, Italy). SP-D stained with DAB (3-3'-Diaminobenzidine) (brown).

MES 8 – MPM Sarcomatoid

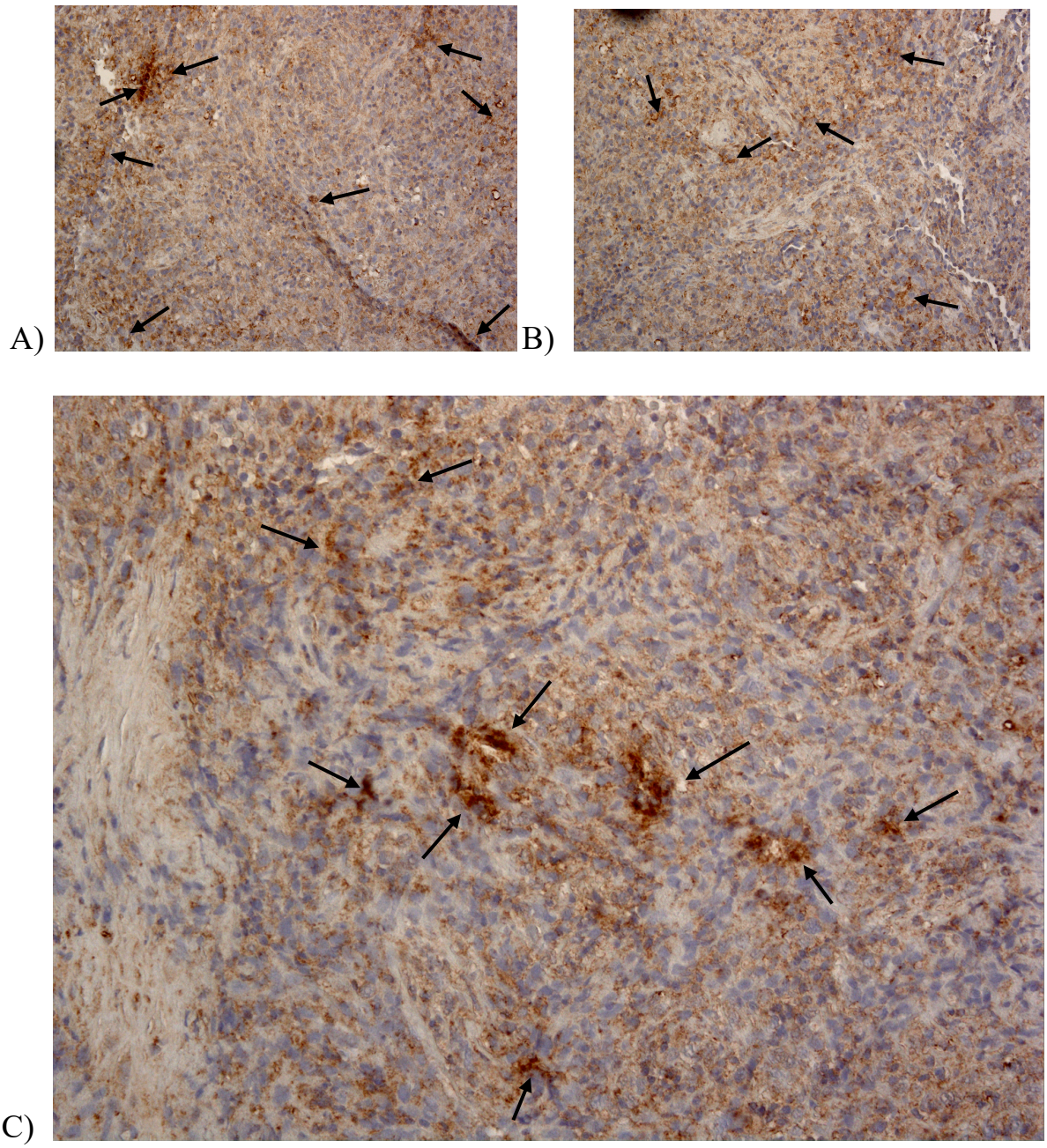

Figure 10: Immunohistochemical analysis at 100x (A) (B) and 200x (C) magnification showing SP-D (brown) in human mesothelioma (MPM) sarcomatoid. A, B and C are sarcomatoid MPM and shown in different sections of the same tissue. SP-D shown as brown see black arrows for guidance. Hematoxylin (deep blue/purple) stains the nucleus. Primary antibody - Anti-SP-D (1:300) polyclonal rabbit anti-human (MRC Immunochemistry Unit, Oxford). Secondary antibody - Biotinylated secondary antibody solution (Vectastein Elite ABC® kit (Vector Laboratories®, DBA, Italy). SP-D stained with DAB (3-3'-Diaminobenzidine) (brown).

Negative controls for human SP-D

A)

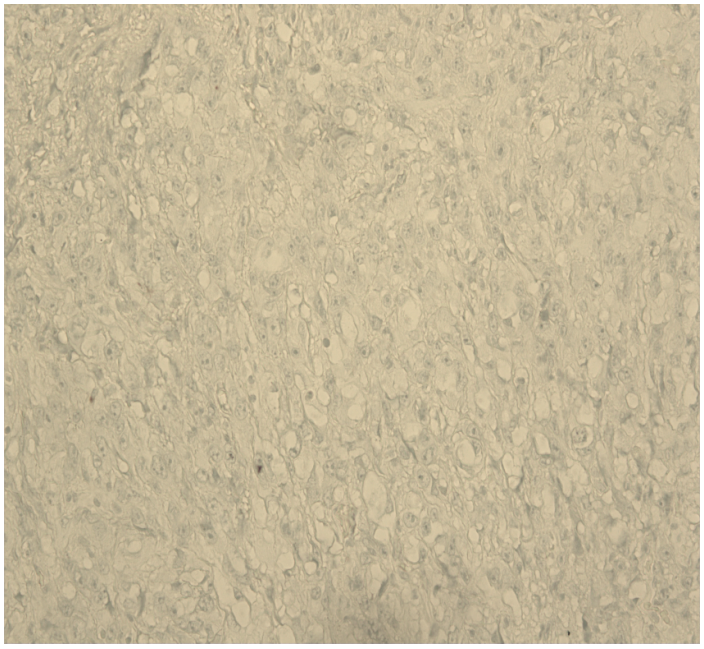

B)

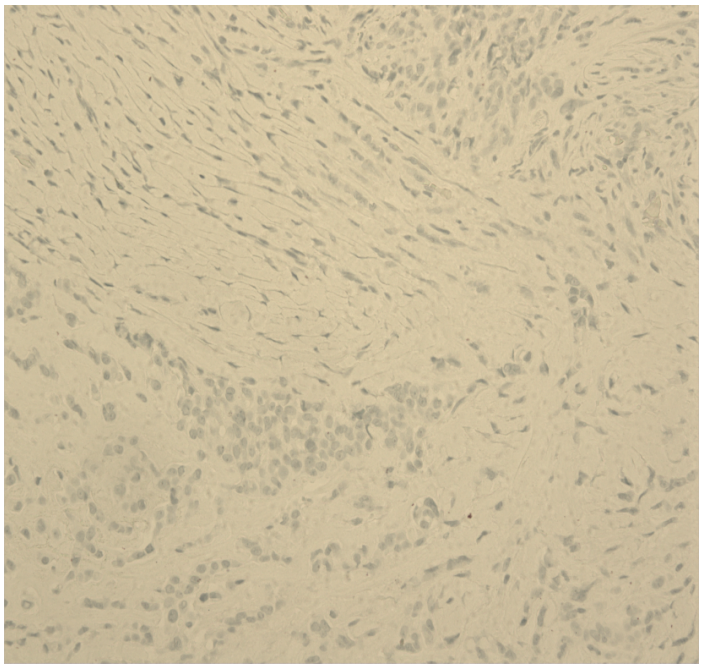

Figure 11: Negative control - Immunohistochemical at 100x magnification (A) (B). A and B showing the negative control in human mesothelioma (MPM). A) Epithelioid histotype of MPM. B) Biphasic histotype of MPM. Negative control - only Vectastain Elite ABC® kit and DAB was used in negative control – unrelated primary rabbit anti-human antibody was used; absent of the primary antibody - Anti-SP-D polyclonal rabbit anti-human. Secondary antibody - Biotinylated secondary antibody solution (Vectastein Elite ABC® kit (Vector Laboratories®, DBA, Italy). SP-D stained with DAB (3-3'-Diaminobenzidine) (brown).

After immunohistochemistry was established, immunofluorescence analysis was carried out to detect human SP-D in permeable malignant pleural mesothelioma tissue (Mes16) (Figure 12A and B). Calretinin was used as a control (Figure 12B), it is a calcium-binding protein, has been reported to be a selective marker for mesothelioma and largely is absent from adenocarcinoma on histologic material. There is a clear indication of the presence of SP-D (Figure 12A) in malignant pleural mesothelioma (MES 16). MES 16 is a primary MPM cancer cell line isolated from MPM biopsies. Its unique permeable membrane (MES 16) suggest SP-D is translocated outside the cells into the surrounding matrix.

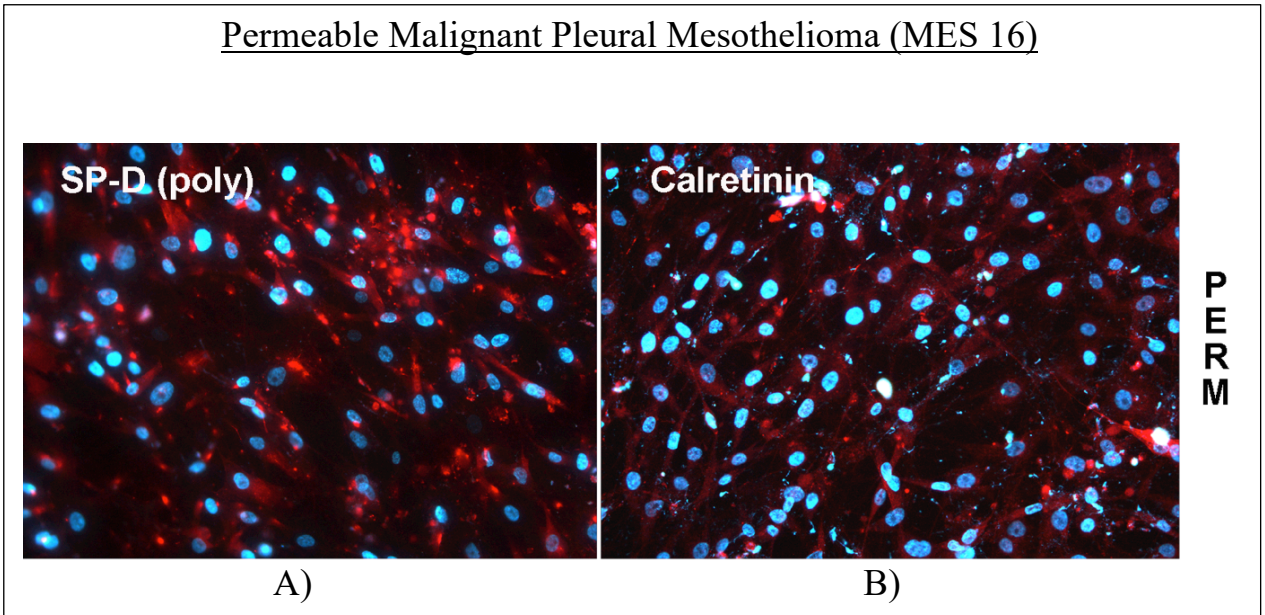

Figure 12: Immunofluorescence microscopy at 400x magnification on MES16 to establish the presence of human SP-D in MPM tissue. A) MPM tissue (MES 16). Primary antibody -polyclonal rabbit anti-human SP-D (MRC Immunochemistry Unit, Oxford) (1:200). Secondary antibody - Anti-rabbit (1:20000) (red). DAPI containing mounting medium was used for nuclear staining (light blue). B) Mesothelioma tissue (MES16). Primary antibody - Anti-calretinin antibody (1:20). Secondary antibody- rabbit anti-human (1:20) (red). DAPI containing mounting medium was used for nuclear staining (light blue).

Based on the IHC images (Figure 8, 9 and 10), it is clearly shown that SP-D is highly concentrated in MPM tissue of various histotypes. Spiral arteries are distinctively brown which strongly indicates SP-D positive, and the wall of the blood vessels as well as the mesothelioma cells are strongly stained with SP-D positive. Tumour growth is shown to be highly concentrated with SP-D compared to the surrounding tissue, further distant to the tumour growth, shown as light blue. Leucocytes infiltration and saturation is also observed in tumour growth (Figure 10C).

4.2 rfhSP-D binds to MSTO cell line

Immunofluorescence microscopy analysis was carried out to determine whether rfhSP-D (10 µg/ml) binds to MSTO (tumorigenic, MPM; blue fluorescence) cell line. Immunofluorescence microscopy revealed membrane localization of rfhSP-D followed by 1 h of incubation at 4°C (Figure 14). Figure 13 (negative control) presents MSTO cells (blue fluorescence; spheroid cells) incubated without rfhSP-D treatment, and no binding was observed. This is to determine presence of any background interferences or unexpected binding from other proteins, and essentially to validate the observation of rfhSP-D binding to MSTO cell line.

Immunofluorescence Microscopy - MSTO cell line
(Negative control - absence of rfhSP-D)

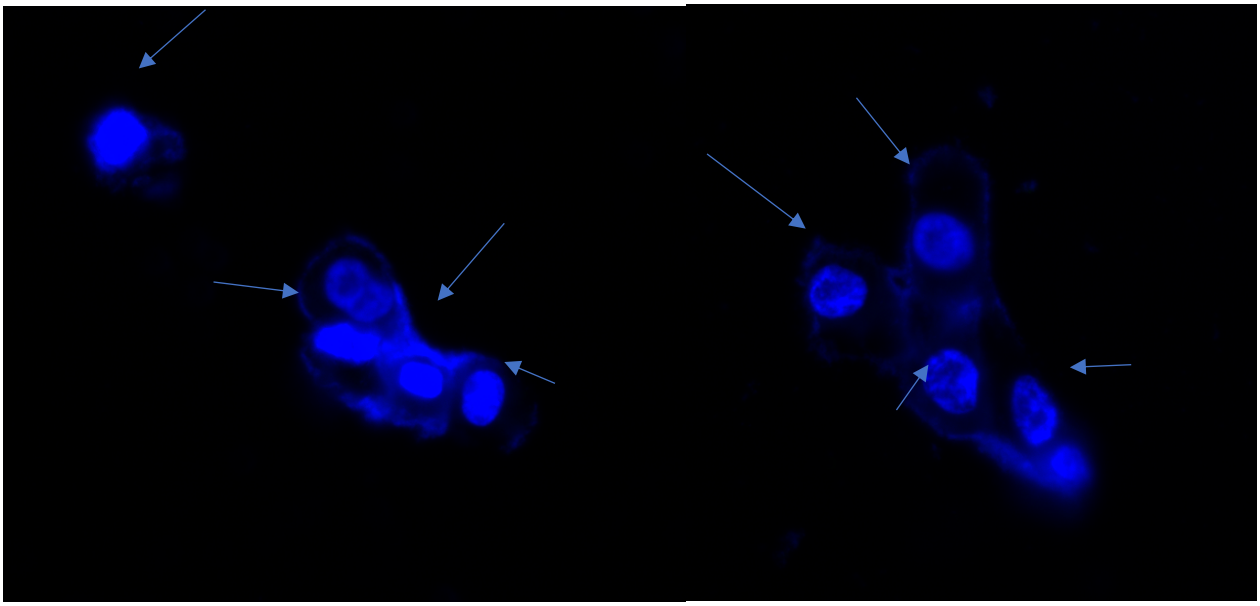

Figure 13: Immunofluorescence micrscopy at 1000x magnification– MSTO cell line (tumorigenic, MPM). Leica®, DM4000 microscope. The nucleus of the cells was stained with Hoechst (1:1000, Thermo Fisher®) (blue florescence; see blue arrows for guidance). The cells were probed with primary antibodies rabbit anti-human SP-D and with secondary antibodies Alexa Flour® 488 (1:200, Thermo Fisher®). Absence of rfhSP-D in this negative control experiment; to observe any false positive.

The rfhSP-D probed with primary human anti-rabbit SP-D followed by secondary antibody (Alexa Flour® 488 and Hoechst; ThermoFisher ® Invitrogen™). The binding of rfhSP-D to MSTO cells appeared evenly bound and distributed in clusters on the cell membrane (green fluorescence; yellow arrows Figure 14), along with nucleus stained positively with Hoechst (blue fluorescence) (Figure 14). A clear localised membrane binding of rfhSP-D to MSTO cell line are observed (Figure 14).

Immunofluorescence - MSTO cell line treated with rhSP-D

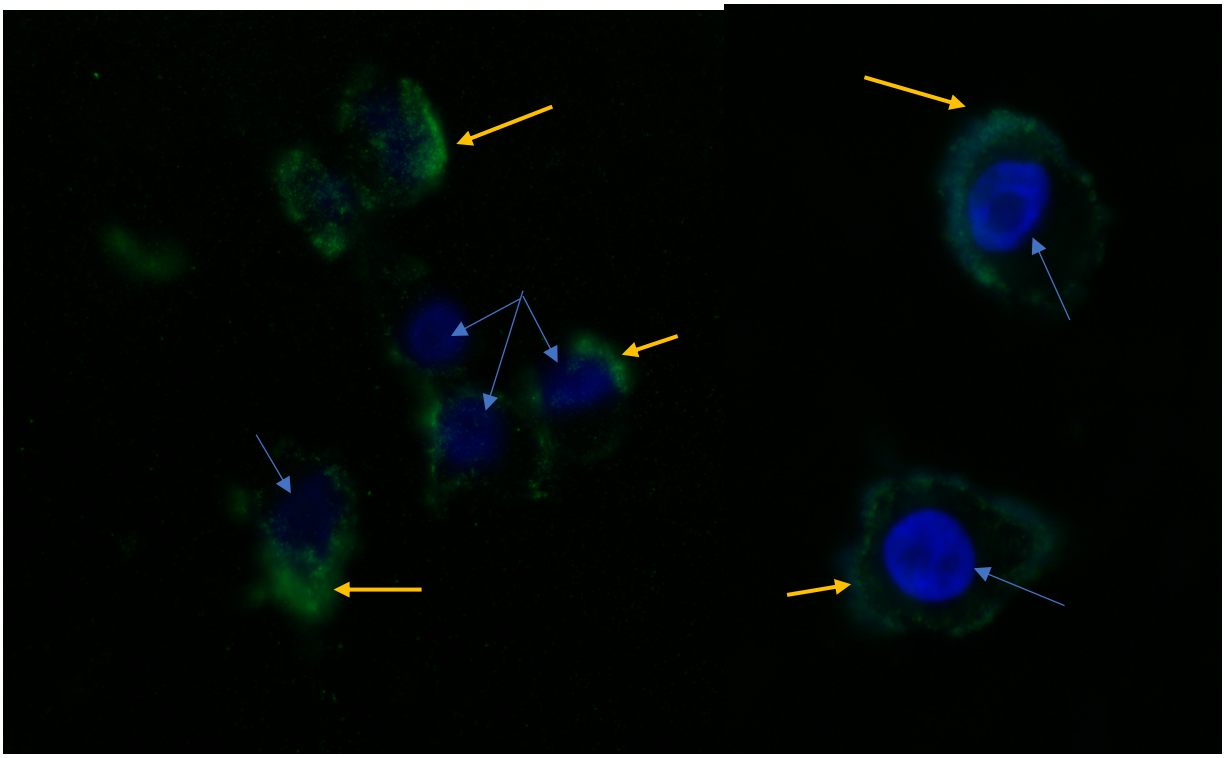

Figure 14: Immunofluorescence microscopy at 1000x magnification – MSTO cell line (tumorigenic, mesothelioma). Leica, DM4000 microscope. The nucleus of the cells was stained with Hoechst (1:1000, Thermo Fisher) (blue florescence, see blue arrows for guidance). The cells bound with rfhSP-D were probed with primary antibodies rabbit anti-human SP-D and with secondary antibodies Alexa Flour® 488 (1:200, Thermo Fisher); rfhSP-D (10 µg/ml) (green florescence; see yellow arrows for guidance) clearly visible and cofinally localized around the cell membrane.

Immunofluorescence reveals a clear interaction of rfhSP-D (green fluorescence) to the cell surface membrane (MSTO; blue fluorescence), as it is dispersed and distributed evenly throughout the membrane (Figure 14). This can be confirmed using ELISA, whereby wells will be coated with MPM cell lines, MSTO as well as with Met-5A (non-tumorigenic MPM cell line), and incubated with rfhSP-D, using controls, this will confirm and validate the immunofluorescence data received.

4.3 Expression, purification and characterisation of recombinant fragment of human SP-D

rfhSP-D is composed of a triple collagen helix of eight repetitious amino acid sequence Glycine-X-Y repeat (where X and Y are frequent proline and hydroxyproline), trimeric α-helical coiled-coil neck region and CRD of human SP-D was expressed in *E. coil* BL21 (λDE3) pLysS under T7 RNA polymerase. Figure 15 represent the end result of the large-scale purification of rfhSP-D (20 kDa) displaying the difference between induced with IPTG (Sigma-Aldrich, UK) (Figure 15; Lane 2 to 6) and un-induced sample (without IPTG) (Figure 15; Lane 1). IPTG (Figure 15; Lane 2 to 6) binds to the repressor of the Lac operon and allows the T7 RNA polymerase to carry out transcription, therefore producing the desired recombinant protein, rfhSP-D. Without IPTG, the repressor remains bound to the Lac operon and therefore transcription does not occur, and rfhSP-D is not produced. Notice on Figure 15 Lane 1, where IPTG was not used, show an absent of a thick band at around 20 kDa (rfhSP-D absent), this confirms that IPTG is an essential molecule and vital in the process in initiating the transcription of rfhSP-D on the Lac operon, therefore without IPTG rfhSP-D cannot be synthesised and repressors will remain bound onto the Lac operon preventing transcription. After the purification process and endotoxin removal, rfhSP-D was collected in Eppendorf tubes and the optical density of each batch was taken using a spectrophotometer (OD; A_{280}). Table 3 represents raw data (OD; A_{280}) of various batches of rfhSP-D collected, as can been seen. An OD (A_{280}) of 0.6 to 0.8 represents a good batch of rfhSP-D and can be used for experimental analysis, any readings lower than 0.5 OD (A_{280}) is insufficient for experimental use, as low OD (A_{280}) is associated with low rfhSP-D concentration therefore not ideal for use in experimental analysis, including *in vivo* and *in vitro* assays.

Table 3 – Optimal range of purified rfhSP-D readings (OD, A_{280}) that is sufficient for experimental use

OD (A_{280})	Estimation of the concentration (μg/ml) of rfhSP-D based on its OD range
0.634	634
0.662	662
0.715	715
0.694	694
0.622	622
0.611	611
0.663	663
0.667	667
0.655	655
0.628	628
0.696	696
0.671	671

Based on Table 3, a good batch of rfhSP-D collected through the purification process will have a reading of between 0.6 – 0.8 OD (A_{280}). This was measured using a spectrophotometer at 280 nm. The concentration of rfhSP-D is estimated based on the OD, which provides some guidance as to the quality of the process and an estimation of the concentration of rfhSP-D collected. The concentration of rfhSP-D based on its OD readings can then be accurately measured using the bicinchoninic (BCA) colorimetric assay (Pierce™ BCA Protein Assay Kit; Fisher scientific®, UK), in which a standard curve is created based on a range of known standards. BCA and bovine serum albumin (BSA) protein concentrations is used as known standards. The OD taken from each batch of samples (Table 3) containing rfhSP-D is read against the standards on a plotted curve and the concentration is accurately determined.

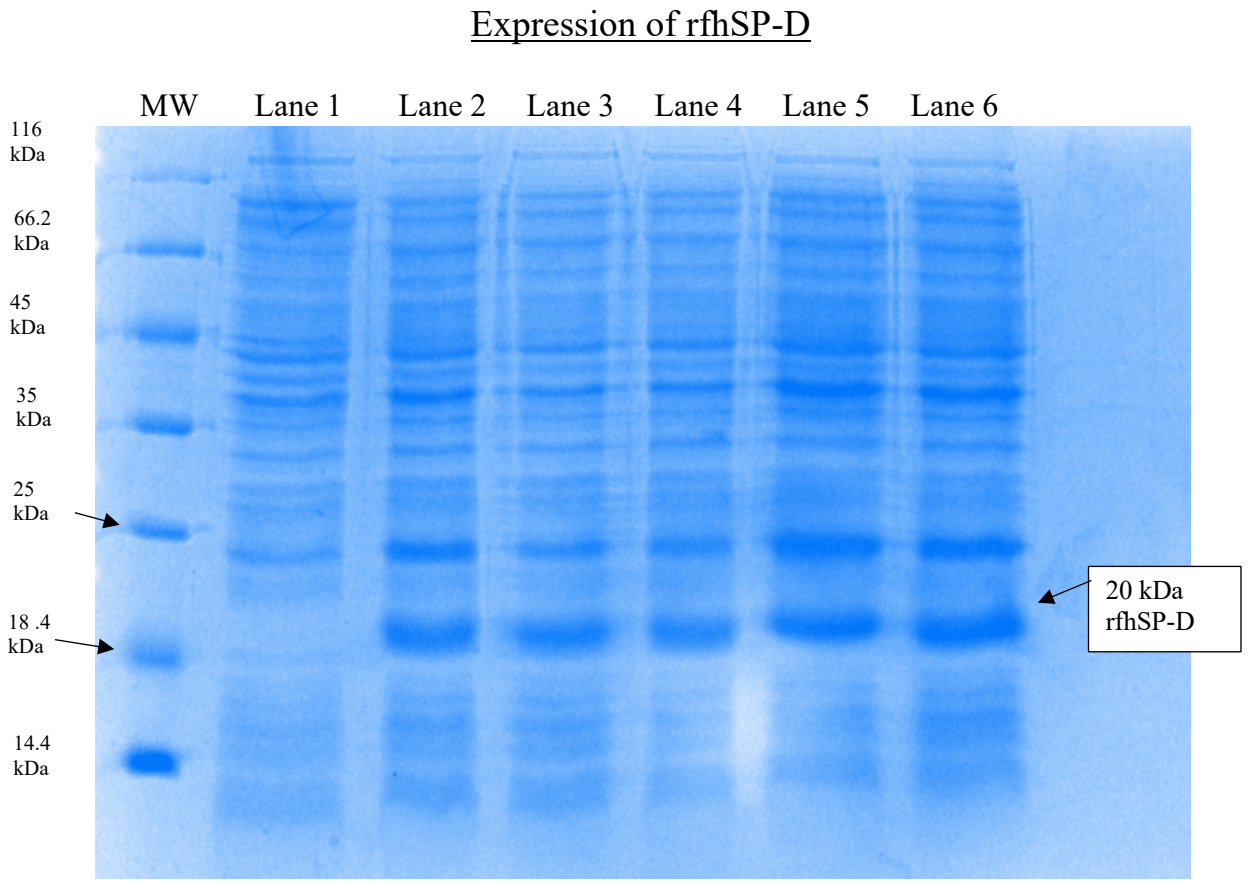

Figure 15: Large scale expression of rfhSP-D. 15% SDS-PAGE – rfhSP-D expressed in batches. Protein expressed at ~20kDa. Molecular marker (MW) - Unstained protein molecular weight protein marker (Thermo Fisher™ Pierce™), Lane 1 – un-induced (without IPTG), Lane 2 – Induced with IPTG (represents rfhSP-D, 20 kDa), Lane 3 – induced with IPTG (represents rfhSP-D, 20 kDa), Lane 4 – Induced with IPTG (represents rfhSP-D, 20 kDa), Lane 5 –induced with IPTG (represents rfhSP-D, 20 kDa), Lane 6 – Induced with IPTG (represents rfhSP-D, 20 kDa) .

Following induction of IPTG, which is used to stimulate the Lac operon, as a result rfhSP-D is produced as can be seen on Figure 15, Lane 2 to 6, where it has a molecular weight of ~ 20 kDa. The insoluble proteins in inclusion bodies were recovered after lysis and sonication of the induced cells (Figure 16, Lane 4). The inclusion body pellet was solubilised initially with urea at 4M concentration and by stepwise dialysis the proteins were re-folded and purified through affinity chromatography using maltose-agarose matrix column, this can be seen on Figure 16 Lane 4, where the proteins haven't yet folded fully and as a result the molecular weight will be at 25 kDa. As the proteins are folded correctly, rfhSP-D can be seen with a molecular weight of 20 kDa. Measuring the molecular weight of each step of the process provides an accurate guidance as to whether the proteins has the correct structure and has folded correctly by possessing the correct molecular weight, which can be used for experiment analysis.

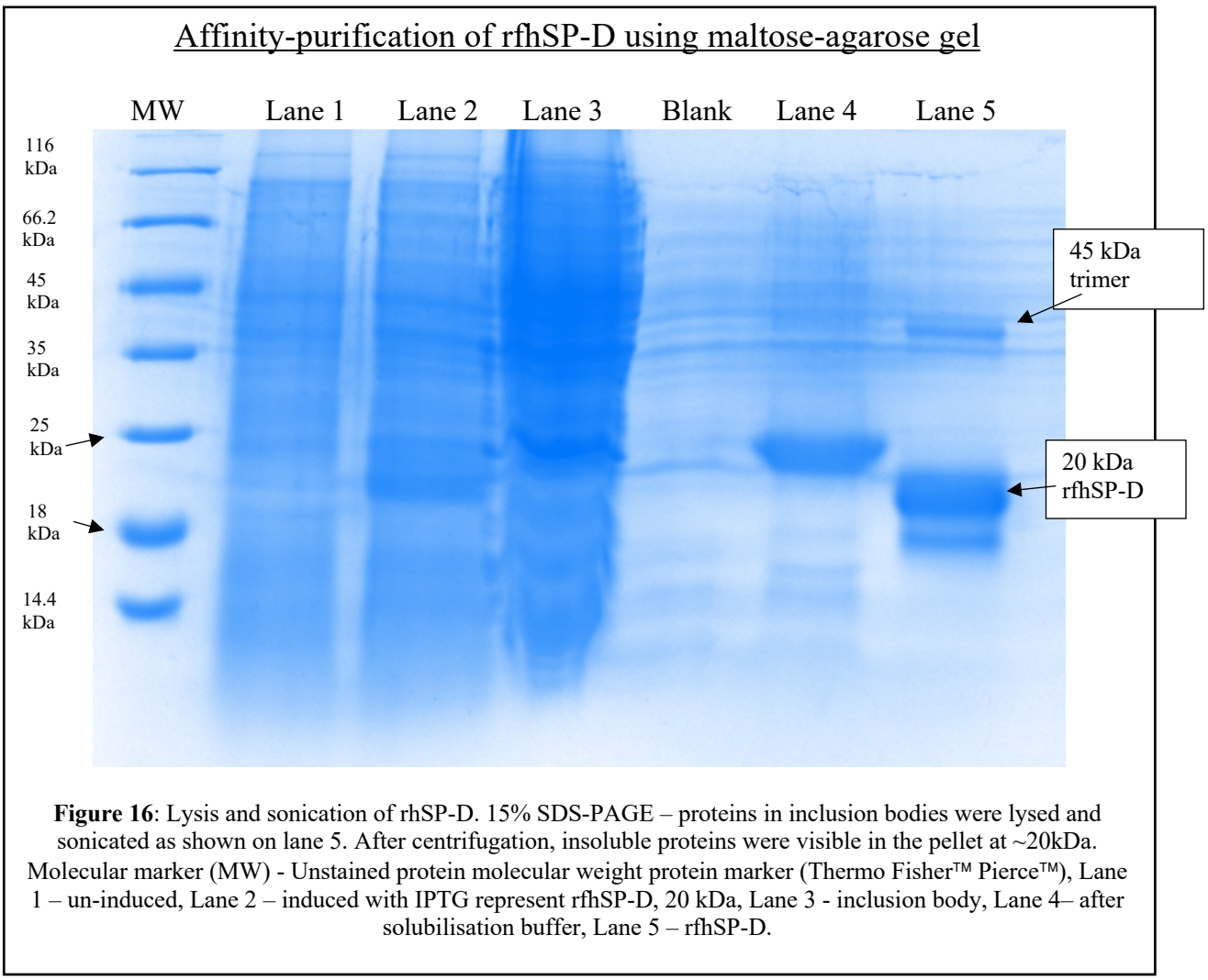

Figure 16: Lysis and sonication of rhSP-D. 15% SDS-PAGE – proteins in inclusion bodies were lysed and sonicated as shown on lane 5. After centrifugation, insoluble proteins were visible in the pellet at ~20kDa. Molecular marker (MW) - Unstained protein molecular weight protein marker (Thermo Fisher™ Pierce™), Lane 1 – un-induced, Lane 2 – induced with IPTG represent rfhSP-D, 20 kDa, Lane 3 - inclusion body, Lane 4– after solubilisation buffer, Lane 5 – rfhSP-D.

As rfhSP-D protein has the ability to bind to a maltose-agarose column through its CRD domain structure, it is then eluted with 10 mM of EDTA (elution buffer), which breaks the bonds between the CRD, of the rfhSP-D protein, and the maltose-agarose purification resin beads from the column chromatography. As the bonds are broken using EDTA, rfhSP-D can then flow through the column and be collected into Eppendorf tubes. The rfhSP-D collected can then be collected and used in SDS-PAGE to confirm the molecular weight of the purified rfhSP-D, which should be 20 kDa (Figure 15; lane 2 to 6 and Figure 16; Lane 2 and 5). The ability of rfhSP-D to bind to maltose in a calcium-dependent manner also provides justification of the protein's bioactivity. The ability to bind to the maltose-agarose resin, shows that it is biologically active and possess the correct biological structure.

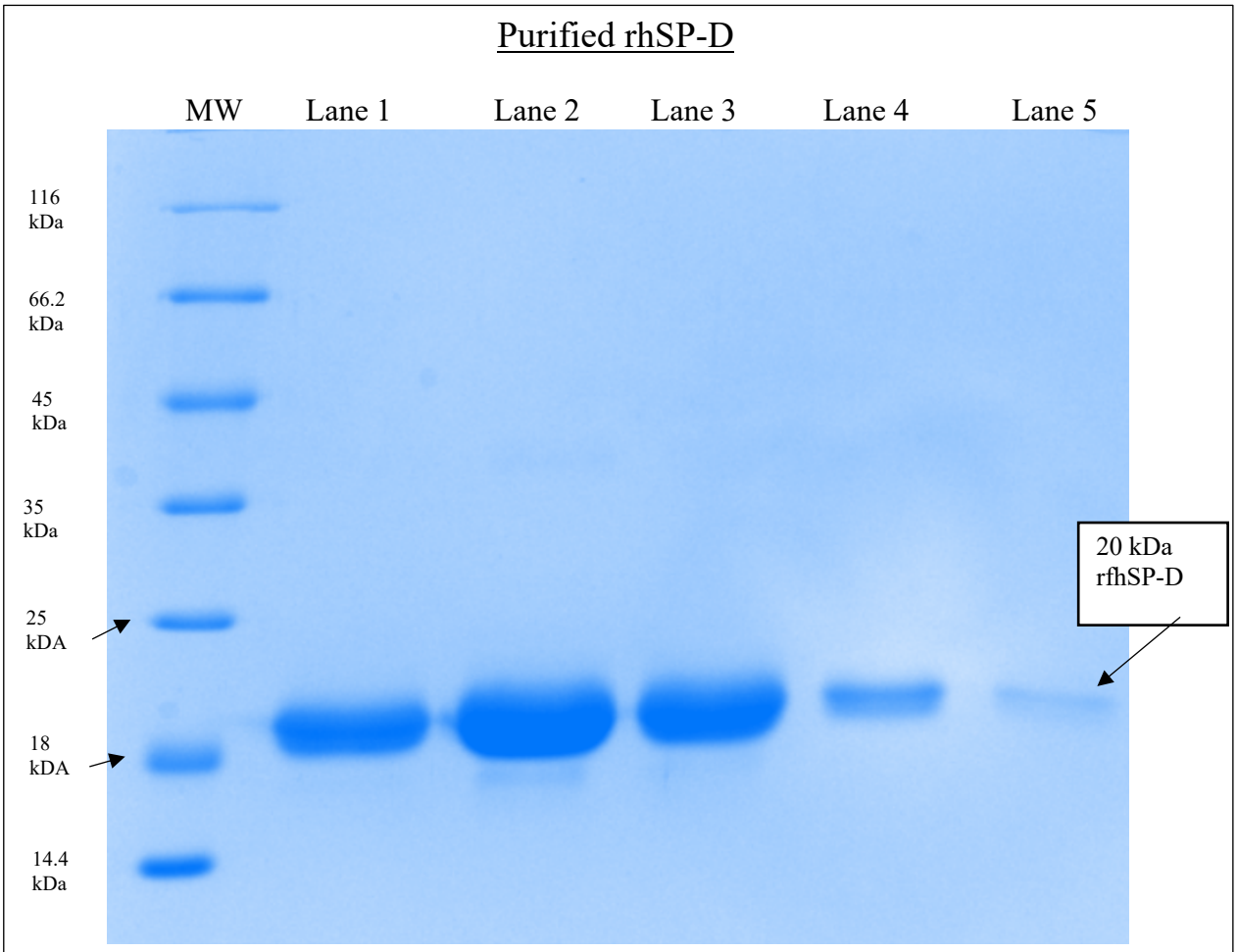

Figure 17: purification of rfSP-D by affinity chromatography. 15% SDS- PAGE – rhSP-D was purified through maltose-agarose matrix by affinity chromatography eluted with 10 mM EDTA (elution buffer). Purified proteins are seen at 20kDA. Molecular weight (MW) - Unstained protein molecular weight protein marker (Thermo Fisher™ Pierce™). Lane 1, 2, 3, 4, 5 – rfhSP-D (20 kDa).

In order to verify if the rfhSP-D protein was present in the induced samples from the large-scale purification process, a western blot was carried out and protein was detected at ~20kDa after IPTG induction (Figure 18). The thick band at 20 kDa from Lane 1 to 4 on Figure 18 represent the fully formed structure of rfhSP-D. This validates the experimental process from transformation to the expression of the Lac operon to the purification process leading to the synthesis of rfhSP-D. Figure 17 represent the bands for the first batch of purified rfhSP-D, as can be seen from Figure 17 Lane 1 to 3 shows a thicker band at 20 kDa, this means that the concentration is most highest from the first three batches of collecting rfhSP-D, thereafter the concentration of rfhSP-D is reduced as can be seen on lane 4 and 5 where the bands are very faint. This represent a bell-shaped curve, during the purification process the first three batches

shows the highest concentration of rfhSP-D, and the last batches with reduced concentration of rfhSP-D.

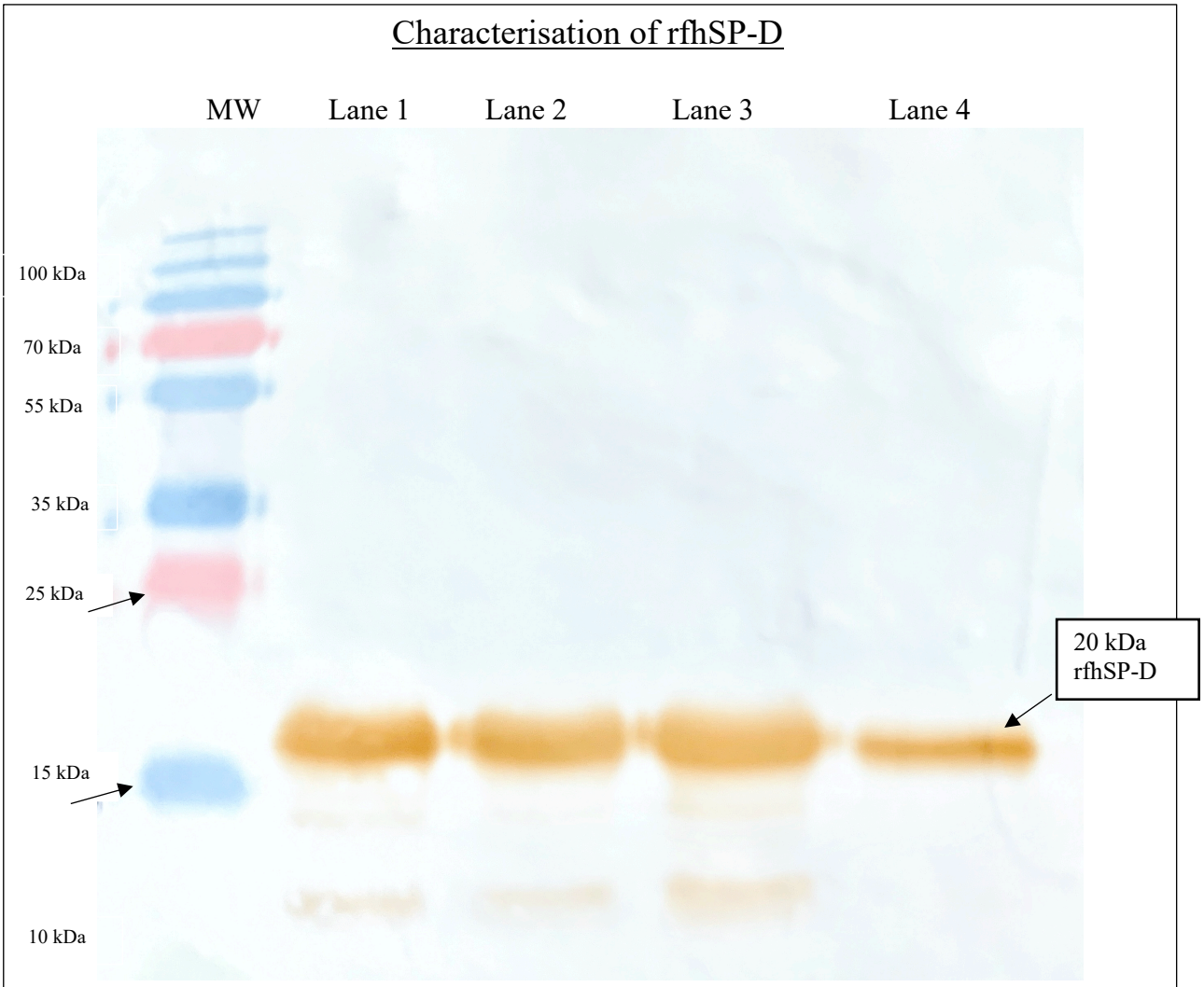

Figure 18: Western blot – detection of recombinant fragment SP-D after large -scale purification. After transfer, membrane was blocked in 5% non-fat milk powder/PBS for 1 hour at +4°C. The nitrocellulose membrane (0.2 µM) (Thermo Fisher™ Pierce™) was incubated in primary antibody (rabbit anti-human SP-A; 1:1000) for 1hrs at room temperature (22°C), after washing 3 times in PBS tween 20, 0.05%, secondary antibody (Protein A; 1:1000) was added and incubated for 1hour. After washing, DAB tablets dissolved in water were used to detect for SP-D. Molecular weight (MW) – Pre-stained protein molecular weight protein marker (Thermo Fisher™ Pierce™). Lane 1, 2, 3, 4 - rfhSP-D (20 kDa).

After confirming the presence of rfhSP-D in large scale production of this protein (Figure 18), supernatant collected from culturing MSTO (MPM) cell line (MPM; fibroblast spheroid cells derived from lungs; pleural effusion) was taken and used on a Western blot assay to determine whether this cell line synthesise human SP-D. Western blot (Figure 19) was carried out to analyse the presence of human SP-D from MPM cell line, and to determine whether this cell

line has the capability to produce or exudes SP-D, as a defensive mechanism against the tumorigenic cell line, from its cell membrane *in vitro* (Figure 19). The assay confirmed that MSTO cell line do not produce SP-D *in vitro* conditions.

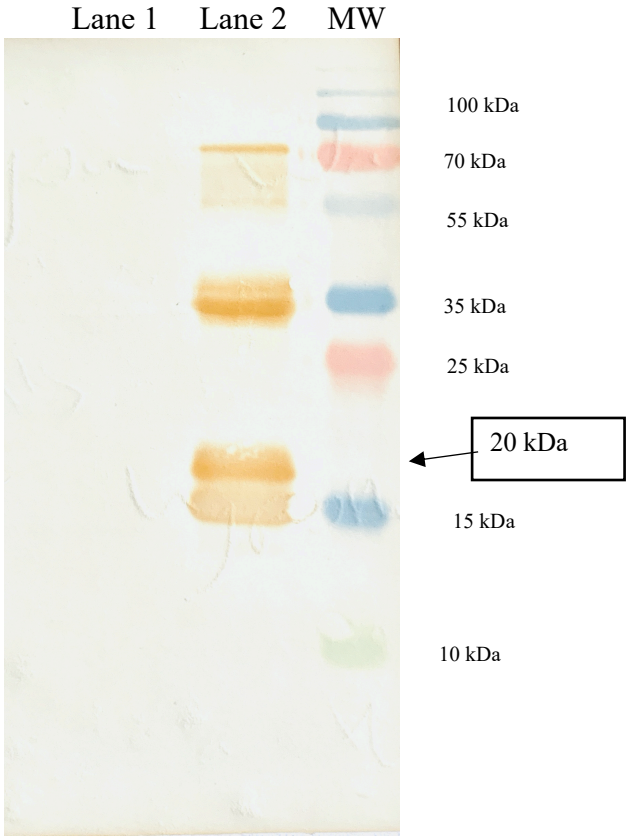

Figure 19: Western blot – detection of human SP-D in supernatant from MSTO cell line (tumorigenic, mesothelioma). Molecular weight (MW) – Pre-stained protein molecular weight protein marker (Thermo Fisher™ Pierce™). Lane 2- purified rfhSP-D (20 kDa). Lane 1 – supernatant from MSTO (MPM tumorigenic cell line) cell line to see whether it is capable to produce or exude human SP-D from its cells into the microenvironment; however no bands present signifies the absence of SP-D (no bands shown on Lane 1).

Lane 1 (Figure 19) revealed the absence of human SP-D in the supernatant of MSTO cell line, which suggests that the cells from MPM tumorigenic mesothelioma do not exude or release SP-D from outside its cell membrane. The formation of trimeric and dimeric SP-D is also apparent (Figure 19; Lane 2), whereby various bands are shown at 15 kDa, 35 kDa and 75 kDa, this is caused by improper folding and cross-linking of the cysteine residues in rfhSP-D structure, which results in some rfhSP-D molecules to form irregular and inconsistent structures such as dimers and trimers. Denatured proteins are also observed at 18 kDa, which

may be caused by improper storage conditions, exposure to excess heat or not been kept on ice during experimental use which limits the preservation of its structure. rfhSP-D should be stored at –20°C; otherwise the structure of rfhSP-D may denature as it is sensitive and any sudden changes to its conditions will denature the protein. Other possible causes are external stress on the protein, such as solvents, inorganic salts, and contamination with acids or bases during experimental use.

4.4 rfhSP-D reduces cell viability in MSTO cell line confirmed by using MTT assay

An MTT assay was chosen for this particular experiment to analyse cellular metabolic activity of MSTO cells (tumorigenic, MPM mesothelioma cell line) to measure and determine cellular viability, proliferation and cytotoxicity. MTT assay is a colorimetric assay based on the reduction of a yellow tetrazolium salt (3-(4,5-dimethylthiazol-2-yl)-2,5-diphenyltetrazolium bromide or MTT) (ThermoFisher ® Invitrogen™) to purple formazan crystals only achieved by metabolically active cells. The viable cells (MSTO) contain NAD(P)H-dependent oxidoreductase enzymes, which is capable of reducing the MTT to insoluble formazan. The insoluble formazan crystals are dissolved using a solubilization solution and the resulting coloured solution is quantified by measuring absorbance at 500-600 nanometres using a multi-well spectrophotometer. The darker the solution, the greater the number of viable, metabolically active cells (Hasegawa *et al*., 2015). rfhSP-D (5 μg/ml, 10 μg/ml and 20 μg/ml) were incubated with MSTO (tumorigenic, MPM mesothelioma cell line) cells for 48 hours. The cell viability MTT assay was carried out on three occasions using identical methods and conditions in order to receive three readings to carry out statistical analysis. 12 mM of MTT revealed clear reduction of cell viability following incubation with rfhSP-D throughout the concentrations (Figure 20). A clear trend was observed in all three identical experiments. Repeating the experimental assay at least three times was carried out to provide greater reliability and validates the data collected. This also enables statistics to be carried out to signify significance within the data collected. Significant reduction was observed consistently with 20 μg/ml rfhSP-D (~30%), in all three experiments carried out (Figure 20).

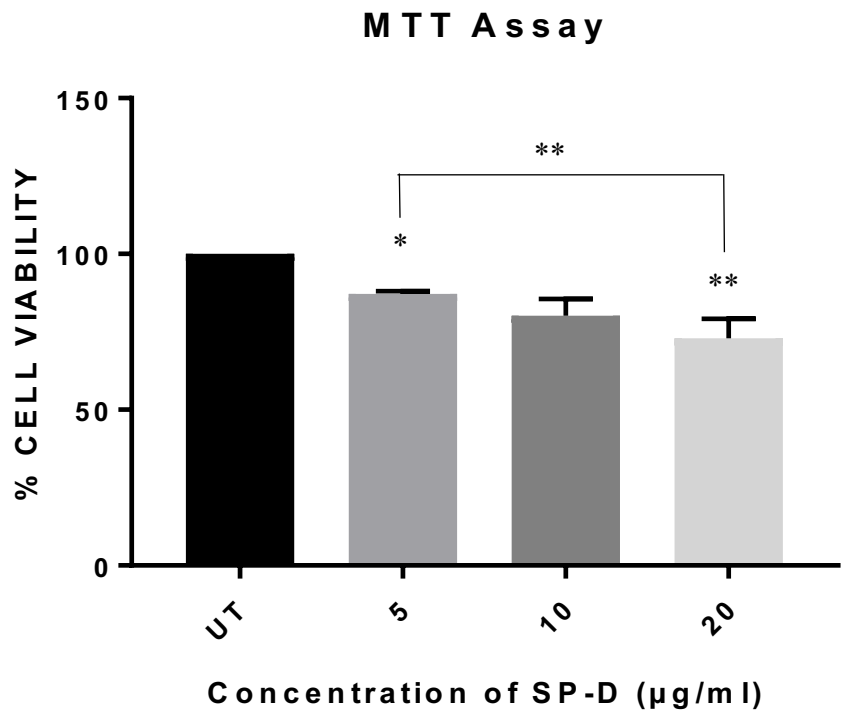

Figure 20: Measuring cell viability by MTT assay following treatment with rfhSP-D (5, 10 & 20 µg/ml) and untreated (UT) for 48 h on MSTO cell line. Optical absorbance was taken at 540 nm. Statistical analysis applied to all three MTT (48-hour, cell viability) assays (±SEM, of three independent experiments). Significance was established using unpaired one-way ANOVA and Tukey's multiple comparisons test. *P < 0.0024 (UT vs 5 µg/ml), **P < 0.0416 (UT vs 20 µg/ml) and P > 0.0573 (UT vs 10 µg/ml) (n = 3).

Statistical analysis was applied to determine significance in all three different concentrations of rfhSP-D. MSTO cells exhibit greatest reduction in cell viability when treated with 20 µg/ml of rfhSP-D, therefore showing statistical significance at 20 µg/ml of rfhSP-D; **P < 0.0416 (UT vs 20 µg/ml) (n = 3), as can be seen on Figure 20. This data suggest an anti-proliferative effect whereby MPM cells (MSTO) degrade and undergo apoptosis (Figure 20).

A pilot test of using cell viability MTT assay was performed initially on MSTO cells incubated with rfhSP-D (5 µg/ml, 10 µg/ml and 20 µg/ml) in various incubations periods, including 24, 48 and 72 hours. This was carried out to identify the optimal incubation time, and statistical significance within the various incubation periods in relation to different concentrations of rfhSP-D. At 24 hours and 2 hours of incubation with rfhSP-D (not shown) shows no clear indication of apoptosis or proliferation, and the trend of cell viability was not consistent. At 24 of incubation with rfhSP-D data (not shown) suggest no clear changes when treated with rfhSP-D (5 µg/ml, 10 µg/ml and 20 µg/ml). It was found in this pilot study that 48

hours of incubation with rfhSP-D showed greatest anti-proliferative effects. None of the data collected, including incubation period of 24 and 72 hours with rfhSP-D, showed proliferative effects. This was taken into consideration and future plans to adjust and optimise the methodology, as described in the discussion.

4.5 rfhSP-D induces apoptosis in MSTO cells confirmed by using flow cytometry

To establish whether rfhSP-D induces apoptosis in MSTO cell line, FITC annexin V apoptotic detection kit with PI (BioLegend™) was used. This enables us to differentiate between apoptotic and necrotic cells. Annexin V (human vascular anti-coagulant) is a calcium dependent phospholipid protein, member of the annexin family of intracellular proteins. FITC conjugated Annexin V has a high affinity for phosphatidylserine (PS) and binds in a calcium dependent manner. In normal and healthy cells, PS is located on the intracellular (cytoplasmic surface) of plasma membrane. As cells undergo apoptosis or necrosis, the PS located on its intracellular membrane is translocated from the inner side to the external leaflet (extracellular side) of the plasma membrane, resulting in structural changes and loss of membrane asymmetry. This then exposes PS, for which fluorochrome-labelled Annexin V conjugated with FITC (Fluorescein isothiocyanate; green dye) can be attached and bind to PS on the plasma membrane. This is only unique to cells undergoing apoptosis, as healthy and normal cells do not undergo any plasma membrane or structural changes, therefore unable for PS to bind to Annexin V. Annexin V cannot differentiate between cells undergoing apoptosis and necrosis, however with the use of propidium iodide (PI) this can be achieved. Cells undergoing early apoptosis will exclude PI, whereas late stage apoptotic cells and necrotic cells will be stained positive for PI. This is because the passage of PI into the cells and nucleus ultimately binding to the DNA of the cells. Whereas in normal cells and cells undergoing early apoptosis, the nucleus remains intact therefore blocking the passage of PI and unable to bind to the DNA. PI targets DNA in necrotic cells and stains with red fluorescence, and excited by 488 nm laser. Fluorescently labelled components of each cells are excited by the laser emitting light at specific wavelength, which is then detected by the flow cytometer (NovoCyte™ ACEA Bioscience, Inc) detecting a combination of scattered and fluorescent light. The data is then analysed using a software (NovoExpress®) based on the gathered information, such as physical and chemical structure of the cells (Hasegawa *et al*., 2015).

Flow cytometry was carried out in this study because it is a highly sensitive test and imperative in detecting and measuring the physical and chemical characteristics of a population of MPM cells. Furthermore, flow cytometry was used to analyse apoptotic or necrotic activity

in MSTO cells (tumorigenic, MPM cell line) treated with varied concentrations of rfhSP-D. Each sample contained MSTO cells from MPM patients and treated with a four different concentrations of rfhSP-D and incubated for 24, 48 and 72 hours and analysed using flow cytometry (NovoCyte™; ACEA Bioscience, Inc). After pilot studies to identify the optimal conditions, without background interferences or contamination that will jeopardise growth or death of the cells, apoptosis and necrosis was confirmed, as seen on Figure 21, 18 and 19.

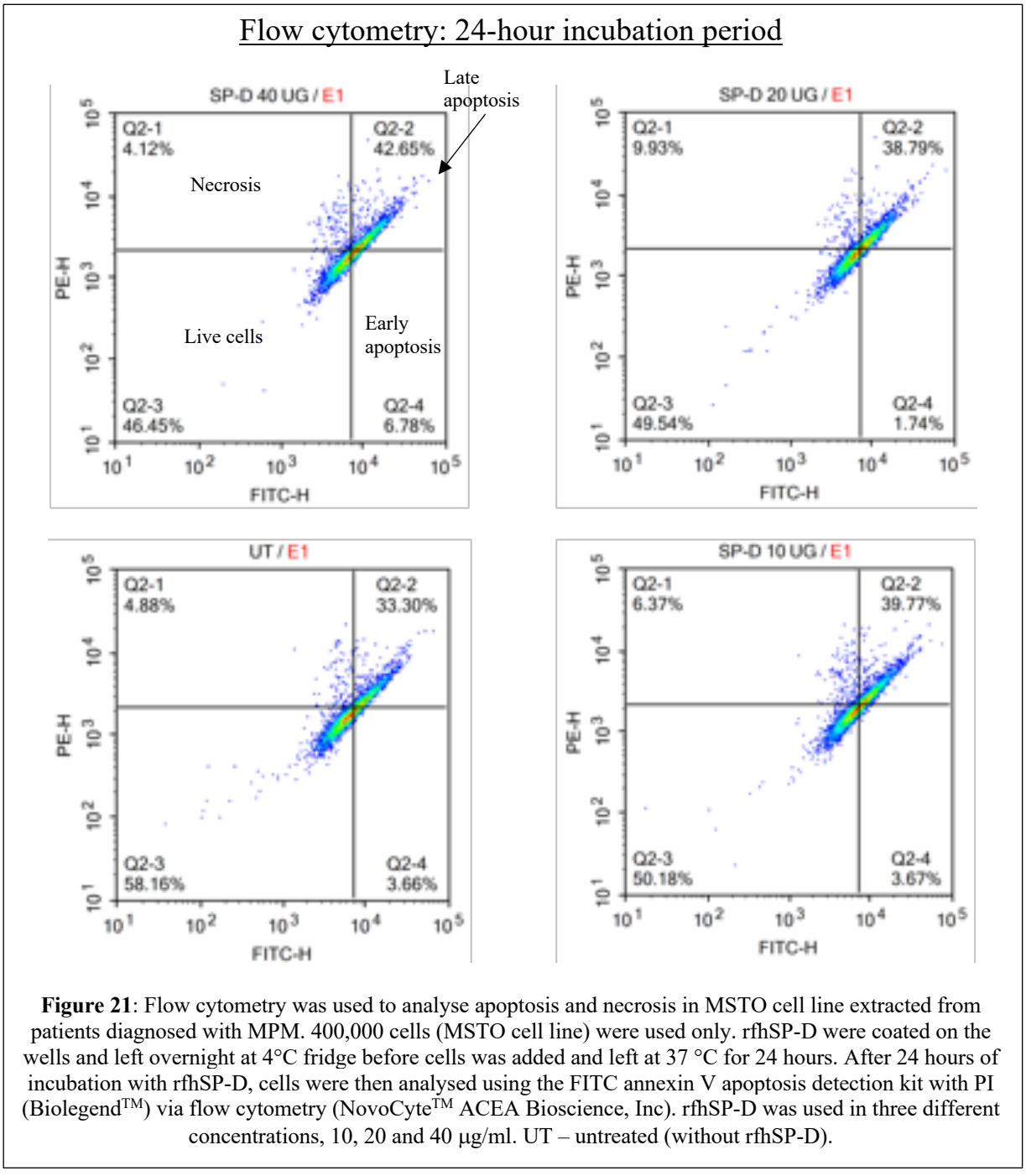

Figure 21: Flow cytometry was used to analyse apoptosis and necrosis in MSTO cell line extracted from patients diagnosed with MPM. 400,000 cells (MSTO cell line) were used only. rfhSP-D were coated on the wells and left overnight at 4°C fridge before cells was added and left at 37 °C for 24 hours. After 24 hours of incubation with rfhSP-D, cells were then analysed using the FITC annexin V apoptosis detection kit with PI (Biolegend™) via flow cytometry (NovoCyte™ ACEA Bioscience, Inc). rfhSP-D was used in three different concentrations, 10, 20 and 40 µg/ml. UT – untreated (without rfhSP-D).

Flow cytometry: 48-hour incubation period

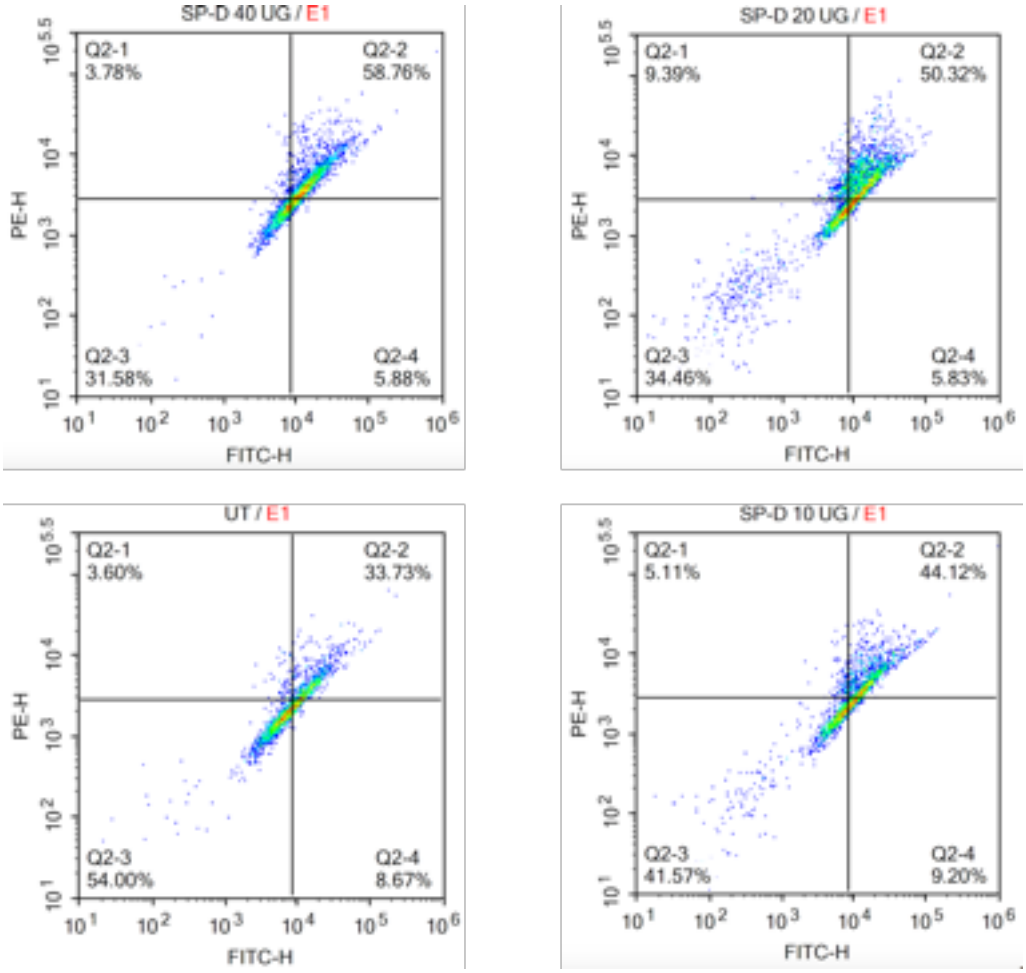

Figure 22: Flow cytometry used to analyse apoptosis and necrosis in MSTO cell line extracted from patients diagnosed with MPM. 400,000 cells (MSTO cell line) were used only. rfhSP-D were coated on the wells and left overnight at 4°C fridge before cells was added and left at 37 °C for 48 hours. After 48 hours of incubation with rfhSP-D, cells were then analysed using the FITC annexin V apoptosis detection kit with PI (Biolegend™) via flow cytometry (NovoCyte™ ACEA Bioscience, Inc). rfhSP-D was used in three different concentrations, 10, 20 and 40 µg/ml. UT – untreated (without rfhSP-D).

Flow cytometry: 72-hour incubation period

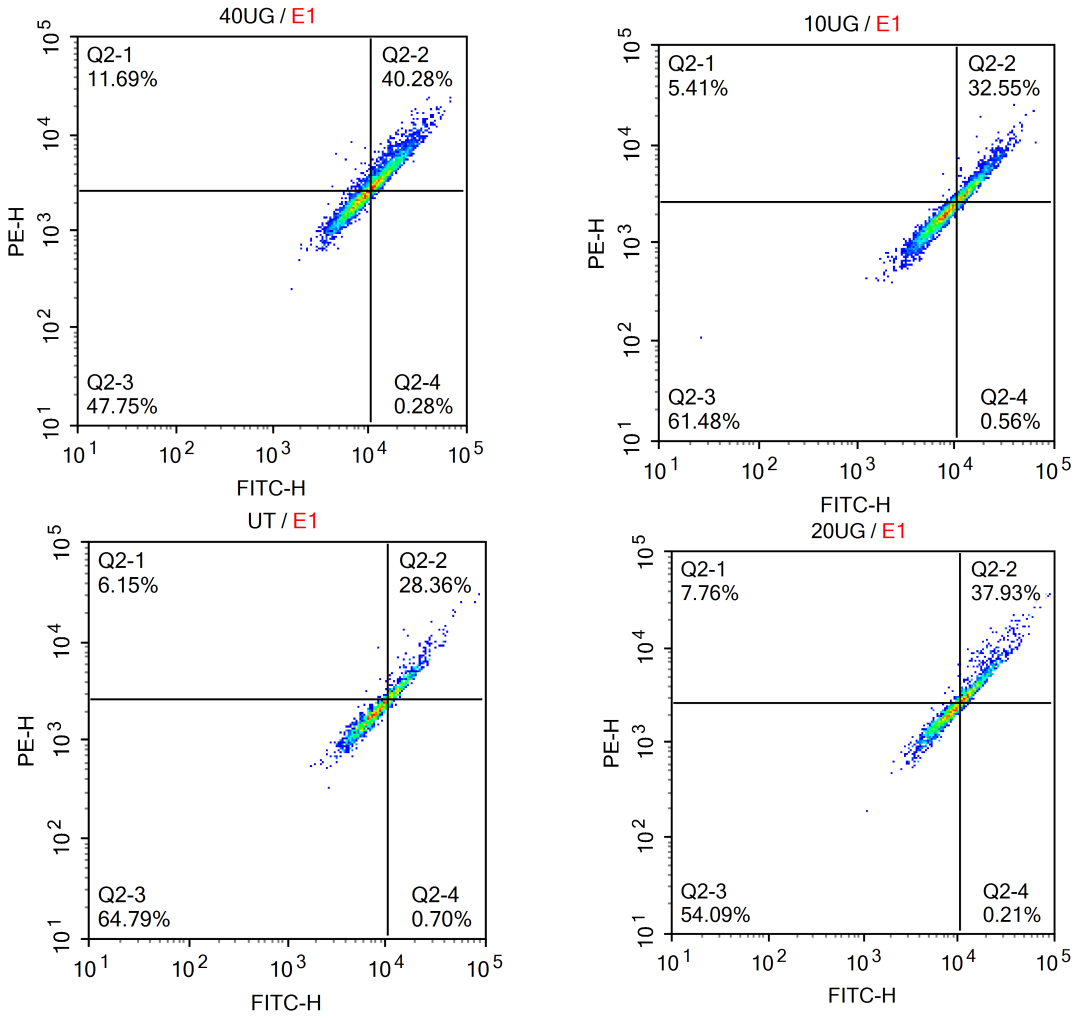

Figure 23: Flow cytometry was used to analyse apoptosis and necrosis in MSTO cell line extracted from patients diagnosed with MPM. 400,000 cells (MSTO cell line) were used only. rfhSP-D were coated on the wells and left overnight at 4°C fridge before cells was added and left at 37 °C for 72 hours. After 72 hours of incubation with rfhSP-D, cells were then analysed using the FITC annexin V apoptosis detection kit with PI (Biolegend™) via flow cytometry (NovoCyte™ ACEA Bioscience, Inc). rfhSP-D was used in three different concentrations, 10, 20 and 40 µg/ml. UT – untreated (without rfhSP-D).

Three separate experiments were carried out with three different incubation periods including 24-hours, 48-hours and 72-hours, all treated with different concentrations of rfhSP-D as shown on Figure 21, 22, and 23. Based on my findings on the MTT cell viability assay (Figure 20), I found that the optimal incubation period was at 48 hours whereby rfhSP-D induces apoptosis and confirmed statistically significant. This preliminary data was used in order to optimise the conditions in flow cytometry analysis for the detection of apoptosis and necrosis. The incubation period at 24 and 72 hours was used to justify and confirm the optimal incubation period of 48 hours. Treatment with rfhSP-D was used in three different concentrations, 10, 20 and 40 μg/ml and an untreated control (UT – untreated), whereby no rfhSP-D was incubated with the cells. The control was essential at this stage, as it enables the justification of the effects of rfhSP-D and used to determine any background interferences or false positive results that can jeopardise the data and overall conclusion. The data displayed on Figures 21, 22 and 23 contains four different quadrants. To understand the meaning of the graph, it is divided into four distinct regions, known as quadrants. The upper left of the quadrant are cells that underwent necrosis and the upper right of the quadrant is where cells have undergone late apoptosis. The lower left are live cells and the lower right of the quadrant is where cells have undergone early apoptosis. The data was gathered and analysed using flow cytometry and data software analysis (NovoExpress®). The flow cytometer (NovoCyte™ ACEA Bioscience, Inc) enables the ability to characterise each cell at a highly sensitive level and quantify cells that are undergoing necrosis, apoptosis and cells that are not affected with the treatment of rfhSP-D, in which case it is known as live cells (Thakur et al., 2017).

Based on the incubation period of 24 hours with rfhSP-D (Figure 21), when treated with 40 μg/ml of rfhSP-D 42.65% of MSTO cells undergone apoptosis, and at 20 μg/ml of rfhSP-D only 38.79% of cells underwent apoptosis. This was compared to the lowest value of MSTO cells undergoing apoptosis which was when cells were treated with only 10 μg/ml of rfhSP-D reaching a figure of 39.77%. This general trend was seen throughout the three different incubation periods, including at 48 and 72 hours. However, with optimal conditions, MSTO cells undergoing apoptosis reached the highest level of 50.32% (20 μg/ml of rfhSP-D incubated for 48 hours), as can be seen on Figure 22. Figure 22 represent the optimal conditions whereby the majority of MSTO cells was seen to undergo apoptosis.

In reference to the three different incubation periods with rfhSP-D (Figure 21, 22 and 23) using flow cytometry, it is established that the highest mortality percentage is at 48-hour also when treated with 40 μg/ml rfhSP-D, whereby 58.76% of cells underwent apoptosis. This

suggests that 48-hours is the optimal length of time for rfhSP-D to take into effect and induce apoptosis to the majority of the cell population (MSTO cell line). Although MSTO cells treated with 40 μg/ml induced the highest apoptotic rate, it is not an efficient concentration of rfhSP-D to be used when considering the effects on cells. Incubating 20 μg/ml of rfhSP-D for 48 hours is shown to be the optimal conditions for inducing apoptosis on MSTO cell line.

5 Discussion and Future direction

MPM is an aggressive neoplasm with very poor prognosis stemming from its resistance to current forms of treatment, including chemotherapy and radiotherapy. MPM has a high mortality rate, this is because it is almost always diagnosed at a late stage where the tumour has already spread and developed, at which first-line treatment or other forms of treatment become less effective. Current forms of treatment used against MPM does not improve prognosis for patients suffering with this disease, but merely reliefs pain elicited from the symptoms. Therefore, a novel form of treatment is highly required in order to reduce the growing number of deaths and essentially reduce mortality rate. This provides an opportunity to explore and study a potential alternative form of therapy. Studies on SP-D are promising and has been reported to have anti-microbial and anti-allergic properties at mucosal surface (Kaur *et al*., 2018). Studies on SP-D provide strong evidence to suggest it acts as an innate immune surveillance molecule against various cancers, such as pancreas, prostate and lung adenocarcinoma (Kumai *et al*., 2019). The purpose of his study is to establish the presence of human SP-D in MPM to further understand its role and contribution in cancer and determine whether rfhSP-D induces apoptosis in MPM cell lines.

SP-D is overexpressed in ovarian cancer tissue (serous cystadenocarcinoma) compare to its counter healthy controls. SP-D has also been reported to be widely expressed in clear cell adenocarcinoma, mucinous adenocarcinoma, serous adenocarcinoma and endometroid adenocarcinoma of ovarian cancer tissue, and also in lung adenocarcinoma (Kumai *et al*., 2019). We report here, for the first time, that SP-D is present in all the histological variants examined, including biphasic, sarcomatoid and epithelioid specimens of MPM tissue. From this finding we know that SP-D is present in lung adenocarcinoma, ovarian cancer and other forms of cancer, and now in MPM. This is evident from the immunohistochemical analysis (Figure 8, 9 and 10). Based on a recent study using *in silico* findings conducted by Mangogna *et al.* (2018), on a variety of cancers (using oncomine data analysis), has revealed that low levels of mRNA expression of SP-D correlates to significant improvement in overall survival

and progression-free survival, as opposed to higher levels of SP-D expression in cancer. Furthermore, a study conducted has shown high mRNA level expression of SP-D in gastric and breast cancer (Mangogna *et al*., 2018). In addition, non-small cell lung cancer (NSCLC) has revealed that high levels of SP-D in lungs of patients suffering from NSCLC correlates with poor prognosis and metastasis (Chong *et al.,* 2006). A study has examined and revealed low expression of SP-D in gastric, lung and breast cancers, compared to its counter controls (healthy individuals). The presence of SP-D in lung cancer is correlated to favourable prognosis. In contrast, studies have shown that in ovarian and breast cancer, the presence of SP-D is correlated to poor prognosis (Mangogna *et al.* 2018). These studies on SP-D expression, suggest a higher order of complexity of SP-D in terms of its function and regulation in cancer, and suggest that SP-D acts in a cell- and tissue-specific manner, which may be dependent on the tumour microenvironment. SP-D may be overly-expressed in tissue to compensate for the tumour microenvironment (saturated with HA) as HA binding to SP-D may negate the anti-tumour effects of human SP-D, since HA has high affinity for binding to tumour cells as it forms the extracellular matrix of tumour therefore blocking the protective functions of SP-D, this warrants for further investigation with HA *in vitro* studies. In contrast to this theory, high levels of SP-D in MPM, shown from our data and other studies, is established because patients undergoing dexamethasone treatment (chemotherapy drug), has shown to induce significantly higher levels of SP-D, as opposed to patients not receiving dexamethasone (Bo-Hui *et al*., 2020), and as the tumour produces HA to bind to SP-D, the tumour suppressive functions of SP-D is negated. These theories based on studies, and data collected so far, require additional investigation and further gathering of data, including a wider repertoire of cell lines and clinical samples collected from patients.

Based on future prospective, studying the microenvironment of MPM can contribute in devising a novel therapeutic strategy against MPM. ELISA and flow cytometry analysis are essential tools to determine binding between hyaluronic acid (HA) and rfhSP-D (Agostinis *et al*., 2017). From our group, we know that the interaction of C1q with HA causes an inflammatory response based on the study conducted by Agostinis *et al*. (2017). Therefore, based on this my future work will also involve examining whether SP-D can bind to HA or its induction will influence C1q and HA interaction, as well as SP-D binding to HA in response to inflammation, and whether it promotes apoptosis or mask apoptosis inducer. The reason to involve HA, is because MPM is associated with inducing high level of HA, and forms a major constituent in tumour environment, and HA is shown to be highly expressed in MPM, supported by a study conducted by Agostinis *et al*. (2017). In normal tissue, HA is shown to

be responsible for the lubrication of pleural membranes and is secreted by mesothelial cells. HA and SP-D are both highly abundant in MPM tissues, and HA has shown in recent studies to induce proliferation and migration of MPM cells through its interaction with hyaluronan receptor CD44 (Cedeño-Arias *at al*., 2011). Flow cytometry will be an essential tool here as it can be used to determine binding between the two molecules, and maintains low assay variation, which is highly advantageous (Agostinis *et al*., 2017). Flow cytometry has stability-indicating properties, which can be useful to detect changes in binding of monoclonal antibodies degraded samples. Using this technique, primary cell lines can be analysed to identify whether it expresses Hyaluronic acid (HA) or the HA receptor, CD44. To identify whether SP-D interacts and binds to HA and CD44, can enable possible future goals to establish if they are pro-apoptotic or anti-apoptotic, and whether SP-D influences HA interaction with its receptor CD44 in inflammation. In previous studies, C1q and HA have been shown to bind forming a complex which enhances adhesion, migration and proliferation of MES cell line (MPM), therefore promoting tumour growth (Agostinis *et al*., 2017). Based on this study my future proposal is to determine whether rfhSP-D binds to hyaluronic acid (HA), a prominent tumour microenvironment molecule, and the effects exerted from rfhSP-D binding to HA on MPM cells, and whether rfhSP-D acts as a binding molecule between CD44 (an HA receptor found abundantly on MPM cells) and HA. This can be achieved using immunofluorescence microscopy and flow cytometry analysis to determine and display binding to rfhSP-D. To assess the effects of rfhSP-D binding to HA in MPM cell lines, anti-apoptotic and pro-apoptotic assays can be carried out to determine any differences in response with and without treatment of HA. This will be essential to our understanding of tumour microenvironment and how it can influence SP-D in MPM.

Immunofluorescent analysis confirmed the presence of SP-D in MPM (MES 16; Figure 12), which appears to be diffusely present and associated with the cell membrane of the cells. Further observation revealed areas where SP-D was found to be associated with small vessels (Figure 8, 9 and 10). After establishing the presence of SP-D in various histotypes of MPM, we can deduce that SP-D potentially exhibit a pro-angiogenic activity on the basis that it is confined around vascular structures on immunohistochemical data (Figure 10). This can be further investigated by assessing proliferation and migration properties of rfhSP-D. The effects of rfhSP-D on cell migration can be assessed by using a scratch wound healing assay, monitoring the mobilization of MPM cell lines towards the scratched area filling the denuded region within a specified period of time (usually 18 h). This may show that MPM cell lines can be stimulated by rfhSP-D by entering the scratched area and migrate farther than control cells

without treatment with rfhSP-D. Cell migration can also be assessed using rfhSP-D-induced migration of labelled MPM cell lines. The percentage of cell migration of MPM cells treated with rfhSP-D can then be comparable to untreated MPM cells. More specifically, a trans-well migration assay is a commonly used test to study the migratory response of MPM cells to rfhSP-D. This assay is commonly known as the Boyden or modified Boyden chamber assay. During this assay, MPM cells can be placed on the upper layer of a cell culture insert with permeable membrane and a solution containing rfhSP-D is placed below the cell permeable membrane, this is used to assess enhancing migratory properties.

After confirming SP-D is present in various histotypes of MPM tissue extracted from patients, including epithelioid, sarcomatoid and biphasic, the next stage was to produce and purify a recombinant form of human SP-D in order to analyse this protein against MPM cell lines *in vitro*. Removing endotoxins from large-scale expression and purification of rfhSP-D was essential to avoid LPS killing off MPM cells. Furthermore, LPS was removed to prevent endotoxic shock, inflammation and/or sepsis in tissue culture cells used for this study. Endotoxins is produced during the transformation and purification process of rfhSP-D from *E. coli*, which produced in large quantities. Endotoxins (LPS) can interfere with the metabolic process in MPM cell lines and enhance release of certain cytokines and other proteins that can interfere with cell signalling process, which may ultimately create false positive and unreliable outcome. This was carried out align with various other studies using rfhSP-D as a form of *in vivo* treatment to maintain consistency throughout our findings (Kumai *et al*., 2019; Kaur *et al*., 2018).

After purifying LPS-free rfhSP-D, we then established whether it induces apoptosis in MSTO cell line. In reference to the MTT cell viability assay (Figure 20), a reduction of almost 20% in cell viability was observed, mainly with 5 μg/ml and 20 μg/ml of treated rfhSP-D, as values were considered significant based on the p-value. This suggests an anti-proliferative effect to the cells, as cells growth reduced and declined. However, based on a recent study involving pancreatic cancer, cell lines of from pancreatic cancer treated with 20 μg/ml of rfhSP-D induced greater reduction in cell viability (almost 60% reduction) in 24 hours (Kaur, et al 2018), compared to our data using MPM (MSTO cell line) (Figure 20) which was only reduced by 15%. This is a significant difference in comparison to other studies using rfhSP-D. This may be caused by trapped lipid raft during the experiment. An alternative way to avoid trapped lipid raft is to add an additional 20 μg/ml of rfhSP-D, just after the 24 hours incubation, and take a reading at 48 hours, which was carried out and an average was taken. This will allow

the cells to be treated with two doses of 20 μg/ml of rfhSP-D during the 48-hour incubation period and may avoid the problem of trapped lipid raft.

Although, cell viability of MPM cell line was reduced by 15% overall using the cell viability assay (MTT assay), it is supported by the flow cytometry data (Figure 21, 22, 23), which shows a far greater decline in growth of the MPM cell line. In fact, during the optimal conditions at 48-hours of incubation treated with 40 μg/ml of rfhSP-D, 34% of cells underwent apoptosis compared to 21% when treated with 20μg/ml of rfhSP-D, and 12% when treated with 10 μg/ml of rfhSP-D. This suggest that the flow cytometry data is able to support the cell viability assay (MTT assay) to confirm that MPM cells underwent apoptosis when treated with rfhSP-D at 48 hours. Although this data also suggest that rfhSP-D induces apoptosis in MPM cell line (MSTO), other studies have shown that it has anti-proliferative properties in pancreas and prostate cancer, all of which are of epithelial origin. This is in agreement with other studies to support the theory that SP-D is an innate immune surveillance molecule in cancer (Kumai *et al*., 2019).

In this study, apoptotic induction has been validated via FITC-conjugated Annexin V-positive kit using flow cytometry analysis. To supplement this finding, determining the presence of apoptotic enzymes, such as caspase 9 and 3, that could be involved will strengthen this finding. Pro-apoptotic response and transcriptional up-regulation of pro-apoptotic markers, such as TNF-α, Bax, and Fas, known to initiate apoptosis are crucial components of the apoptosis process. This can be achieved by setting up a western blot for the detection of apoptotic markers, such as the activation cleavage of caspase 8 and 9 (initiator caspase) and 3 (executioner caspase), using anti-rabbit cleaved caspase 3 and 8 followed by secondary anti-rabbit IgG HRP-conjugate. In addition, analysis of the annexin V binding using fluorescent microscopy is also an essential tool here to analyse apoptosis. To further determine apoptotic pathways, gene expressions can be used to assessed pro-apoptotic genes Bax (intrinsic pathway marker), and Fas (extrinsic pathway marker) using western blot analysis in MPM cell lines treated with rfhSP-D using rabbit anti-human Fas followed by secondary anti-rabbit IgG HRP-conjugate, to differentiate whether induction of apoptosis is through intrinsic or extrinsic pathways. Previous studies have shown that rfhSP-D induces apoptosis by p53 mediated apoptosis pathway in an eosinophilic leukemic cell line, AML14.3D10 (Mahajan *et al*., 2013; Mahajan *et al*., 2008). rfhSP-D induces apoptosis in pancreatic cancer cell lines via Fas-mediated pathway (Kaur *et al*., 2018). Based on these studies, our future proposition can involve establishing apoptotic signalling pathway in MPM by assessing gene expressions for

pro-apoptotic genes such as Bax, an intrinsic pathway marker, and Fas, an extrinsic pathway marker. We can use the studies carried out previously on rfhSP-D on expression levels of Bax and Fas, and adopt similar experiment conditions, such as time-points ranging from 2 h to 24 h in all MPM cell lines for analysis to explore the apoptotic pathway. Furthermore, as TNF-α and NF-κB are crucial factors in the apoptotic pathway which is able to also regulate Fas expression, the effect of rfhSP-D on the gene expression of TNF-α and NF-κB as well as translocation of NF-κB from the cytoplasm to nucleus, will be targeted for investigation in MPM with rfhSP-D to further understand the underlying mechanism of rfhSP-D in MPM.

Further to this point, up-regulation of Fas, an apoptosis stimulator, and pro-apoptotic TNF-α (and associated transcription factor, NF-κB) at a certain time-point with consistency with the cleavage of caspase 8 and 3 will enable us to establish whether cell death in MPM using rfhSP-D is likely to occur via TNF-α/Fas-mediated apoptosis pathway. This is because caspase-3 is activated during apoptosis both by extrinsic (death ligand) and intrinsic (mitochondrial) pathways, and capsase-8 (cysteine protease) plays a crucial role in the extrinsic apoptotic signalling pathway via death receptors. To further elucidate the mechanism of the cell activation and expand our knowledge in signally pathways in MPM using rfhSP-D, we need to analyse the signalling pathway biomarkers likely to be involved in cell adhesion, migration and proliferation. These biomarkers include three members of the MAPK family, ERK1/2, SAPK/JNK, and P38 signalling molecules, consistent with a recent study conducted by Agostinis *et al*. (2017). The analysis of TNF-α mRNA expression levels in MPM cell lines and transcriptional regulation for NF-κB using immunofluorescence microscopy could further confirm whether NF-κB could play a key role in deciding the apoptotic fate of the MPM cell lines following the rfhSP-D treatment (Agostinis *et al*., 2017). NF-κB (nuclear factor kappa-light-chain-enhancer of activated B cells) is a protein complex that controls transcription of DNA, cytokine production and cell survival. Incorrect regulation of NF-κB has been linked to the development of cancer. (Agostinis *et al*., 2017).

Future analysis on this study will be to focus on a wider portfolio of cell lines as well as primary cell lines from patients diagnosed with MPM. Examining a wide range of different cell lines will enable us to confirm and ascertain our current finding of rfhSP-D in inducing apoptosis. A wider portfolio of cell lines will enable us to gain a more reliable trend and improve our understanding by categorising which cell lines may respond more quickly or cell lines that has the least effect on rfhSP-D in inducing apoptosis. This will enable us to learn more about why different lines may react differently with or without treating with rfhSP-D. Tissue characterisation using immunofluorescence and immunohistochemical staining (IHC)

will also be helpful to localise human SP-D in a wide range of histological samples. It is also imperative to examine the immunomodulatory effect SP-D can potentially have on tissues under inflammatory conditions. A variety of cell lines and primary cell lines extracted from patients diagnosed with MPM, will enable us to establish which cell lines are affected most from treatment with rfhSP-D, and which has the least effect, as different cell lines may behave in different ways and have different responses.

This current study has demonstrated that SP-D is significantly present in various histological types of MPM but may be immunosuppressed by pro-tumorigenic substances released by the tumour microenvironment. The role of SP-D is more complex than previously thought and may be dependent on the tumour microenvironment. Previous studies have shown that HA, a major constituent of the tumour microenvironment, can actively inhibit the immunological effects of SP-D (Kaur *et al*., 2018; Mahajan *et al*., 2008). Furthermore, the role of rfhSP-D has been investigated on MSTO (MPM cell line) in which has significantly induced apoptosis. The possible explanation of this is due to intrinsic apoptotic pathway in which is based on previous investigation on other types of epithelium malignancies (prostate, ovarian and breast), but further investigation into apoptotic pathway is required. This study demonstrated the potential role of rfhSP-D as anti-cancerous modality in MPM. Further investigation is required to establish the element involved in inhibiting SP-D actions within MPM microenvironment, as well the underlying cellular mechanism of rfhSP-D involved in initiating the anti-proliferative effects on MPM cells. Therefore, further investigation is required to validate our finding in this study and widen our understanding of SP-D and rfhSP-D in inducing apoptosis in MPM.

6 References

Agostinis C, Vidergar R, Belmonte B, Mangogna A, Amadio L, Geri P, Borelli V, Zanconati F, Tedesco F, Confalonieri M, Tripodo C, Kishore U, Bulla R. (2017). Complement Protein C1q Binds to Hyaluronic Acid in the Malignant Pleural Mesothelioma Microenvironment and Promotes Tumor Growth. Frontiers Immunology; 20 (8), 1559

Agostinis C, Bulla R, Tripodo C, Gismondi A, Stabile H, Bossi F, et al (2010). An alternative role of C1q in cell migration and tissue remodeling: contri- bution to trophoblast invasion and placental development. J Immunol; 185:4420–9

Anraku M., Cunningham K.S., Yun Z., Tsao M.-S., Zhang L., Keshavjee S., Johnston M.R., de Perrot M (2008). Impact of tumor-infiltrating T cells on survival in patients with malignant pleural mesothelioma. J. Thorac. Cardiovasc. Surg; 135:823–829

Bibby, A et al. (2016). Malignant pleural mesothelioma: an update on investigation, diagnosis and treatment. European Respiratory Review; 2 (25), 472-486

Bianchi, S. M., Prince, L. R., McPhillips, K., Allen, L., Marriott, H. M., and Taylor, G. W. (2008). Impairment of apoptotic cell engulfment by pyocyanin, a toxic metabolite of Pseudomonas aeruginosa. Am. J. Respir. Crit. Care Med; 177, 35–43

Boutin C, Dumortier P, Rey F, Villiat JR, De Vuyst P. 1996. Black Spots concentrate oncogenic asbestos fibres in the parietal pleura. Am J Respir Crit Care Med; 153:444–449

Boffetta P. (2007). Epidemiology of peritoneal mesothelioma: A review. Ann Oncol; 18:985–990
Cancer Research UK. (Feb 2018). Mesothelioma statistics. Available: http://www.cancerresearchuk.org/health-professional/cancer-statistics/statistics-by-cancer-type/mesothelioma#heading-Zero.

Bo-Hui Jeon, Yeong-Min Yoo, Eui-Man Jung and Eui-Bae Jeung. (2020). Dexamethasone Treatment Increases the Intracellular Calcium Level Through TRPV6 in A549 Cells. International Journal of molecular Sciences; 21 (1050), 1-15

Bulla R, et al. (2016). C1q acts in the tumour microenvironment as a cancer-promoting factor independently of complement activation. Nat Commun; 7:10346

Bulla R, et al. (2008). Decidual endothelial cells express surface-bound C1q as a molecular bridge between endovascular trophoblast and decidual endothelium. Mol Immunol; 45:2629–40

Carbone, M et al. (2012). Malignant Mesothelioma: Facts, Myths, and Hypotheses. Journal of Cellular Physiology; 227 (1), 44-58

Cedeño-Arias M, Sánchez-Ramírez J, Blanco-Santana R, and Rengifo-Calzado E. (2011). Validation of a Flow Cytometry Based Binding Assay for Evaluation of Monoclonal Antibody Recognizing EGF Receptor. Scientia Pharmaceutica; 79 (3), 569-581

Ceresoli GL, Zucali PA, Favaretto AG, et al. (2006). Phase II study of pemetrexed plus carboplatin in malignant pleural mesothelioma. J Clin Oncol; 24: 1443–8

Ceresoli GL, Zucali PA, De Vincenzo F, et al. (2011) Retreatment with pemetrexed-based chemotherapy in patients with malignant pleural mesothelioma. Lung Cancer; 72:73–7

Chong IW, Chang MY, Chang HC, Yu YP, Sheu CC, Tsai JR, et al. (2006). Great potential of a panel of multiple hMTH1, SPD, ITGA11 and COL11A1 markers for diagnosis of patients with non-small cell lung cancer. Oncol Rep; 16:981–8

Cugell DW, Kamp DW. (2004). Asbestos and the pleura: a review. Chest; 125:1103-111

Cui A, Jin X-G, Zhai K, et al. (2014). Diagnostic values of soluble mesothelin-related peptides for malignant pleural mesothelioma: updated meta-analysis. BMJ Open; 4: e004145

Dodagatta-Marri E, Qaseem AS, Karbani N, Tsolaki AG, Waters P, Madan T, et al. (2014). Purification of surfactant protein D (SP-D) from pooled amniotic fluid and bronchoalveolar lavage. Methods Mol Biol; 1100:273–90

Duncan A.R, Winter G. (1988). The binding site for C1q on IgG. Nature; 332 , 738-740

Eggleton P, Reid K.B.M, Tenner A.J (1998). C1q — how many functions? how many receptors? Trends Cell Biol; 8, 428-431

Favaretto AG, Aversa SM, Paccagnella A, et al. (2003) Gemcitabine combined with carboplatin in patients with malignant pleural mesothelioma: a multicentric phase II study. Cancer; 97:2791–7

Foreman MG, Kong X, DeMeo DL, Pillai SG, Hersh CP, Bakke P, et al. (2011). Polymorphisms in surfactant protein-D are associated with chronic obstructive pulmonary disease. Am J Respir Cell Mol Biol; 44:316-322

F Zhang., et al. (2010). mTOR complex component Rictor interacts with PKCzeta and regulates cancer cell metastasis. Cancer Res; 70, 9360-9370

Griese M, Steinecker M, Schumacher S, Braun A, Lohse P, Heinrich S. (2008). Children with absent surfactant protein D in bronchoalveolar lavage have more frequently pneumonia. Pediatr Allergy Immunol; 19:639-647

Hartshorn, K.L., White, M.R., Mogues, T., Ligtenberg, T., Crouch, E.C., Holmskov, U., 2003. Lung and salivary scavenger receptor glycoprotein- 340 contribute to the host defense against influenza A viruses. Am. J. Physiol. Lung Cell Mol. Physiol; 285, L1066–L1076

Haas A R & Sterman D H. (2013). Malignant Pleural Mesothelioma: Update on Treatment Options with a Focus on Novel Therapies. Clinics in Chest Medicine; 34 (1), 99-111

Haagsman, H.P., van Golde, L.M. (1991). Synthesis and assembly of lung surfactant. Annu. Rev. Physiol; 53, 441–464

Hasegawa Y, Takahashi M, Ariki S, Asakawa D, Tajiri M, Wada Y, et al. (2015). Surfactant protein D suppresses lung cancer progression by downregulation of epidermal growth factor signaling. Oncogene; 34:4285-4286

Haslett, C., Savill, J. S., Whyte, M. K., Stern, M., Dransfield, I., and Meagher, L. C. (1994). Granulocyte apoptosis and the control of inflammation. Philos. Trans. R. Soc. Lond. B Biol. Sci; 345, 327–333

Herías MV, Hogenkamp A, van Asten AJ, Tersteeg MH, van Eijk M, Haagsman HP (2007) Expression sites of the collectin SP-D suggest its importance in first line host defence: power of combining in situ hybridisation. RT-PCR and immunohistochemistry. Mol Immunol; 44(13):3324–3332

Hollevoet K, Reitsma JB, Creaney J, et al. (2012) Serum mesothelin for diagnosing malignant pleural mesothelioma: an individual patient data meta-analysis. J Clin Oncol; 30: 1541–1549

Holmskov, U., Thiel, S., Jensenius, J.C. (2003). Collections and ficolins: humoral lectins of the innate immune defense. Annu. Rev. Immunol; 21, 547–578.

Illei PB, Rusch VW, Zakowski MF, et al. (2003). Homozygous deletion of CDKN2A and codeletion of the methylthioadenosine phosphorylase gene in the majority of pleural mesotheliomas. Clin Cancer Res; 9: 2108–2113

Ismail, K R et al. (2006). Malignant Pleural Mesothelioma: A Comprehensive Review. Cancer Control; 13 (3), 225-263

Ishii T, Hagiwara K, Ikeda S, Arai T, Mieno MN, Kumasaka T, et al. (2012). Association between genetic variations in surfactant protein d and emphysema, interstitial pneumonia, and lung cancer in a Japanese population. COPD; 9:409-416.

Ikegami M, Na CL, Korfhagen TR, Whitsett JA. (2005). Surfactant protein D influences surfactant ultrastructure and uptake by alveolar type II cells. Am J Physiol Lung Cell Mol Physiol; 288:L552-61

Janssen, W. J., McPhillips, K. A., Dickinson, M. G., Linderman, D. J., Morimoto, K., Xiao, Y. Q., and Oldham, K. M. (2008). Surfactant proteins A and D suppress alveolar macrophage phagocytosis via interaction with SIRP alpha. Am. J. Respir. Crit. Care Med; 178, 158–167

Joseph W. Belluck. (2018). The facts, figures and and statistics of mesothelioma. Available: https://www.mesotheliomahelp.org/mesothelioma/statistics/.

Kaur A, Riaz MS, Murugaiah V, Varghese PM, Singh SK and Kishore U. (2018). A Recombinant Fragment of Human Surfactant Protein D induces Apoptosis in Pancreatic Cancer Cell Lines via Fas-Mediated Pathway. Front. Immunol; 9:1126

Kaur A, Riaz MS, Singh SK and Kishore U. (2018) Human Surfactant Protein D Suppresses Epithelial-to- Mesenchymal Transition in Pancreatic Cancer Cells by Downregulating TGF-β. Front. Immunol; 9:1844

Kumai J et al. (2019). Surfactant Protein D as a Potential Biomarker and Therapeutic Target in Ovarian Cancer. Frontiers in Oncology; 9:542

K Uematsu, S Kanazawa, L You, B He, Z Xu, K Li, B Peterlin, F McCormick and D Jablons. (2013). Wnt Pathway Activation in Mesothelioma. American Association for Cancer Research; 63 (15), 4547-4551

Kishore U, Greenhough TJ, Waters P, Shrive AK, Ghai R, Kamran MF, et al. (2006). Surfactant proteins SP-A and SP-D: structure, function and receptors. Mol Immunol; 43:1293-1315

Kishore U., Strong, P., Perdikoulis, M. V., and Reid, K. B. (2001). A recombinant homotrimer, composed of the alpha helical neck region of human surfactant protein D and C1q B chain globular domain, is an inhibitor of the classical complement pathway. J. Immunol; 166, 559–565.

Kishore, U., Reid, K.B.M., 2001. Structures and functions of mammalian collectins. In: Crocker, P. (Ed.), Mammalian Carbohydrate Recognition Proteins. Results and Problems in Cell Differentiation Series, vol. 33, Springer, Berlin, pp. 225–248.

Kishore, U., Madan, T., Sarma, P.U., Singh, M., Urban, B.C., Reid, K.B.M., 2002. Protective roles of pulmonary surfactant proteins, SP-A and SP- D, against lung allergy and infection caused by Aspergillus fumigatus. Immunobiology; 205, 610–618.

Kouki, I. (2008). Pathology of mesothelioma. Environmental health and protective medicine; 13 (2), 60-64.

Lee CW, Murray N, Anderson H, et al. (2009) Outcomes with first-line platinum-based combination chemo- therapy for malignant pleural mesothelioma: a review of practice in British Columbia. Lung Cancer; 64:308–13

Lingappa JR, Dumitrescu L, Zimmer SM, Lynfield R, McNicholl JM, Messonnier NE, et al. (2011). Identifying host genetic risk factors in the context of public health surveillance for invasive pneumococcal disease. PLoS One; 6:e23413.

Liu J., Stevens J., Rote C. A., Yost H. J., Hu Y., Neufeld K. L., White R. L., Matsunami N. (2001). Siah-1 mediates a novel β-catenin degradation pathway linking p53 to the adenomatous polyposis coli protein. Mol. Cell; 7: 927-936

Lorusso G and Ruegg C. (2008). The tumour microenvironment and its contribution to tumour evolution toward metastasis. Histochem Cell Biol; 130:1091–103

Marcq E., Siozopoulou V., De Waele J., van Audenaerde J., Zwaenepoel K., Santermans E., Hens N., Pauwels P., van Meerbeeck J.P., Smits E.L.J (2017). Prognostic and predictive aspects of the tumor immune microenvironment and immune checkpoints in malignant pleural mesothelioma. Oncoimmunology; 6:e1261241

Madan T, Kishore U, Singh M, Strong P, Clark H, Hussain EM, et al. (2001). Surfactant proteins A and D protect mice against pulmonary hypersensitivity induced by Aspergillus fumigatus antigens and allergens. J Clin Invest; 107(4):467-75.

Madsen, J., Tornoe, I., Nielsen, O., Lausen, M., Krebs, I., Mollenhauer, J., Kollender, G., Poustka, A., Skjodt, K., Holmskov, U., 2003. CRP-ductin, the mouse homologue of gp-340/deleted in malignant brain tumors 1 (DMBT1), binds Gram-positive and Gram-negative bacteria and interacts with lung surfactant protein D. Eur. J. Immunol; 33, 2327–2336

Madsen J, Kliem A, Tornøe I, Skjødt K, Koch C, Holmskov U. (2000). Localization of lung surfactant protein D (SP-D) on mucosal surfaces in human tissues. J. Im- munol; 164:5866–70

Mahani, et al. (2008). Recombinant surfactant protein-D selectively increases apoptosis in eosinophils of allergic asthmatics and enhances uptake of apoptotic eosinophils by macrophages. International Immunology. 20 (8), 993–1007

Maloney T, Phelan R, Simmons N. (2018). Saving the horseshoe crab: A synthetic alternative to horseshoe crab blood for endotoxin detection. PLoS Biology; 16 (10)

Matsuzawa S. I., Reed J. C. (2001). Siah-1, SIP, and Ebi collaborate in a novel pathway for β-catenin degradation linked to p53 responses. Mol. Cell; 7: 915-926,

Mauney, M. (2018). History of Asbestos. Available: https://www.asbestos.com/asbestos/history/. Last accessed 24/02.2018

Mahajan L, Madan T, Kamal N, Singh VK, Sim RB, Telang SD, et al. (2008). Recombinant surfactant protein-D selectively increases apoptosis in eosinophils of allergic asthmatics and enhances uptake of apoptotic eosinophils by macrophages. Int Immunol; 20:993-1007.

Mahajan L, Pandit H, Madan T, Gautam P, Yadav AK, Warke H, et al. (2013). Human surfactant protein D alters oxidative stress and HMGA1 expression to induce p53 apoptotic pathway in eosinophil leukemic cell line. PLoS One; 8: e85046.

Mahajan L, Gautam P, Dodagatta-Marri E, Madan T, Kishore U. (2014). Surfactant protein SP-D modulates activity of immune cells: proteomic profiling of its interaction with eosinophilic cells. Expert Rev Proteomics 11:355-369

Mangogna A, Belmonte B, Agostinis C, Ricci G, Gulino A, Ferrara I, et al. (2018) Pathological significance and prognostic value of surfactant protein D in cancer. Front Immunol; 9:1–12

MesotheliomaHelp.org. (Jan 2017). Mesothelioma Statistics. Available: https://www.mesotheliomahelp.org/mesothelioma/mesothelioma-statistics/. [Last accessed 17/03/2018]

Mesothelioma Cancer Alliance at Mesothelioma.com. (2018). Pleural Mesothelioma. Available: https://www.mesothelioma.com/mesothelioma/types/pleural.htm. Last accessed [Accessed 4/06/2018].

Miles, E. (2008) Clinical consequences of asbestos-related diffuse pleural thickening: A review. Journal of Occupational Medicine and Toxicology; (3):20

Mudhar H.S., Wallace W.A.H (2002). No relationship between tumour infiltrating lymphocytes and overall survival is seen in malignant mesothelioma of the pleura. Eur. J. Surg. Oncol; 28:564–565

Nayak A, Dodagatta-Marri E, Tsolaki AG, Kishore U. (2012). An Insight into the Diverse Roles of Surfactant Proteins, SP-A and SP-D in Innate and Adaptive Immunity. Front Immunol; 3:131

O'Brien ME, Watkins D, Ryan C, et al. (2006). A randomised trial in malignant mesothelioma (M) of early (E) versus delayed (D) chemotherapy in symptomatically stable patients: the MED trial. Ann Oncol; (17): 270–275

Pass HI, Lott D, Lonardo F, et al. (2005). Asbestos exposure, pleural mesothelioma, and serum osteopontin levels. N Engl J Med; 353:1564-1573

Pandit, et al. (2014). Surfactant Protein D Inhibits HIV-1 Infection of Target Cells via Interference with gp120-CD4 Interaction and Modulates Pro-Inflammatory Cytokine Production. Public Library of Science; 9 (7), 1-11

Païdassi, H., Tacnet, P., Garlatti, V., Darnault, C., Ghebrehiwet, B., Gaboriaud, C., Arlaud, G. J., and Frachet, P. (2008). C1q binds phosphatidylserine and likely acts as a multiligand bridging molecule in apoptotic cell recognition. J. Immunol; 180, 2329–2338

Ricklin D, Hajishengallis G, Yang K, Lambris JD. (2010). Complement: a key system for immune surveillance and homeostasis. Nat Immunol; 11:785–97

Rimner A, Zauderer MG, Gomez DR, et al. (2016). Phase II study of Hemithoracic Intensity-Modulated Pleural Radiation Therapy (IMPRINT) as part of lung-sparing multimodality therapy in patients with malignant pleural mesothelioma. J Clin Oncol; 34: 2761–2768

Robinson BW, Lake RA. (2005). Advances in malignant mesothelioma. N Engl J Med; 353: 1591–1603

Robinson BW, Creaney J, Lake R, et al. (2003). Mesothelin-family proteins and the diagnosis of mesothelioma. Lancet; 362:1612-1616

Scherpereel, A et al. (2010). Guidelines of the European Respiratory Society and the European Society of Thoracic Surgeons for the management of malignant pleural mesothelioma. European Respiratory Journal; 35 (3), 479-495.

Sekido Y. (2013). Molecular pathogenesis of malignant mesothelioma. Carcinogenesis; 34: 1413–1419

Sellar, G.C., Blake, D.J., Reid, K.B.M., 1991. Characterization and organization of the genes encoding the A, B and C chains of human complement subcomponent Clq. The complete de-rived amino acid sequence of human Clq. Biochem. J; 274, 481-490

Silveyra P, Floros J. (2012). Genetic variant associations of human SP-A and SP-D with acute and chronic lung injury. Front Biosci (Landmark Ed); 17:407-429

Singh M, Madan T, Waters P, Parida SK, Sarma PU, Kishore U. (2003). Protective effects of a recombinant fragment of human surfactant protein D in a murine model of pulmonary hypersensitivity induced by dust mite allergens. Immunol Lett; 86:299–307.

Sluis-Cremer GK. (1991). Asbestos disease at low exposures after long residence times. Ann NY Acad Sci; 643:182–193

Sluis-Cremer GK, Liddell FDK, Logan WPD, Bezuidenhout BN. (1992). The mortality of amphibole miners in South Africa, 1946-80. Br J Ind Med; 49:566–575

Stahlman MT, Gray ME, Hull WM, Whit- sett JA. (2002). Immunolocalization of sur- factant protein-D (SP-D) in human fetal, newborn, and adult tissues. J. Histochem. Cytochem; 50:651–60

Soerensen C M, Nielsen O L, Willis A, Heegaard P M H, and Holmskov U. (2005). Purification, characterization and immunolocalization of porcine surfactant protein D. Immunology; 114 (1), 72-82

Tanaka M, Arimura Y, Goto A, Hosokawa M, Nagaishi K, Yamashita K, et al. (2009). Genetic variants in surfactant, pulmonary-associated protein D (SFTPD) and Japanese susceptibility to ulcerative colitis. Inflamm Bowel Dis; 15:918-925

Thakur et al. (2017). Involvement of mitochondrial intrinsic pathway in rhSP-D (recombinant human Surfactant Protein D) induced apoptosis of prostate cancer cells Can J Biotech; 1:172

Ujma S, Horsnell WG, Katz AA, Clark HW, Schafer G. (2017). Non-Pulmonary Immune Functions of Surfactant Proteins A and D. J Innate Immun; 9:3-11

Uematsu K., Kanazawa S., You L., He B., Xu Z., Li K., Peterlin B.M., McCormick F., Jablons D.M. (2003). Wnt pathway activation in mesothelioma: Evidence of Dishevelled overexpression and transcriptional activity of beta-catenin. Cancer Research; 63:4547–4551

Vandivier, R., Ogden, C., Fadok, V. A., Hoffmann, P., Brown, K., Botto, M., Walport, M. J., Fisher, J. H., Henson, P. M., and Greene, K. E. (2002). Role of surfactant proteins A, D, and C1q in the clearance of apoptotic cells in vivo and in vitro: calreticulin and CD91 as a common collectin receptor complex. J. Immunol; 169, 3978–3986

Vieira F, Kung JW and Bhatti F. (2017). Structure, genetics and function of the pulmonary associated surfactant proteins A and D: The extra-pulmonary role of these C type lectins. Annels of Anatomy; 11 (211), 184-201

Wert SE, Yoshida M, LeVine AM, Ikegami M, Jones T, Ross GF, et al. (2000). Increased metalloproteinase activity, oxidant production, and emphysema in surfactant protein D gene-inactivated mice. Proc Natl Acad Sci U S A; 97:5972-5977

Wright, J.R., Dobbs, L.G. (1991). Regulation of pulmonary surfactant secretion and clearance. Annu. Rev. Physiol; 53, 395–414

Wyllie, A. H., Kerr, J. F., and Currie, A. R. (1980). Cell death: the significance of apoptosis. Int. Rev. Cytol; 68, 251–306

Yamada N., Oizumi S., Kikuchi E., Shinagawa N., Konishi-Sakakibara J., Ishimine A., Aoe K., Gemba K., Kishimoto T., Torigoe T., (2010). CD8+ tumor-infiltrating lymphocytes predict favorable prognosis in malignant pleural mesothelioma after resection. Cancer Immunol. Immunother; 59:1543–1549

Zalcman G, Mazieres J, Margery J, Greillier L, Audigier-Valette C, Moro-Sibilot D, et al. (2016) Bevacizumab for newly diagnosed pleural mesothelioma in the Mesothelioma Avastin Cisplatin Pemetrexed Study (MAPS): a randomised, controlled, open-label, phase 3 trial. Lancet; 387:1405–14

Zucali PA, Ceresoli GL, Garassino I, et al. (2008) Gemcitbine and vinorelbine in pemetrexed-pretreated patients with malignant pleural mesothelioma. 176. Cancer; 112(7):1555–61